

OFR
82-994

DEPARTMENT OF THE INTERIOR
GEOLOGICAL SURVEY

*Shallow Subsurface Temperatures and
Some Estimates of Heat Flow from the
Colorado Plateau of Northeastern Arizona*

UNIVERSITY OF UTAH
RESEARCH INSTITUTE
EARTH SCIENCE LAB.



OPEN-FILE REPORT 82-994
FLAGSTAFF
1982

United States Department of the Interior

Geological Survey

SHALLOW SUBSURFACE TEMPERATURES AND SOME ESTIMATES OF HEAT FLOW
FROM THE COLORADO PLATEAU OF NORTHEASTERN ARIZONA

by

J. H. Sass, Claudia Stone[†], and Donald J. Bills

U.S. Geological Survey Open-File Report 82-994

1982

This report is preliminary and has not been reviewed for conformity with U.S. Geological Survey editorial standards and stratigraphic nomenclature.

[†]State of Arizona, Bureau of Geology and Mineral Technology, Geological Survey Branch, Tucson, Arizona 85719; present address: 5933 East Pima Street, Tucson, Arizona 85712

Table of Contents

	<u>page</u>
Abstract -----	3
Introduction -----	4
Acknowledgments -----	6
Regional Geology and Stratigraphy -----	7
San Francisco Volcanic Field -----	7
Black Mesa -----	13
South-Central Colorado Plateau -----	14
Regional Hydrologic Characteristics -----	16
Introduction -----	16
Regional Climate and Hydrology -----	16
Regional Hydrogeology -----	17
Regional Aquifers -----	17
San Francisco Volcanic Field -----	18
Black Mesa -----	19
South-Central Colorado Plateau -----	21
Temperature data -----	23
San Francisco Volcanic Field -----	23
Black Mesa -----	23
South-Central Colorado Plateau -----	23
Variation of Extrapolated Surface Temperature with Elevation -----	33
Thermal Conductivity -----	36
Heat-flow Estimates -----	40
San Francisco Volcanic Field -----	40
Black Mesa -----	40
South-Central Colorado Plateau -----	40
Discussion -----	46
References -----	48
Appendix A: Individual temperature profiles and tabulations for the San Francisco Volcanic Field -----	52
Appendix B: Individual temperature profiles and tabulations for the Black Mesa region -----	77
Appendix C: Individual temperature profiles and tabulations for the South-Central Colorado Plateau -----	94

Abstract

Temperature data to depths of a few hundred meters were obtained from 29 wells in northeastern Arizona; 12 in the region surrounding the San Francisco Volcanic Field, 8 in the Black Mesa area, and 9 in the south-central Colorado Plateau which includes the White Mountains. Although there was evidence for local hydrologic disturbances in many temperature profiles, most wells provided an estimate of the conductive thermal gradient at the site. A few thermal conductivities were measured and were combined with published regional averages for the north-central part of the Colorado Plateau to produce crude estimates of regional heat flux. None of the wells was accessible below the regional aquifers. To these depths, heat flow in the area of the San Francisco Volcanic Field appears to be controlled primarily by regional lateral water movement having a significant downward vertical component of velocity. The mean heat flow of $27 \pm 5 \text{ mWm}^{-2}$ is only a third to a quarter of what we would expect in this tectonic setting. The heat that is being carried laterally and downward probably is being discharged at low enthalpy and low elevation in springs and streams of the Colorado Plateau and Mogollon Rim. In the vicinity of Black Mesa, heat-flow averages about 60 mWm^{-2} , characteristic of the "cool interior" of the Colorado Plateau. North of the White Mountain Volcanic Field, the average heat flow is about 95 mWm^{-2} .

INTRODUCTION

The thermal regime of the Colorado Plateau provides important constraints on models for the evolution and tectonic state of this major physiographic province. Early heat-flow maps (e.g., Blackwell, 1971; Sass and others, 1971b; Roy and others, 1972) depicted the Colorado Plateau as primarily a province of low-to-normal heat flow although they all recognized that the southeastern part of the plateau in New Mexico (which seems to interact tectonically with the western margin of the Rio Grande Rift Zone) was a region of higher than normal heat flow. Subsequent work by Marshall Reiter, Edward R. Decker, David S. Chapman and their associates has revealed that the Colorado Plateau is quite complicated thermally and contains a number of distinct thermal provinces. Data from Shearer and Reiter (1981) and Bodell and Chapman (1982) indicate high heat flow along the eastern and southeastern margins of the plateau as well as in the southeastern $\sim 1/3$ of the province. Such data as exist also indicate high heat flow along the western margin of the plateau consistent with the observed active normal faulting and young volcanism. Preliminary results from the southwestern margin of the plateau, in particular near the San Francisco volcanic field and the Mogollon Rim, indicate a conductive component of heat flow in the low-to-normal range (20-50 mWm^{-2}) (Shearer and Reiter, 1981; Bills and Sass, 1982); this, despite the evidence for late Tertiary and Quaternary normal faulting and volcanism. Shearer and Reiter (1981) attribute the low heat flow to groundwater movement, and Bills and Sass (1982) provide hydrogeologic and hydrologic data confirming this interpretation.

In this study, we combine the temperature data obtained by Bills and Sass (1982) for the San Francisco volcanic field with temperature data obtained by the Arizona Bureau of Geology and Mineral Technology over the remainder of the study area (Figure 1) and with data from a heat-flow well (CVL, Figure 1) drilled by the USGS in 1979. With the exception of CVL and the "TGE" wells near the White Mountain volcanic field (Figure 1), no conductivity samples were available. Thus, the present study generally is limited to presenting the temperature profiles and discussing their implications for the hydrology and heat flow of the region. We do, however, make some crude estimates of heat flow to investigate whether our results are in accord with earlier published values. Throughout this paper, we look at three individual subprovinces within this portion of the Colorado Plateau; namely, the San Francisco volcanic field, Black Mesa, and a somewhat arbitrarily defined "south-central Colorado Plateau" combining the White Mountain volcanic field and Mogollon Rim.

Standard techniques were used to obtain the data. Temperatures were measured to an overall precision of $\pm 0.01^\circ\text{C}$ (for relative temperatures) using variants of the "portable mode" described by Sass and others (1971b) in which the wheatstone bridges have been replaced by digital ohmmeters. Thermal conductivities were measured on divided-bar-type apparatuses (see e.g., Birch, 1950), and all but four of the measurements were made on drill cuttings using the technique described by Sass and others (1971a).

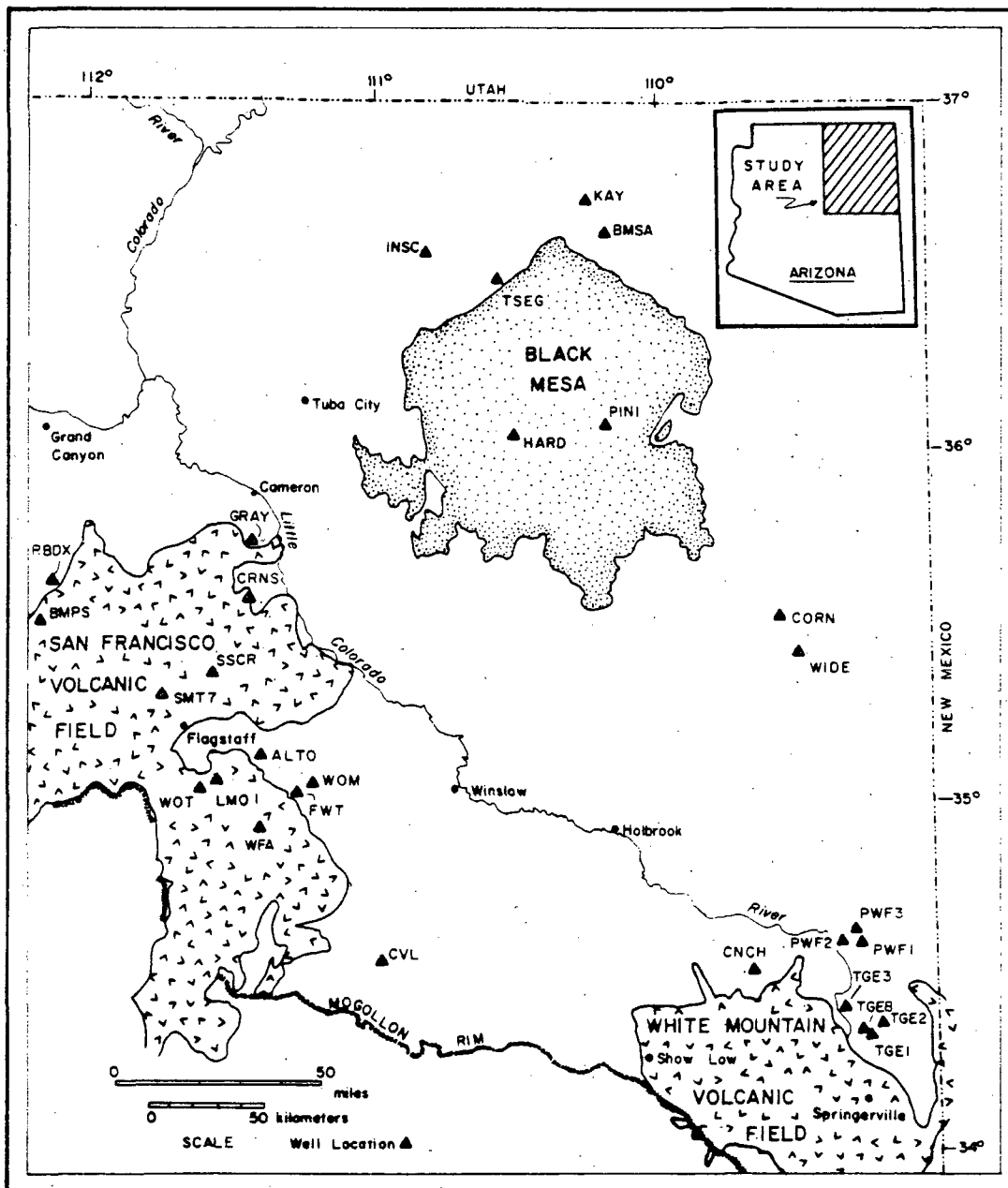


Figure 1. Map showing locations of wells and principal physiographic and geologic features of the study area.

The primary aims of this study are: 1) To make the temperature data available to interested workers; 2) to interpret these data to the extent possible in terms of the geology and hydrology of the region, and 3) to suggest some further studies which may help to unravel the complicated interaction between the earth's heat and groundwater in the region.

Acknowledgments. Many people working in the field offices of the Navajo Indian Tribe, Water and Sanitation Department, Navajo Tribal Utility Authority, and the U.S. Public Health Service, Office of Environmental Health and Engineering, generously assisted us in locating open or abandoned wells from which we could obtain temperature logs for this study. To them we extend our sincere appreciation and gratitude.

REGIONAL GEOLOGY AND STRATIGRAPHY

The Colorado Plateau physiographic province of northeastern Arizona comprises relatively flat-lying undeformed sedimentary rocks that are slightly tilted to the northeast. Broad regional arching and sagging, mesas, dissected canyons and local flexures and faults characterize much of the plateau country. The major regional structures are the Defiance positive along the Arizona-New Mexico border, Black Mesa basin in the central area, and the Kaibab positive to the west. Much of the plateau exceeds 1,800 m in elevation, and some areas attain more than 2,700 m.

Precambrian rocks are exposed only in the Grand Canyon but have been encountered in drill holes at depths varying from 300 to 2,300 m. Granitic, quartzitic, and metamorphic Precambrian rocks have been identified. Lower Paleozoic strata, where present, are generally thin and discontinuous. Upper Paleozoic rocks are more abundant, with the Permian System being thicker than all other Paleozoic units combined (Peirce, 1976). Due to regional tilting and to pre-Late Cretaceous erosion that beveled the land surface, progressively younger rocks crop out to the north and northeast. Permian rocks form most of the surface outcrops south and west of the Little Colorado River; Mesozoic strata are the principal surface exposures north and east of the river. Extensive areas of Triassic and Jurassic rocks crop out around Black Mesa, while Cretaceous units form the erosion surface of Black Mesa itself and crop out farther south, in the eastern part of the Mogollon Rim. The Cretaceous rocks form a sequence of continental and transitional margin "red beds" that are noted for vertical and lateral-facies changes. Minor exposures of middle Tertiary to early Quaternary alluvium are present locally in river and stream channels. (See Table 1 for representative geologic sections and Table 2 for descriptions of rock units.)

Three young volcanic fields exist along the south and southwest margins of the plateau. Extrusions of predominantly basaltic Tertiary-Quaternary lavas cover large areas in the White Mountain and San Francisco volcanic fields. Numerous cinder cones stud the northern (younger) part of these fields. Young intermediate to silicic lavas (≤ 3 m.y.), which erupted contemporaneously with the basalts, form stubby flows, domes, and dome complexes in the San Francisco field. On the southern flank of Black Mesa basin, the Pliocene Hopi Buttes volcanic field erupted principally alkalic lamprophyres. Maar craters and volcanic plugs characterize this field today.

The San Francisco volcanic field lies within a southeast-trending zone through northwest and central Arizona where historical seismicity (1830-1980) coincides with Quaternary faulting (DuBois and others, 1981). In contrast, Black Mesa and the south-central Colorado Plateau lie within a region of sparse historical seismicity.

San Francisco Volcanic Field. Volcanic rocks of the San Francisco volcanic field cover an area greater than 5,000 km² along the southwestern margin of the Colorado Plateau (Figure 1). The lavas rest on a stripped surface of predominantly Permian and some remnant Triassic sedimentary rocks that dip slightly (less than 1°) to the northeast (Moore, Wolfe, and Ulrich, 1974). In this area, the Permian System (Kaibab Limestone, Coconino

of northeastern Arizona (See Table 2 for descriptions of rock units.)

ERA	SYSTEM	BLACK MESA	SAN FRANCISCO VOLCANIC FIELD	SOUTH-CENTRAL COLORADO PLATEAU	GEOHYDROLOGIC CHARACTERISTICS	
<i>WELL</i>	<i>LOCATIONS</i>	<i>(A-23-19) 8ad</i>	<i>(A-19-6) 17da</i>	<i>(A-10-30) 27ac</i>		
CENOZOIC	TERT-QUAT		Volcanics		Water-bearing	
MESOZOIC	CRETACEOUS	Wepo Fm			Water-bearing	
		Toreva Fm			Aquiclude	
		Mancos Sh				
		Dakota Ss				
	JURASSIC	Morrison Fm				D Multi-Aquifer
		Cow Springs Ss				
		Entrada Ss				Aquitard
	JTR	Navajo Ss				
	TRIASSIC	Kayenta Fm				N Multi-Aquifer
		Moenvae Fm				
Wingate Fm					Water-bearing	
Chinle Fm					Aquitard	
Moenkopi Fm				Moenkopi Fm		
PALEOZOIC	PERMIAN	De Chelly Ss	Kaibab Ls	Kaibab Ls	C Multi-Aquifer	
		Supai Fm	Coconino Ss	Coconino Ss		
		Supai Fm	Supai Fm	Supai Ss		
	PENN-PERM	Naco Fm	Naco Fm		Water-bearing ?	
	MISS.	Redwall Ls	Redwall Ls		Limestone Aquifer	
	DEVONIAN	Ouray Fm	Martin Fm		?	
		Elbert Fm				
CAMBRIAN	Aneth Fm				Aquitard	
	Bright Angel Sh				Water-bearing	
	Tapeats Ss					
PRECAMBRIAN	PRECAMBRIAN	Granite	Granite	Granite	Aquiclude ?	

TABLE 2. Description of major sedimentary rock units
of the Colorado Plateau of NE Arizona
(from Bahr, 1962; Geologic Atlas of the Rocky Mountain Region, 1972;
Johnson and Sanderson, 1968; Peirce and others, 1970; Sobels, 1962;
Twenter, 1962; Wilson, 1974)

Age		Formation	Description and Thickness
Cenozoic	Quaternary	Glacial outwash	alluvium, colluvium, glacial fluvial and morainal deposits
		Verde Formation	Pleistocene-Pliocene, white to pinkish gray limestone and marl, yellowish green and reddish brown mudstone and claystone, grayish orange-pink and light brown sandstone 500-1000 m
		Bidahochi Formation	limestone, claystone and silt beds with interbedded sandstone and water-laid rhyolite tuffs and ash
	Tertiary	Chuska Sandstone	gray to brown, fine-to-medium grained, cross-stratified sandstone, to 100 m
		Datil Formation	reddish brown to gray sandstone, mudstone and conglomerate and beds of volcanic ash
		Eagar Formation	reddish sandstone, shale and conglomerate
Mesozoic	Jurassic	Yale Point Sandstone	yellowish gray sandstone, to 100 m
		Wepo Formation	gray siltstone, mudstone, sandstone, and coal, 90-230 m
		Toreva Formation	lower and upper light-colored, cross-stratified sandstone separated by variegated siltstone, and dark carbonaceous mudstone and coal; 43-100 m
		Mancos Shale	grayish, fossiliferous mudstone and siltstone, 145-235 m
		Dakota Sandstone	lower and upper light-colored, cross-stratified sandstone separated by carbonaceous siltstone and coal, 15-45 m

TABLE 2. Description of major sedimentary rock units of the Colorado Plateau of NE Arizona -- continued (from Bahr, 1962; Geologic Atlas of the Rocky Mountain Region, 1972; Johnson and Sanderson, 1968; Peirce and others, 1970; Sobels, 1962; Twenter, 1962; Wilson, 1974)

Age	Formation	Description and Thickness
Mesozoic	Jurassic	Morrison Formation variegated claystone and sandy claystone, 0-75 m; grayish to yellowish, cross-stratified sandstone and minor mudstone, 0-90 m; reddish sandstone and mudstone, 0-100 m; interstratified cross-stratified sandstone and greenish to grayish mudstone, 0-120 m
		Cow Springs Sandstone grayish, planar cross-stratified sandstone, 0-105 m
		Bluff Sandstone orange-gray to gray medium-to-coarse-grained eolian sandstone, 6-20 m
		Summerville Formation grayish orange-pink to reddish brown siltstone and sandstone, 15-45 m
		Entrada Sandstone lower sandy orangish cross-stratified sandstone, 0-106 m; silty reddish sandy siltstone, 0-45 m; upper sandy orangish sandstone, 0-73 m
		Carmel Formation horizontally stratified, reddish siltstone and minor sandstone, 0-60 m
	Triassic	Navajo Sandstone light brown, planar cross-stratified sandstone, 0-490 m
		Kayenta Formation northeastern assemblage of reddish cross-stratified sandstone and a southwestern assemblage of reddish siltstone and minor sandstone, 0-210 m
		Moenave Formation upper pale red, cross-stratified sandstone, 0-85 m and lower reddish orange to reddish brown siltstone and sandstone, 0-105 m
		Wingate Sandstone light brown, cross-stratified sandstone, 0-150 m; reddish brown, horizontally stratified siltstone and minor cross-stratified sandstone, 0-150 m
		Chinle Formation lenticular sandstone, claystone and clayey sandstone, 12-85 m
		Moenkopi Formation reddish brown siltstone and lesser sandstone, 0-150 m

TABLE 2. Description of major sedimentary rock units
of the Colorado Plateau of NE Arizona -- continued
(from Bahr, 1962; Geologic Atlas of the Rocky Mountain Region, 1972;
Johnson and Sanderson, 1968; Peirce and others, 1970; Sobels, 1962;
Twenter, 1962; Wilson, 1974)

Age		Formation	Description and Thickness
Paleozoic	Permian	Kaibab Limestone	yellowish to light-gray dolomitic limestone, 100-200 m
		Toroweap Formation	very pale orange cross-bedded sandstone, 45-105 m
		DeChelly Sandstone	crossbedded, reddish orange, massive sandstone, 0-300 m
		Coconino Sandstone	very pale orange to pale yellowish-orange massive crossbedded sandstone, 100-300 m
		Cutler Formation	fine-to-medium grained arkosic sandstone, siltstone and mudstone, 75-230 m
		Supai Formation	fine-grained yellow-red-brown crossbedded sandstone, interbedded red shale, siltstone, and bluish gray limestone at base, 275-300 m
	Penn.	Naco Formation	interbedded red and gray shale and limestone, 0-85 m
		Redwall Limestone	thick-bedded, bluish gray, cherty, crystalline limestone, 135-245 m
		Martin Formation	interbedded dolomite, limestone, gray and green shale, sandstone, and cg., 0-95 m
	Devonian	Ouray	dark brown limestone, locally dolomited and massive, 0-35 m
Elbert Formation		light colored quartzitic sandstone, shaley dolomite and minor green and red shale, 0-150 m	
Aneth Formation		dense, dark colored dolomite, generally argillaceous with minor interbeds of dark gray shale, 0-60 m	

TABLE 2. Description of major sedimentary rock units
of the Colorado Plateau of NE Arizona -- continued.
(from Bahr, 1962; Geologic Atlas of the Rocky Mountain Region, 1972;
Johnson and Sanderson, 1968; Peirce and others, 1970; Sobels, 1962;
Twenter, 1962; Wilson, 1974)

Age		Formation	Description and Thickness
Paleozoic	Cambrian	Muav Limestone	limestone with beds and partings of silt, shale and dolomite, 90-180 m
		Bright Angel Shale	green and buff micaceous shale and thin beds of sandstone, limestone and dolomite, 60-185 m
		Tapeats Sandstone	brown and white crossbedded sandstone, shale partings, and conglomerate lenses, 15-105 m
Prec.		Granitic quartzitic and metamorphic rocks	

Sandstone, and Supai Formation) has an average thickness between about 650 and 825 m, which exceeds the combined total thickness of the remaining Paleozoic units. Depth to Precambrian granitic rock is about 1,100 m.

Eruptions of basaltic lavas south and west of the San Francisco volcanic field began in the Transition Zone approximately 15 m.y. ago (Luedke and Smith, 1978). Eruptive centers and flows very roughly decrease in age to the northeast. In the San Francisco volcanic field, itself, basaltic volcanism began about 6 m.y. ago and has been nearly continuous for the past 3 m.y. Ages continue to decrease generally to the north-northeast. The youngest K-Ar date on a basaltic rock (0.046 m.y.) was obtained on a basaltic andesite from Strawberry Crater (Damon, Shafiqullah, and Leventhal, 1974) in the northeastern part of the field. Basaltic rocks are mostly alkali olivine basalt, alkali-rich high-alumina basalt, and basaltic andesite.

Intermediate to silicic lavas were erupted contemporaneously with lavas of basaltic composition. They occur as isolated domes, dome complexes, and stubby flows. Rock types and K-Ar dates of the five principal silicic centers (Leudke and Smith, 1978) are listed below.

Bill Williams Mountain	dacite	4.1 to 3.47 m.y.
Sitgreaves Mountain	rhyolite	3.8 to 0.94 m.y.
Kendrick Peak	dacite, rhyolite	1.9 m.y.
San Francisco Mountain	dacite, andesite	1.77 to 0.56 m.y.
O'Leary Peak	dacite	0.233 m.y.

The silicic centers form two distinct northeast-trending, en echelon chains. To the west, Bill Williams Mountain, Sitgreaves Mountain and Kendrick Peak, respectively, decrease in age to the northeast. Shoemaker, Squires, and Abrams (1974) pointed out that these eruptive centers appear to be localized along the Mesa Butte fault system. To the east, San Francisco Mountain and O'Leary Peak show a similar northeast alignment.

The youngest K-Ar date on silicic lava (0.021 m.y.) is from a rhyolite from South Sugarloaf Mountain (Damon, Shafiqullah, and Leventhal, 1974) on the northeast side of San Francisco Mountain. However, the very last eruption, which produced a volcano now called Sunset Crater, has been determined from tree ring studies to have taken place in 1064 A.D. (Smiley, 1958).

Black Mesa. Northern Arizona east of the Colorado River is often called the Black Mesa basin region because of the large structural basin that underlies much of the area. The basin encompasses the area approximately from the Defiance positive, west to the Kaibab positive, and from the Mogollon slope north nearly to the Utah border.

Black Mesa, which overlies the central part of Black Mesa basin, is an erosional remnant and a topographic high that stands 150 to 300 m above the surrounding terrain (Figure 1). The top of Black Mesa slopes to the southwest, with elevation changing from 2,400 to 1,800 m. Because surface streams drain to the southwest, the south and west margins of Black Mesa are dissected and embayed into large canyons and mesas. The northwest and northeast margins are relatively straight and continuous.

The top of Black Mesa is an erosional surface developed on the Cretaceous Wepo Formation. The other Mesaverde Group formations underlie the Wepo and crop out along the marginal scarps. These formerly extensive rocks of Cretaceous age were stripped away from the structurally higher areas of north-central and northeastern Arizona but were preserved at Black Mesa due to downwarping of the basin. The maximum in-place thickness of stratigraphic units beneath Black Mesa is approximately 2,750 m and consists of approximately half Mesozoic and half Paleozoic strata (Peirce and others, 1970).

Peirce and others (1970) estimated that Black Mesa contains coal reserves, within 500 m of the surface, amounting to about 20 billion short tons. The reserves are contained in the Cretaceous Dakota sandstone, and Toreva and Wepo Formations.

The Hopi Buttes volcanic field is located on the southern flank of Black Mesa basin. Eruptions of the nearly 200 Pliocene volcanoes were largely controlled by N. 60° W. and N. 40° E. regional fractures (Sutton, 1974). The field is nearly circular in plan and about 65 km in diameter. Volcanic rocks belong to the suite of alkalic lamprophyres called monchiquite or limburgite. They were intruded as dikes and sills, and erupted as flows, domes, and pyroclastics (Sutton, 1974). Violent phreatic explosions, which probably occurred in ancient "Hopi Lake," created numerous circular maar-type craters. Other topographic features prominent in the volcanic field are lava-capped mesas and conspicuous volcanic necks that formerly filled the diatremes.

South-Central Colorado Plateau. The south-central Colorado Plateau lies within the Mogollon slope, a broad structural homocline that extends from the Mogollon Rim northward to the Defiance positive and Black Mesa basin, and from Springerville on the east to Flagstaff on the west (Figure 1). The main structural features of the Mogollon slope are a gentle dip of 6 to 7 m per km to the northeast and small asymmetrical anticlines that trend generally northwest.

Drilling logs indicate that Precambrian basement in this area is principally granitic rock that varies in depth from about 700 to 1,400 m. The sedimentary rocks of the Mogollon slope range in age from late Pennsylvanian to Quaternary. Permian rocks, principally the Kaibab Limestone, Coconino Sandstone, and Supai Formation, comprise the predominant stratigraphic sequence. The Triassic Chinle and Morrison Formations are present but wedge out in this area. During pre-Late Cretaceous time, erosion removed the entire Jurassic System. The Tertiary Eagar and Datil Formations are present locally along the Arizona-New Mexico border. A single deep borehole east of Springerville (Peirce and Scurlock, 1972) confirms the continuation of Paleozoic units beneath the White Mountain volcanic field, but exactly how far south they occur and where they wedge out is unknown.

Three episodes of volcanism occurred in the White Mountain volcanic field between middle Tertiary and less than 200,000 years ago. The rocks are principally basaltic, with minor trachyandesite and rhyolite flows. The initial phase of volcanism began about 38 m.y. ago in the Transition Zone, and progressed northward with decreasing age. The second (Mount Baldy) episode began about 12 m.y. ago. A date of 8.6 m.y. was obtained from a

late-state rhyolite flow from the top to Mount Baldy (Merrill, 1974), a predominantly basaltic edifice. Dates on youngest basaltic rocks in the northern part of the field range from about 6.03 to 0.19 m.y. (Damon and Shafiqullah, personal communication, 1979). Numerous young cinder cones dot the northern part of the field. An AFM diagram clearly shows that the lavas of the three major volcanic episodes were not generated by continuous differentiation from a single source (Merrill and Péwé, 1977).

REGIONAL HYDROLOGIC CHARACTERISTICS

Introduction. Northeastern Arizona is characterized by a bedded sequence of sedimentary rocks generally unaltered by severe deformation and bisected by a largely superimposed stream network that in places has become deeply entrenched. The climate varies widely from semi-arid in the desert lowlands to relatively humid on the high plateaus and in the southern Alpine environments; however, precipitation and temperatures have a fairly uniform relation to altitude and orographic effects of the physiography particularly on the Navajo and Hopi Reservations (Cooley and others, 1969). Ground water underlies most of the area as either very local, discontinuous, and largely unconfined local aquifers, or as one of a series of generally continuous, occasionally confined, and possibly interconnected multi-aquifers. A basal group of Precambrian rock, for which very little hydrologic data exists, represents a bottom confining layer for the aquifers above, except where it may be highly fractured and faulted.

Regional climate, recharge, discharge, and runoff patterns have not changed significantly throughout recent times.

Regional Climate and Hydrology. Northeastern Arizona includes the Northeast, Plateau, and parts of the Central climate boundaries of Sellers and Hill (1974). These areas vary widely in climate and topography. The Mogollon Rim (Figure 1), which extends from near the San Francisco Peaks to the White Mountains represents a major orographic barrier to air masses moving across the state. As a result, it generally receives large amounts of precipitation [600 mm (25 inches) per year or more]. By contrast, Black Mesa, located in a rain shadow of this and other barriers, generally receives less than 250 mm (10 inches) per year. Other areas of notably low precipitation are the Painted Desert from Tuba City to Holbrook and along the Colorado River near the Utah border (Figure 1) where annual rainfall rarely exceeds 250 mm (10 inches) per year (Sellers and Hill, 1974). Most precipitation throughout occurs as a result of locally intense summer thunderstorms while winter and spring months produce occasionally heavy snows.

Most streams that drain northeastern Arizona are ephemeral. Exceptions are the Colorado River, which derives almost all of its controlled flow from outside Arizona, and perennial streams at the southern margin such as Oak Creek, White River, and Black River that drain the Mogollon Rim to the south and out of the area. Ground water also supplies locally perennial reaches either as large springs issuing from exposed contacts or in streams where a water table is intersected. Total runoff, however, is largely dependent on irregular precipitation. Much of the mean annual precipitation that falls on northeastern Arizona is lost to evaporation and/or infiltration. Cooley (1969) indicated that transmission losses alone can amount to 50% or more of the average annual runoff within reservation lands. Unit runoff values in the vicinity of the San Francisco Peaks are only around 1 to 3 mm/year, probably because of the excellent infiltration characteristics of the surrounding and underlying volcanic materials. Elsewhere along the Mogollon Rim, values seldom exceed 200 mm/year (E. H. McGavoch, U.S. Geological Survey, oral communication, 1980). Most of these losses are due to evaporation and transpiration while lesser amounts infiltrate into the underlying aquifers.

Regional Hydrogeology. Several hydrologic basins can be found in northeast Arizona and locally, ground water is exchanged between them (Cooley and others, 1969). Generally, ground water drains from the north and south toward the central part of the area (i.e., toward the Little Colorado River) and then flows north to northwestward until it encounters the Colorado River. Along the margins, some ground water flows out of the study area especially from the north into the San Juan Basin and from ground water divides along the Mogollon Rim to the south into the Verde and Salt River Basins.

Aquifer characteristics are not uniform and vary noticeably throughout the study area and from unit to unit. They are controlled regionally by lithology and bedding, locally by joint fractures and faults. Individual well yields and production characteristics from which aquifer characteristics are generally obtained are probably more dependent on how an individual well was developed and fitted. However, efficient, properly constructed wells do provide useful data on the nature of aquifer characteristics in various locations.

Substantial recharge occurs where favorable conditions exist (i.e., areas of high primary permeability or secondary permeability at the surface caused by extensive faulting, solution, joint fractures, and/or folds). Recharge in the alpine and high plateau environments is mostly the result of melting snow in the spring and early summer months. Short intense summer thunderstorms generally result in flashy runoff that produces comparatively little recharge to these areas. However, losing streams in the lower lying areas will absorb substantial amounts of the runoff and what is not evaporated is transmitted to the aquifers below. Direct recharge to consolidated sedimentary rocks is restricted by their relatively low permeabilities.

Regional Aquifers. Four regional multi-aquifers are found in the Mesozoic and Paleozoic sediments underlying the Colorado Plateau of northeastern Arizona. In descending order, they are the D, N, and C multi-aquifers (Cooley and others, 1969), and a limestone aquifer (Table 1). All are underlain by a basal unit of Precambrian rocks that are generally non-waterbearing. The D and N multi-aquifers are generally restricted to the Black Mesa subprovince since erosion has stripped Mesozoic sediments from most of the surrounding areas. The C multi-aquifer and a limestone aquifer probably underlie most of northeastern Arizona, although in the south-central Colorado Plateau, well logs from oil test holes in the vicinity of the White Mountains seldom encounter the Early to Middle Paleozoic Limestones which comprise the limestone aquifer. How far south these units actually occur is not known. The C multi-aquifer is continuous and extends outside the study area to the south, west, and east. Local and regional peculiarities of these aquifers as well as some additional local aquifers are discussed below in our review of the individual thermal subprovinces.

Throughout the Colorado Plateau, the C multi-aquifer is referred to by several names depending on location. In the Black Mesa subprovince, it is the C multi-aquifer centrally, and the DeChelly aquifer toward the eastern boundary of the state where the Coconino Sandstone grades into its lateral equivalent the DeChelly Sandstone (Cooley and others, 1969). In the south-central Colorado Plateau, it is referred to occasionally as the Coconino aquifer (Mann, 1976; Harper and Anderson, 1976) even though it is a continuation of

the aquifer as it exists in Black Mesa. In the San Francisco Volcanic Field subprovince, the C multi-aquifer is referred to as the Coconino or Regional aquifer (Levings and Mann, 1980; Appel and Bills, 1980, 1981), the latter primarily because it becomes hydraulically connected to Early and Middle Paleozoic Limestones as well as to younger sediments of the Verde Formation. For simplicity, this discussion will call it the C multi-aquifer throughout.

San Francisco Volcanic Field. In this subprovince, occasionally large amounts of water are found in unconsolidated alluvium and volcanic material where confining layers, such as clay beds or dense basalt, below the main water-bearing unit are relatively intact (Appel and Bills, 1981). Glacial Outwash in the Inner Basin of the San Francisco Peaks is particularly productive, and the Moenkopi Formation and Kaibab Limestone yield small amounts of water locally to wells where they are heavily interbedded with clay or cherty limestone that can act as aquitards. All of these water-bearing zones are perched to as much as 1,000 meters above the water-bearing units of the C multi-aquifer. The Kaibab Limestone at the eastern margin of the San Francisco Volcanic Field is under water-table conditions and hydraulically connected to the underlying Coconino Sandstone (Appel and Bills, 1981). But, toward the west, it, too, becomes perched well above the C multi-aquifer and eventually goes dry. Drainage patterns in the local aquifers tend to follow those expressed at the surface by topography. When these shallow water tables are intersected, water will briefly flow at the surface as springs, but it is soon either evaporated and transpired off, or infiltrates deeper into the subterranean environment. Most of these water-bearing zones respond directly to seasonal changes in climate, and during extended dry periods, many will go dry. Little is known about the individual aquifer characteristics of some of these local aquifers, and the available data transfers poorly to other areas. Generally, well yields are low, rarely greater than 200 L/M, and are more the result of pump type and limits on pump size than of actual aquifer characteristics. The Glacial Outwash provides the only exception with well yields in excess of 3,000 L/M and well-defined field constants (Harshbarger and Associates, 1974).

In the San Francisco Volcanic Field, erosion has removed most of the Mesozoic sediments that contain the major aquifers of the other subprovinces. Here, instead, the C multi-aquifer found in Middle to Late Paleozoic sediments is the principal aquifer. The main water-bearing unit, however, varies with location. To the east, the aquifer is still saturated and confined by the overlying Moenkopi Formation as a continuation of conditions that dominate in the South Central Plateau. To the west, the sediments that make up the C multi-aquifer begin to thicken, and water migrates downward out of the Kaibab Limestone and well into the Coconino Sandstone. Just east of the San Francisco Peaks, the aquifer is only partly saturated and under water-table conditions while to the west of the Peaks, water is encountered only in the Supai Group (Appel and Bills, 1980, 1981). Throughout the subprovince, siltstones in the Supai group may act as aquitards to restrict the vertical movement of water to the underlying limestones. To the south, near areas of recharge, the Coconino Sandstone is still at least partially saturated. But, because of extensive faulting and fracturing, the C multi-aquifer is in good hydraulic connection with the limestone beds below (Levings and Mann, 1981; Appel and Bills, 1981). Ground water moves away from areas of recharge, and a poorly defined ground water divide that stretches along the Mogollon

Rim to the southwest, northwest, and northeast. To the southwest, water flows down gradient and discharges as springs along Oak Creek and the Verde River, as well as migrating downward into the Verde Formation and limestone aquifer. Ground-water flow to the north seems to be split to the northeast and northwest around the San Francisco Peaks. Flow to the northeast turns northwest along the Little Colorado River and is drawn downward near Cameron through heavily fractured and folded parts of the aquifer into the underlying limestones (Appel and Bills, 1981). To the northwest, flow continues to discharge at points outside the study area along the Colorado River and Havasu Creek. Aquifer characteristics vary widely throughout the area and depend largely on the degree of fracture and faulting encountered (Appel and Bills, 1980, 1981). Well yields are low, less than 200 L/M, where the aquifer is unaltered, and high, as much as 3,000 L/M, where fault zones and intense fracturing has occurred.

Black Mesa. Local aquifers in the vicinity of the Black Mesa Basin occur primarily in unconsolidated alluvium along major streams that drain the area while lesser amounts can be found along the southern margin in diatremes, flows, and tuff beds of the Hopi Buttes and, in eolian deposits throughout (Cooley and others, 1969). Ground water is also found in the Bidahochi Formation which occurs quite extensively, if somewhat discontinuously, in the east-central part of northeastern Arizona. The Bidahochi Formation is only partly saturated under water-table conditions throughout its extent. In some places, the Bidahochi aquifer includes a sequence of underlying beds of sandstones from the Wepo and Toreva Formation where they have not been removed by erosion (Mann, 1977; Farrar, 1980). Ground water in the Bidahochi aquifer, and the rest of the local aquifers as well, are hydraulically separated from the multi-aquifers below by the intervening, poorly permeable Mancos Shale. Ground water in these units flows to discharge points along the Puerco and Zuni Rivers or into alluvium where most is lost to evapotranspiration.

Regionally, the main aquifers in this subprovince are the D and N multi-aquifers. The D multi-aquifer is composed of Jurassic and Cretaceous sediments in the extreme northeast corner of the state and in the Black Mesa Basin. The principal water-bearing units are the Dakota Sandstone, Morrison Formation, Cow Springs Sandstone, Bluff Sandstone, Summerville Formation, and Entrada Formation (Table 1). The aquifer has a maximum saturated thickness of about 360 m in the east and northeast that gradually wedges out along the southern margin. To the south-central part of the subprovince, the Summerville Formation and/or Bluff Sandstone may occasionally be absent and to the west, the Morrison Formation is missing. All the units are hydraulically connected, and the D multi-aquifer is under artesian pressure everywhere within the Black Mesa Basin except at the northeast, east, and extreme south margins where the Mancos Shale (the upper confining layer) is not present. Artesian pressure is great enough, especially in the south-central part of Black Mesa, to raise water levels in wells that penetrate the D multi-aquifer several hundred meters; along Polacca Wash, wells flow at the surface (Levings and Farrar, 1977a, b, c, d). In the northeastern corner of the state, the D multi-aquifer is under water-table conditions. The Mancos Shale above, and siltstones in the Entrada Sandstone and the Carmel Formation below represent confining layers that restrict vertical movement of

ground water. Because the Mancos shale acts as an aquiclude and the D multi-aquifer is under substantial pressure head, a downward-component of flow exists that produces some leakage through the Carmel Formation into the N multi-aquifer below (Eychaner, 1981, p. 18). The general direction of ground-water flow is from recharge areas in the north and northeast margins to the west, southwest, and southeast (Levings and Farrar, 1977a, b, c, d) where it is generally lost to evapotranspiration as it is discharged into alluvium and as springs along minor stream beds.

Aquifer characteristics of the D and M multi-aquifers are presented by Cooley and others (1969) as determined from hydrologic laboratory and pump tests. For sandstones in the D multi-aquifer, porosity is around 25%. Hydraulic conductivity and transmissivity vary considerably from unit to unit. Individual well yields are low, less than 90 L/M, and depend on the saturated thickness of the aquifer.

The N multi-aquifer is made up of the Navajo Sandstone, Kayenta Formation, Moenave Formation, and the Lukachukai member of the Wingate Sandstone. The Owl Rock member of the Wingate Sandstone is present only in the southeast part of the Black Mesa Basin. The aquifer underlies all of the Black Mesa subprovince as well as most of the areas to the north and east, and thins to extinction at the south and southeast margin of Black Mesa (Levings and Farrar, 1977a, b, c, d; Farrar, 1979, 1980). All units are hydraulically connected, but most of the water is derived from the Navajo Sandstone. The aquifer is under confined conditions everywhere except at its margins where erosion has stripped away the confining layers. In those areas, mostly under water-table conditions, intertonguing of the Navajo Sandstone with confining siltstone beds in the Kayenta Formation will cause great artesian pressure locally. Some wells near Tuba City drilled in these conditions flow at land surface. In the central part of the subprovince, the N multi-aquifer has a maximum saturated thickness of about 365 m and is overlaid by more than 900 m of additional sediments (Levings and Farrar, 1977a, b). The main water-bearing units thin to about 100 m in the south and southeast and gradually wedge out as they move out of the area. A ground-water divide is located west to northeast between Cedar Hills and White Mesa in the northwestern part of the subprovince (Farrar, 1979) in unconfined conditions. Ground-water movement is generally away from this divide to the northwest, where a large section of Navajo sandstone is dry owing to extensive structural deformation, and to the south toward discharge points along Moenkopi Wash. Elsewhere the aquifer is confined, and water moves away from areas of high artesian pressure in the central part of basin to discharge points in alluvium along Moenkopi and Dinnebito Wash and to the northeast toward Chinle Creek.

Eychaner (1981) indicates that the N multi-aquifer has an overall estimated hydraulic conductivity of .2m/d and estimated transmissivity of 65 m²/d. But, there appears to be no clear regional trend, since values for transmissivity and hydraulic conductivity differ greatly over short distances. Some downward flow occurs from the D multi-aquifer as discussed earlier, but the amounts of leakage is small. Confining beds in the Chinle and Moenkopi Formations that underlie the N multi-aquifer effectively separate it from the C multi-aquifer below. However, some downward movement may occur in the northwest where the Navajo Sandstone is heavily faulted, fractured, and dry. Well yields vary considerably from less than 18 L/M to as high as 1900 L/M

and are dependent on the saturated thickness of the aquifer. Average yields are about 150 L/M but are considerably less all around the subprovince margin (Levings and Farrar, 1977a, b, c, d; Farrar, 1979).

The C multi-aquifer consists of the Shinarump member of the Chinle Formation, Moenkopi Formation, Kaibab Limestone, Coconino Sandstone, and its lateral equal, the DeChelly Sandstone, the Organ Rock tongue of the Cutler Formation, and upper beds of the Supai Formation (Levings and Farrar, 1977a, b, c, d; Farrar, 1979, 1980; Mann, 1977). Only the Moenkopi Formation, Coconino Sandstone with its lateral equivalent, the DeChelly Sandstone, and the Supai Formation are likely to exist continuously throughout the subprovince. The principal water-bearing units are the Coconino Sandstone and Supai Formation although all the units are hydraulically connected. The Chinle and Moenkopi Formations, Kaibab Limestone and the Organ Rock member of the Cutler Formation occur as members of the aquifer primarily at the margins where they wedge out rapidly inward or are eroded away. In the central part of the Black Mesa Basin, the C multi-aquifer is at considerable depth, approximately 1450 m below land surface (Levings and Farrar, 1977), and little is known of its occurrence or movement. The aquifer is exposed to recharge along the Defiance Plateau to the east, and the depth of burial increases rapidly to the west where the aquifer eventually becomes confined in the vicinity of Chinle as well as to the west, north, and throughout most of the margin areas south and southwest of the Puerco River. Ground water moves from areas of recharge to the north, west, and southwest, and, to the east out of the study area. Along the south margins, the Kaibab Limestone is frequently encountered as an upper member of the aquifer (Mann, 1977; Farrar, 1980; Appel and Bills, 1981). Confining conditions still exists except to the west along the Little Colorado River where confining beds and evaporites of the Moenkopi have been eroded away. Ground water here begins to move in a more west-to-northwest direction. Along the western margin, the C multi-aquifer, as verified by test holes, is mostly dry. Only the Chinle Formation is partly to fully saturated and yields small amounts of water to wells (Farrar, 1979). The Coconino Sandstone is encountered by wells but does not yield water. Much deformation that occurs in this area may have created sufficient secondary permeabilities in the Coconino Sandstone for it to drain into the underlying Early to Middle Paleozoic Limestones which are known to bear large amounts of water (Cooley, 1976; Appel and Bills, 1981). Aquifer characteristics are poorly understood mainly because of a lack of sufficient well data in this subprovince. Well yields are generally low, 50 to 500 L/M, and depend on saturated thickness as well as the occurrence and degree of secondary permeability.

South-Central Colorado Plateau. Local aquifers in this subprovince follow a pattern of occurrence similar to those found in the San Francisco Volcanic Field as the result of a similar volcanic environment. In addition, from about Showlow southeast to Springerville, alluvium, rim gravels, and basalts combine with undifferentiated sediments of the upper Cretaceous underlain by poorly permeable shale beds to form the locally extensive Pinetop-Lakeside aquifer (Mann, 1976). Ground water in this unit is under water-table conditions and hydraulically separate from the underlying C multi-aquifer, in some cases by as much as 45 m. The movement of water is northward, paralleling the regional dip until it reaches discharge points along

minor streams or infiltrates downward. Other locally important sources of ground water occur in alluvium along many of the stream beds. These waters are also unconfined and generally perched, receiving their recharge from stream flow. However, near Holbrook and Joseph City, it is more likely that most of the recharge is the result of leakage upward from the C multi-aquifer which in this area is very near the surface and under confining conditions (Mann, 1976).

The C multi-aquifer consists of Kaibab Limestone, Coconino Sandstone, and the upper member of the Supai Formation (Harper and Henderson, 1976; Mann, 1976). Ground water is unconfined in the south and west near areas of recharge but is confined in the north and eastern parts of the area. Less permeable beds in the Moenkopi Formation form the confining layer that lies on top of the aquifer. All of the units are hydraulically connected and generally saturated except to the south and west where they are only partly saturated. In structural highs, along the crest of the Holbrook anticline and near Heber, the Coconino Sandstone is dry, and water is not encountered until the upper beds of the Supai are tapped (Mann, 1976). Water moves from recharge areas along the Mogollon Rim northward to discharge points in springs in the Little Colorado River Valley and its tributaries or continues northward out of the area as underflow (Mann, 1976). Well yields vary considerably from less than 10 L/M to greater than 10,000 L/M. Yields depend on the saturated thickness and amount of fracturing the aquifer has encountered, but the highest yields are the result of artesian pressure (Mann, 1976; Harper and Anderson, 1976).

Early to Middle Paleozoic limestones are encountered in deep oil-test wells in all three subprovinces, and in all cases water is encountered also. The actual occurrence and movement of water in these units is not well understood except between the margins of the Black Mesa and San Francisco Volcanic Field subprovinces and at the southern extent of the San Francisco Volcanic Field. In both these areas, the limestone aquifer is composed mainly of the Redwall Limestone and Martin Formation. Less frequently encountered is the Mauv Formation (Levings and Mann, 1980; Appel and Bills, 1981). The aquifer in these areas is entirely saturated and under water-table conditions. To the south, water moves down gradient to discharge into sediments of the Verde Formation and directly into the Verde River. To the north in the vicinity of Cameron, water is drained from all areas of the C multi-aquifer through faults and fractures into the limestone aquifer and continues to move northwest toward discharge as springs in the Little Colorado River (Cooley and others, 1969; Cooley, 1976). These springs maintain a perennial flow of about 7.5 m³/s at the mouth. The aquifer where tapped by wells is very productive, yields in excess of 10,000 L/M are not uncommon, indicating that it transmits water readily in association with high amounts of secondary permeability.

The lowermost extent of ground-water occurrence is represented by a basal confining layer that is composed of Precambrian sediments, igneous, and metamorphic rock underlying the entire study area. Water does occur in these units where they have been heavily fractured and faulted. Some springs of the Grand Canyon are known to produce small amounts of water from these units (Johnson and Sanderson, 1968). However, few data exist elsewhere on the Colorado Plateau of northeastern Arizona to aid in defining the occurrence and movement of water in these units.

TEMPERATURE DATA

Temperature data for each well are presented, both as graphs and tables, in Appendices A, B, and C corresponding to our three sub-provinces. In this section, we look at the data in the same three groups.

San Francisco Volcanic Field. For this subprovince, information on location and elevation of the wells is presented in Table 3. The profiles (Figure 2), appear to be mostly conductive with evidence for localized water movement in GRAY, WOM, and LM01. The lowermost ~200 m of BMPS within the Supai Formation (Table 4) appears to be dominated by a slow downward water movement. Not shown in Figure 2 is the profile for SMT7 (Figure A-8) which was only accessible to 104 m in cinders and Tertiary basalt. This is the only well for which there was a substantial gradient (albeit poorly controlled, Figure A-8). The low conductivities of the unsaturated rocks of the San Francisco volcanic field are probably primarily responsible for this relatively high gradient. Over the remainder of the volcanic field, gradients range from virtually 0 in WOT to just over $13^{\circ}\text{C km}^{-1}$ in the Kaibab limestone and Coconino sandstone in RBDX (Figure 2 and Table 4). The quartz-rich Permian rocks penetrated by most of the wells in this sub-province are characterized by very high thermal conductivity (Bodell and Chapman, 1982; see also discussions of conductivity and heat-flow low). Nevertheless, the gradients are anomalously low for a region that has experienced vigorous tectonic activity throughout most of the Cenozoic era.

Black Mesa. Temperature data were obtained from eight wells within the Black Mesa subprovince (Figure 3, Tables 5 and 6). Once again, there is evidence for localized water flow in most wells; however, with the exception of TSEG and KAY, there are conductive segments from which gradient information can be obtained. Although well KAY has not been pumped for several years, it is situated within the Kayenta municipal well field which is heavily exploited. Temperatures in this well (see also Figure B-5) suggest downward water movement into the Navajo or N multi-aquifer, which is presently the most extensively exploited water source in the area (Eychaner, 1981). Downward vertical flow within the Navajo sandstone also is indicated in BMSA, TSEG, and PIN1 (Figure 3; Table 6). Conductive temperature gradients for Black Mesa generally are higher than those found beneath the San Francisco volcanic field (cf. Tables 4 and 6).

South-central Colorado Plateau. Temperature data were obtained from nine wells situated (with the exception of CVL, Figure 1) north of the White Mountain volcanic field (Figure 4, Tables 7 and 8). The inclusion of CVL in this group is quite arbitrary and is mainly for convenience in displaying the data. This well could just as easily have been included in the group from the San Francisco volcanic field. Thus, when generalizing for this province, we feel justified in excluding CVL where these data have a significant impact on our conclusions.

The profiles from this subprovince tend to have a convex upward curvature indicating either upward water movement or systematically increasing thermal conductivity with depth. As in the previous case, gradients generally are higher than those beneath the San Francisco volcanic field (cf. Tables 4 and 8).

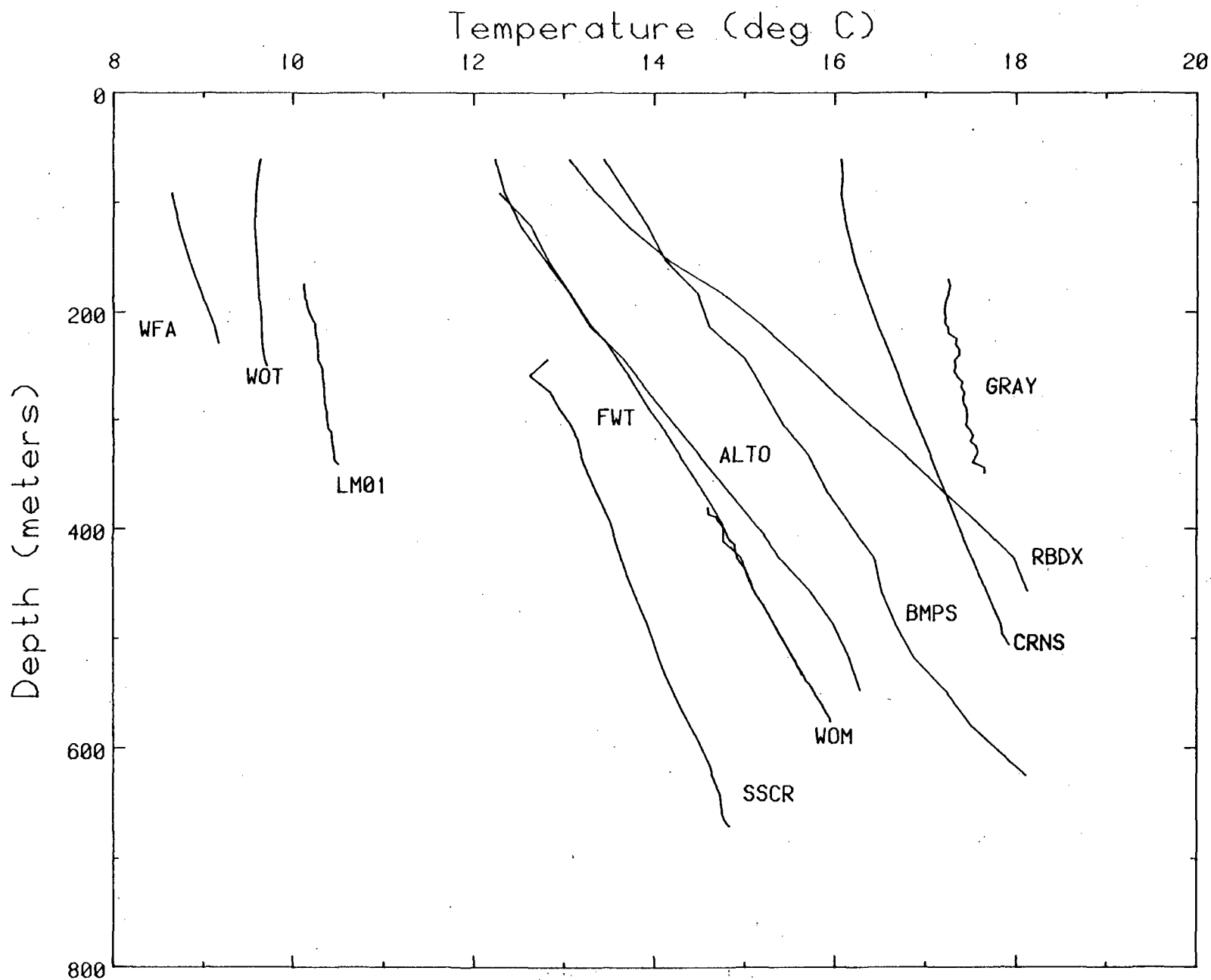


Figure 2. Temperature profiles, San Francisco Volcanic Field (see Figure 1).

TABLE 3. Location information for temperature profiles shown in Figure 2

Abbreviated designation	USGS/WRD designation	N. Lat.	W. Long.	Elev. (m)	Nearest feature or locality or well name
ALTO	(A-21-09) 17 ACC	35° 12' 13"	111° 27' 40"	1963	Alto
BMPS	(A-25-02) 27 ABA	35° 31' 34"	112° 09' 49"	1879	Black Mesa pipeline Pumping Station #3
CRNS	(A-25-09) 06 CCD	35° 34' 12"	111° 28' 46"	1640	Citadel Ruins
FWT	(A-19-10) 24 CDB	35° 00' 35"	111° 17' 24"	1953	Flo Walt #1
GRAY	(A-28-9) 31 CCC	35° 45' 50"	111° 29' 40"	1501	Gray Mountain
LM01	(A-20-08) 18 BBB	35° 07' 16"	111° 35' 44"	2085	Lake Mary #1
RBDX	(A-26-02) 11 AAD	35° 39' 14"	112° 08' 21"	1826	Robidoux Airport
SMT7	(A-23-06) 26 CCD (2)	35° 20' 28"	111° 43' 58"	2588	Summit Property #7
SSCR	(A-23-08) 21 AAD	35° 22' 07"	111° 34' 37"	2124	Sunset Crater
WFA	(A-17-09) 11 BDD	34° 52' 12"	111° 24' 42"	2329	Wifeda #1
WOM	(A-19-10) 24 BDD	35° 00' 58"	111° 17' 18"	1949	Western Oil and Minerals #1
WOT	(A-19-07) 01 DDD	35° 03' 07"	111° 35' 55"	2187	Winfed Oil #1

TABLE 4. Temperature gradient, elevation, and summary lithology
San Francisco Volcanic Field

Well	Depth range logged (m)	Interval (m)	Formation	Gradient ± SE (°C/km)	Elev. (m)	Surface intercept (°C)
ALTO	61-547	61-98	Kaibab ls	NC*	1963	11.3
		98-327	Coconino ss	9.3±0.2		
		327-488	Supai	11.32±0.01		
		488-547	?	NC		
BMPS	61-625	61-180	Kaibab ls	8.3±0.5	1879	12.9
		180-244	Toroweap	8.6±2.6		
		244-415	Coconino ss	7.8±0.2		
		415-625	Supai	NC		
CRNS	61-506	61-152	Kaibab/coc.	NC	1640	15.4
		152-389	Coconino ss	4.8±0.1		
		389-506	Supai	5.2±0.1		
FWT	30-533	122-396	Kaibab ls(?)	7.9±0.1	1953	11.6
		427-533	Coconino ss(?)	6.5±0.2		
GRAY	30-350	30-250	Kaibab/coc.	NC	1501	16.7
		250-320	Coconino ss	2.7±0.3		
		320-350	Supai	4.5±1.5		
LM01	30-341	37-174	Kaibab/coc.	NC	2085	9.8
		174-331	Coconino ss	2.06±0.04		
		331-341	Coc/supai	NC		
RBDX	61-457	61-201	?	NC	1826	12.4
		201-347	Kaibab ls	13.3±0.1		
		347-402	Coconino ss	13.1±0.1		
		402-457	Supai	NC		
SMT7	61-104	61-104	SF volcs.	31±4	2588	2.9
SSCR	61-670	61-274	Volc./kaibab	NC	2124	11.6
		274-305	Kaibab ls	7.5±0.7		
		305-588	Coconino ss	4.7±0.04		
		588-670	Supai	NC		
WFA	91-229	91-219	SF volcs.	3.9±0.1	2329	8.3
		219-229	Kaibab ls	NC		
WOM	381-576	381-457	Supai	NC	1949	11.9
		457-576	Supai	7.09±0.02		
WOT	30-250	30-122	Kaibab ls	NC	2187	9.5
		128-250	Coconino ss	0.8±0.05		

*Not calculated owing to insufficient data points, near-surface microclimatic disturbance, or vertical water movement.

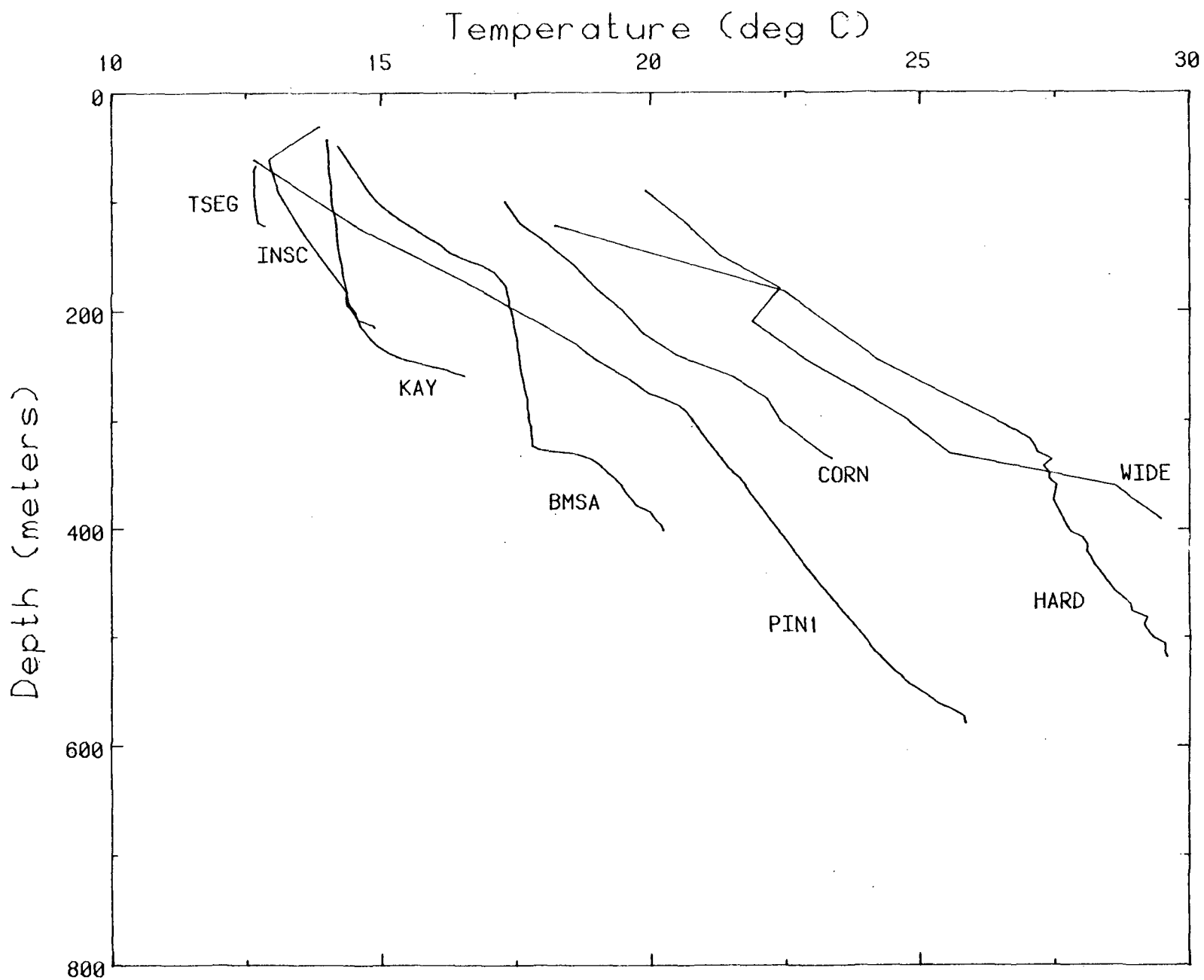


Figure 3. Temperature profiles, Black Mesa region (see Figure 1).

TABLE 5. Location information for temperature profiles shown in Figure 3

Abbreviated designation	Navajo well number	N. Lat.	W. Long.	Elev. (m)	Nearest feature or locality or well name
BMSA	8T-538	36° 38' 50"	110° 10' 08"	1723	WRD BMO #2
CORN	17T-501	35° 39' 40"	109° 36' 40"	1924	Cornfield
HARD	4T-525	36° 02' 35"	110° 31' 35"	1823	Hard Rocks
INSC	2T-517	36° 36' 10"	110° 48' 50"	1963	Inscription House
KAY	8T-500	36° 43' 38"	110° 15' 46"	1749	WRD BMO #3
PIN1	4T-522	36° 05' 29"	110° 12' 27"	1930	Pinon
TSEG	2T-514	36° 31' 43"	110° 35' 50"	1935	WRD BMO #4
WIDE	17T-553	35° 23' 57"	109° 31' 33"	1861	Wide Ruins

TABLE 6. Temperature gradient, elevation, and summary lithology
Black Mesa, Colorado Plateau

Well	Depth range logged (m)	Interval (m)	Formation	Gradient \pm SE ($^{\circ}\text{C}/\text{km}$)	Elev. (m)	Surface intercept ($^{\circ}\text{C}$)
BMSA	50-400	50-81	Entrada	13.9 \pm 0.1	1723	13.5
		81-104	Carmel	14.3 \pm 0.3		
		104-119	Carmel	31.0 \pm 0.5		
		119-329	Navajo ss	NC*		
		329-386	Kayenta	18.8 \pm 0.8		
		386-400	Wingate	14.3 \pm 1.0		
CORN	20-335	100-335	Chinle	26.9 \pm 0.8	1924	14.3
HARD	185-520	185-229	Mancos sh	28.2	1823	14.6
		229-317	Dakota/Morrison	39.2 \pm 0.6		
		317-351	Dakota/Morrison	9.7 \pm 2.8		
		351-442	Entrada ss	11.8 \pm 0.7		
		442-466	Navajo ss	19.7 \pm 1.5		
		466-520	Kayenta	14.3 \pm 1.5		
INSC	60-215	91-183	Navajo ss	14.4 \pm 0.2	1963	11.8
KAY	35-260	35-60	Entrada	NC		
		60-98	Carmel	NC		
		98-260	Navajo ss	NC		
PIN1	60-580	60-76	Torera	NC	1930	10.4
		76-235	Mancos sh	35.6 \pm 0.9		
		235-280	Dakota/Morrison	33.1 \pm 1.0		
		280-366	Dakota/Morrison	17.0 \pm 0.5		
		366-442	Entrada	15.2 \pm 0.1		
		442-466	Carmel	16.8 \pm 0.2		
		466-580	Navajo ss	NC		
TSEG	67-122	67-122	Navajo ss	NC	1935	12.5
WIDE	30-390	210-314	Chinle	31.4 \pm 0.9	1861	
		314-357	DeChelly ss	NC		
		357-390	Supai	NC		

*Not calculated owing to insufficient data points, near-surface microclimatic disturbance, or vertical water movement

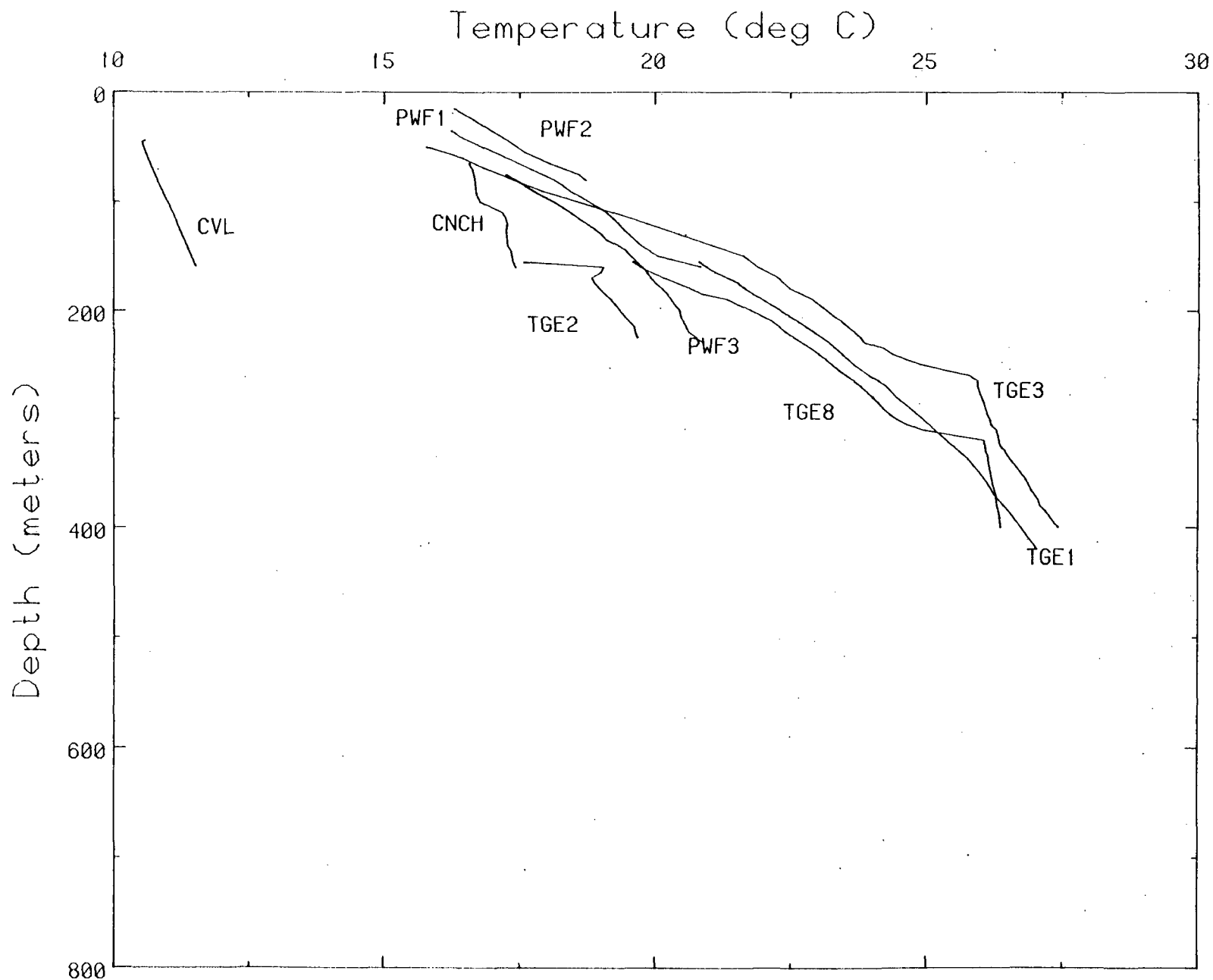


Figure 4. Temperature profiles for the south-central Colorado Plateau (see Figure 1).

TABLE 7. Location information for temperature profiles shown in Figure 4

Abbreviated designation	USGS/WRD designation	N. Lat.	W. Long.	Elev. (m)	Nearest feature or locality or well name
CNCH	(A-13-25) 24 CAD	34° 30' 33"	109° 39' 00"	1771	Concho C-24-1000
CVL		34° 32' 24"	110° 55' 35"	2145	Chevelon
PWF1	(A-13-29) 5 ABD	34° 34' 05"	109° 17' 15"	1777	St. Johns P-5 ob
PWF2	(A-13-28) 3 ABB	34° 34' 10"	109° 21' 30"	1723	St. Johns P-3 ob
PWF3	(A-13-29) 6 ACC	34° 33' 53"	109° 18' 16"	1787	St. Johns P-6 ob
TGE1	(A-11-29) 28 DAA	34° 19' 18"	109° 16' 36"	1989	Lyman Lake
TGE2	(A-11-29) 23 ABA	34° 20' 37"	109° 14' 16"	2039	Lyman Lake
TGE3	(A-11-29) 34 CDC	34° 18' 01"	109° 23' 25"	2023	Lyman Lake
TGE8	(A-11-29) 20 BAA	34° 20' 26"	109° 17' 40"	1988	Lyman Lake

TABLE 8. Temperature gradient, elevation, and summary lithology
South-central Colorado Plateau

Well	Depth range logged (m)	Interval (m)	Formation	Gradient ± SE (°C/km)	Elev. (m)	Surface intercept (°C)
CNCH	45-160	55-79	Moenkopi	10.0±0.7	1771	15.9
		79-107	Kaibab ls			
		107-158	Coconino			
		158-160	Supai			
CVL	46-167	46-167	Coconino ss	8.91±0.02	2145	10.1
PWF1	35-160	35-85	Chinle	42.6±0.5	1777	14.7
		85-152	Chinle	NC*		
		152-160	Moenkopi	NC		
PWF2	15-85	15-58	Chinle	32.8±0.6	1723	15.8
		58-73	Moenkopi	50±3		
		73-85	Kaibab	24		
PWF3	65-230	75-145	Chinle	31.2±0.5	1787	15.0
		145-200	Chinle	18.3±0.3		
		200-230	Chinle-Moenkopi	NC		
TGE1	5-420	5-12	Q-T	NC	1989	14.4
		100-150	Chinle-Moenkopi	55±1		
		150-244	Chinle-Moenkopi	31.7±0.4		
		244-350	Kaibab ls	23.4±0.4		
		350-420	Coconino ss	15.3±0.1		
TGE2	20-225	20-67	Chinle-Moenkopi	NC	2039	13.5
		67-171	Kaibab ls	NC		
		171-225	Coconino ss	17.6±0.3		
TGE3	10-400	50-150	Chinle-Moenkopi	58.6±0.8	2022	12.8
		150-226	Chinle-Moenkopi	29.3±0.7		
		226-343	Kaibab ls	NC		
		343-400	Coconino ss	13.9±0.2		
TGE8	10-400	10-116	Q-T	NC	1988	16.1
		116-293	Chinle-Moenkopi	NC		
		293-400	Kaibab ls	NC		

*Not calculated owing to insufficient data points, near-surface microclimatic disturbance, or vertical water movement.

VARIATION OF EXTRAPOLATED SURFACE TEMPERATURE WITH ELEVATION

One measure of the internal consistency of a group of temperature data is the extent to which the extrapolated surface temperature correlates with elevation. In an homogeneous isotropic medium, there should be a negative correlation with elevation on the order of a few degrees per kilometer. Factors which can influence this relation include lateral variations in albedo, heat flow, thermal conductivity, and depth of surface cover. In steep terrains, there are also azimuthal variations in surface temperatures, south-facing slopes being significantly warmer than those facing north. When plotting results from as large an area as the present one, it should not, therefore, be surprising to find some scatter in the data.

For the San Francisco volcanic field (Figure 5), the correlation between surface temperature and elevation is excellent with a coefficient of correlation of 0.97 and a lapse rate of $11.6^{\circ}\text{C}/\text{km}$ (Table 9). The scatter for the other sub-provinces is much greater (Figure 5), perhaps reflecting a greater heterogeneity in near-surface conditions. The correlation is particularly poor for Black Mesa with a coefficient of only 0.47 (Table 9). The lapse rates for Black Mesa and the South-central sub-province are somewhat lower but not significantly so (on the basis of a two-sample T-test) than that for the San Francisco volcanic field. We thus adopt the lapse rate of $11.9^{\circ}\text{C}/\text{km}$ obtained by performing a linear regression analysis on data from the entire area (Table 9) as being representative of northeastern Arizona. This value is considerably higher than those previously published. Compared with values of $4.5^{\circ}\text{C}/\text{km}$ for the Rocky Mountains (Birch, 1950), 4.7 for the Alps (Clark and Niblett, 1956), 6.6 for the Snowy Mountains of Australia (Sass and others, 1967) and $6.9^{\circ}\text{C}/\text{km}$ for the North-central Colorado Plateau (Bodell and Chapman, 1982), this represents a distinctly anomalous situation. Bills and Sass (1982) suggested that the high lapse rate for the San Francisco volcanic field might be related in some way to the regional hydrology, but it is difficult to extend this reasoning to the other two subprovinces.

TABLE 9. Parameters of the linear regression of surface temperature on elevation, ($\theta = \theta_0 - \Gamma h$), northeastern Arizona

Region	Coefficient of correlation	θ_0 (°C)	Γ (°C/km)
San Francisco Volcanic Field	0.97	34.5	11.6
Black Mesa	0.47	31.4	9.7
South-central Colorado Plateau	0.76	32.5	9.5
Entire study area	0.87	35.8	11.9

THERMAL CONDUCTIVITY

As noted in the introduction, we had no cores or drill cuttings from the great majority of wells studied. We are, however, dealing with a region within which some formations are laterally homogeneous over distances of 100 km or more, and we feel that it is a legitimate exercise to examine our data and compare them with recently published values from other parts of the plateau, then to generalize some values of conductivity (with appropriate limits of uncertainty) from which to make some crude estimates of heat flow.

Bodell and Chapman (1982) have compiled a fairly complete catalog of thermal conductivities for the stratigraphic column of the north-central Colorado Plateau. Not surprisingly, they found that while some formations (most notably the "clean" sandstones) could be characterized adequately by a few determinations of thermal conductivity, there were others (e.g., the Jurassic Carmel formation) that are very heterogeneous and for which detailed and accurate lithologic information (of higher quality than that usually associated with mud logs or summary lithologic logs) is required to specify the thermal conductivity at a given locality.

A comparison of our Table 1 with that of Bodell and Chapman (1982) shows that we are dealing with many of the same formations (although not necessarily the same mineralogic compositions) in our study area. The Coconino sandstone (Table 10) provided the only basis for comparison and our measurements at two sites are in reasonable agreement with those of Bodell and Chapman. Based on this agreement and the similarity of lithologic descriptions for many other formations, we generalized some values for the various formations encountered in our wells (Table 11). In compiling this table, we assigned a larger (percentage) uncertainty to the more heterogeneous formations.

Apart from mineralogical composition, the greatest source of uncertainty is porosity which varies significantly in otherwise homogeneous formations like the Navajo, Wingate, or Coconino sandstones (note the large standard deviations for the porosity measurements listed in Table 10). Most of our own conductivity measurements (Table 10) and those of Reiter and Shearer (1979) and Shearer and Reiter (1981) were made on fragments so that porosity corrections are necessary to specify the formation conductivity.

To illustrate the sensitivity of formation conductivity to porosity and to provide a means of making a quick estimate for a given grain conductivity-porosity data pair, we have constructed a graph of thermal grain conductivity of water-saturated rock as a function of porosity for a wide range of values of grain conductivity (Figure 6). The calculated formation conductivity (K_f) is simply the geometric mean of the grain conductivity (K_s) and the conductivity of water (K_w) weighted according to the fractional porosity (ϕ). That is,

$$K_f = K_s^{(1-\phi)} K_w^\phi$$

(see for example Woodside and Messmer, 1961, Sass and others, 1971a). As we might expect, the sensitivity of formation conductivity to porosity increases as grain conductivity increases.

TABLE 10. Miscellaneous thermal conductivity and porosity data from the Colorado Plateau
(See Tables 1 and 2 for description and stratigraphy)

Locality	Formation	Lithology	N	Thermal Conductivity					
				$W m^{-1} K^{-1}$					
				chip	sd	solid cylinder	sd	ϕ %	sd
NCCP*	Dakota Ss	Ss	1			4.87		11.4	
	Morrison	Ls	1			2.72		0.5	
	Entrada	sltst-Ss	19			3.43	0.67	6.4	2.4
		sltst	10			2.92	0.43	5.0	1.0
	Carmel	ss	9			3.85	0.61	8.5	4.0
		Gypsum-Ls	17			2.75	0.58	2.9	2.7
		mdst	6			2.50	0.38	2.7	1.7
		sltst-Ss	7			3.12	0.50	4.4	3.2
	Navajo	Ls	3			2.85	0.09	3.7	0.4
		Silty ss-ss	14			4.20	0.54	12.5	3.4
		Silty ss	5			3.59	0.30	12.9	5.1
	Kayenta	Ss	9			4.53	0.29	12.2	5.3
		Silty ss-ss	14			4.20	0.54	12.5	3.4
		Silty ss	5			3.59	0.30	12.9	5.1
	Wingate	Ss	9			4.53	0.29	12.2	2.3
		Ss	17			3.86	0.37	14.1	4.8
	Chinle	sltst-Cong.	8			4.11	1.30	6.6	3.9
		sltst	2			3.30	0.21	2.4	0.7
		Ss	3			3.97	0.51	10.5	5.8
		V. coarse ss	2			5.96	0.41	7.3	0.4
Moenkopi	Mdst	1			3.02		4.4		
SCCP* (TGE)	Kaibab	Ls	7	3.48	0.63				
NCCP	Coconino	ss	5			5.01	0.36	16.2	1.5
SCCP (CVL)		ss	4			4.52	0.32	17.7	1.2
SCCP (CVL)		ss	13	6.70	0.68				
SCCP (TGE)		ss	6	5.72	0.64				

*NCCP, North-central Colorado Plateau, data from Table 2 of Bode11 and Chapman, 1982.

SCCP, South-central Colorado Plateau, symbols in parentheses denote locations of samples (Figure 1).

TABLE 11. Generalized thermal conductivities
used in heat-flow estimates on Tables 12 through 14

Formation	Conductivity $W m^{-1} K^{-1}$	Uncertainty
Dakota	4.5	0.5
Morrison	2.7	0.7
Entrada	3.5	0.5
Carmel	2.75	0.5
Navajo	4.5	0.5
Kayenta	4.0	0.5
Wingate	4.0	0.5
Chinle	3.5	0.5
Moenkopi	3.0	1.0
Kaibab	3.5	0.5
Coconino	4.5	0.5
Supai	3.5	0.5

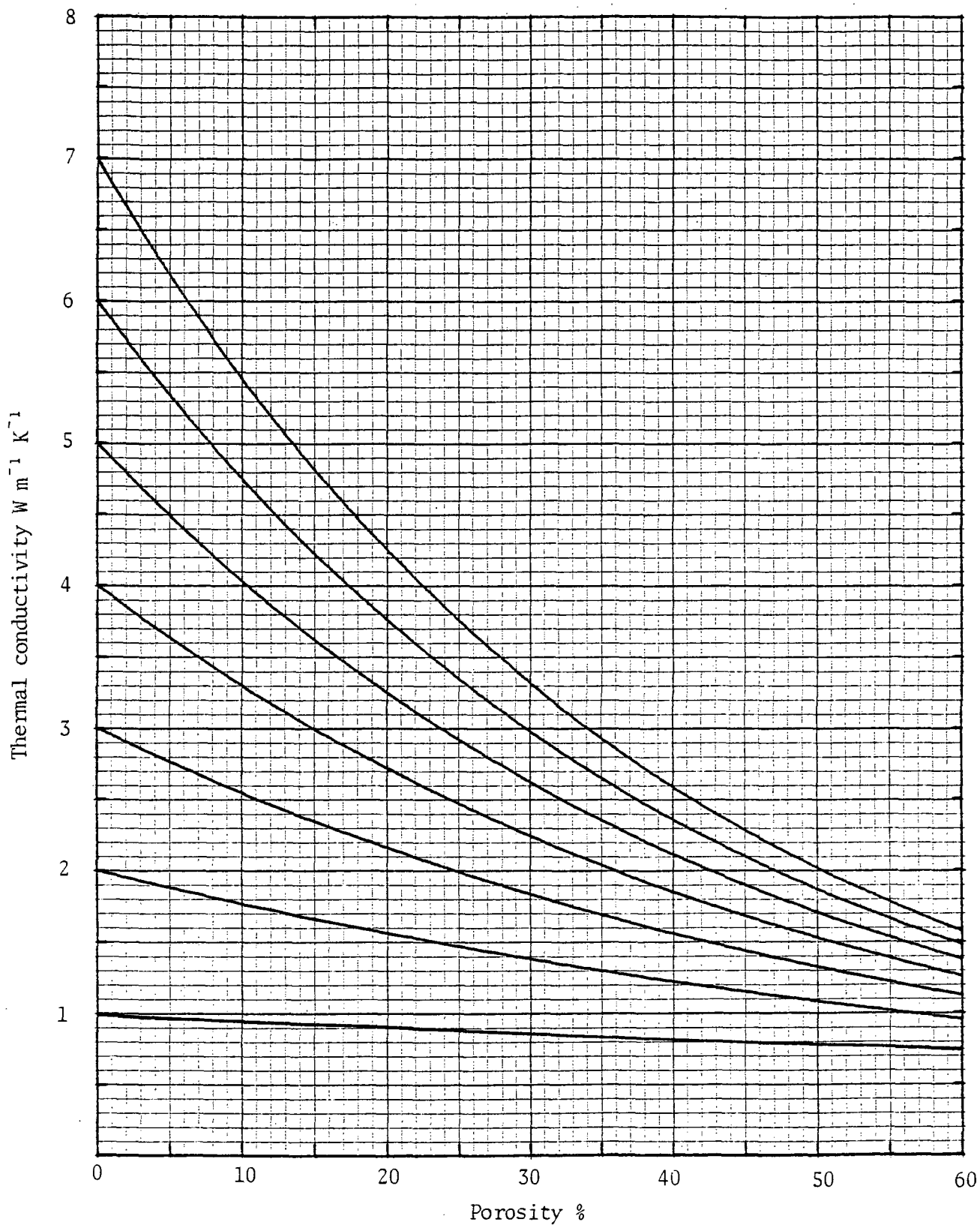


Figure 6. Thermal conductivity as a function of porosity for water-saturated rocks (thermal conductivity of water, $0.58 W m^{-1} K^{-1}$). Thermal conductivity of solid component is intercept for 0 porosity.

HEAT-FLOW ESTIMATES

Based on the gradients from Tables 4, 6, and 8 and the generalized thermal conductivities in Table 11, we have estimated heat flows for the three sub-provinces in Tables 12, 13, and 14. Unfortunately, there were some linear segments of temperature profiles for which we were unable to make even the most rudimentary estimates of heat flow. For example, we had substantial intervals penetrating the Mancos Shale in HARD and PIN1 (Figure 1 and Table 6) where the gradients are well established but where we have no conductivity information at all. In the same wells, the lithologic descriptions did not distinguish between the Dakota sandstone and Morrison formation which have greatly different thermal conductivities (Tables 10 and 11). We calculated vastly different gradients within different sections of the undifferentiated Dakota/Morrison in these wells (Table 6). The only way to reconcile this gradient contrast is for the Morrison Formation to overlie the Dakota sandstone, a reversal of the normal stratigraphic section (Tables 1 and 2).

The above difficulties notwithstanding, we were able to obtain at least one estimate of heat flow from most of the wells, the exceptions being KAY and TSEG, Black Mesa, and CNCH and TGE8, South-central. For these wells, it was simply impossible to extract a gradient that could be ascribed plausibly to one-dimensional vertical heat conduction.

San Francisco Volcanic Field. The heat-flow estimates (Table 12; Figure 7) reflect the low gradients. Where more than one formation is involved in the heat-flow estimate, it is also gratifying that, in most instances, component heat flows are in reasonable agreement, since the gradient determinations and generalized conductivity estimates were truly independent. Geographically (Figure 7) there is little systematic variation of heat flow except for the area directly south of Flagstaff, where heat flow is consistently less than 10 mWm^{-2} .

Black Mesa. As expected from the gradients, heat-flow estimates for Black Mesa are higher than for the San Francisco field. The present values are within the range published by Reiter and Shearer (1979) (Figure 7) and by Reiter and others (1975) for neighboring northwestern New Mexico. Bodell and Chapman (1982) include Black Mesa within their "cooler interior" region (heat flow $\leq 65 \text{ mWm}^{-2}$). Our heat-flow estimates are somewhat lower than those of Reiter and Shearer (1979) and with the exception of CORN and WIDE (Table 13; Figure 7) are less than (or equal to) 65 mWm^{-2} . A minor adjustment to the 65 mWm^{-2} contour of Bodell and Chapman would certainly accommodate these data.

South-Central Colorado Plateau. Our value of $39 \pm 1 \text{ mWm}^{-2}$ for CVL is actually a first-rate determination of heat flow providing confirmation of the low regional conductive flux within and around the San Francisco volcanic field. The remainder of the sites are north of the White Mountain volcanic field (Figure 7). The PWF series (Table 14) yields a mean heat flow in excess of 100 mWm^{-2} , consistent with two values to the North published by Reiter and Shearer (1979) (Figure 7) and two values to the east in New Mexico by Reiter and others (1975). The TGE series (Figure 7, Table 14)

TABLE 12. Heat-flow estimates, San Francisco Volcanic Field

Well	Formation	Heat flow mWm ⁻²
ALTO	Coconino	42±6
	Supai	40±6
	mean	41
BMPS	Kaibab	29±6
	Coconino	35±5
	mean	32
CRNS	Coconino	22±3
	Supai	18±3
	mean	20
FWT	Kaibab	28±4
	Coconino	29±4
	mean	28
GRAY	Coconino	12±3
	Supai	16±7
	mean	14
LM01	Coconino	9±1
RBDX	Kaibab	47±10
	Coconino	59±7
	mean	53
SMT7	SF Volcanics	51±16
SSCR	Kaibab	26±6
	Coconino	21±3
	mean	24
WFA	SF Volcanics	6±1
WOM	Supai	25±4
WOT	Coconino	4±1

TABLE 13. Heat-flow estimates, Black Mesa

Well	Formation	Heat flow mWm ²
BMSA	Entrada	49±7
	Carmel	62±20
	Kayenta	75±13
	Wingate	57±5
	mean	61
CORN	Chinle	94±16
HARD	Entrada	41±8
	Navajo	89±17
	Kayenta	57±13
	mean	62
INSC	Navajo	65±8
PIN1	Entrada	53±8
	Carmel	46±8
	mean	50
WIDE	Chinle	110±19

TABLE 14. Heat-flow estimates, South-central Colorado Plateau

Well	Formation	Heat flow mWm ²
CVL	Coconino	39±1
PWF1	Chinle	149±23
PWF2	Chinle	115±18
	Moenkopi	150±59
	Kaibab	84±15
	mean	116
PWF3	Chinle	109±17
	Chinle	64±10
	mean	86
TGE1	Kaibab	82±13
	Coconino	69±8
	mean	76
TGE2	Coconino	79±10
TGE3	Coconino	63±8

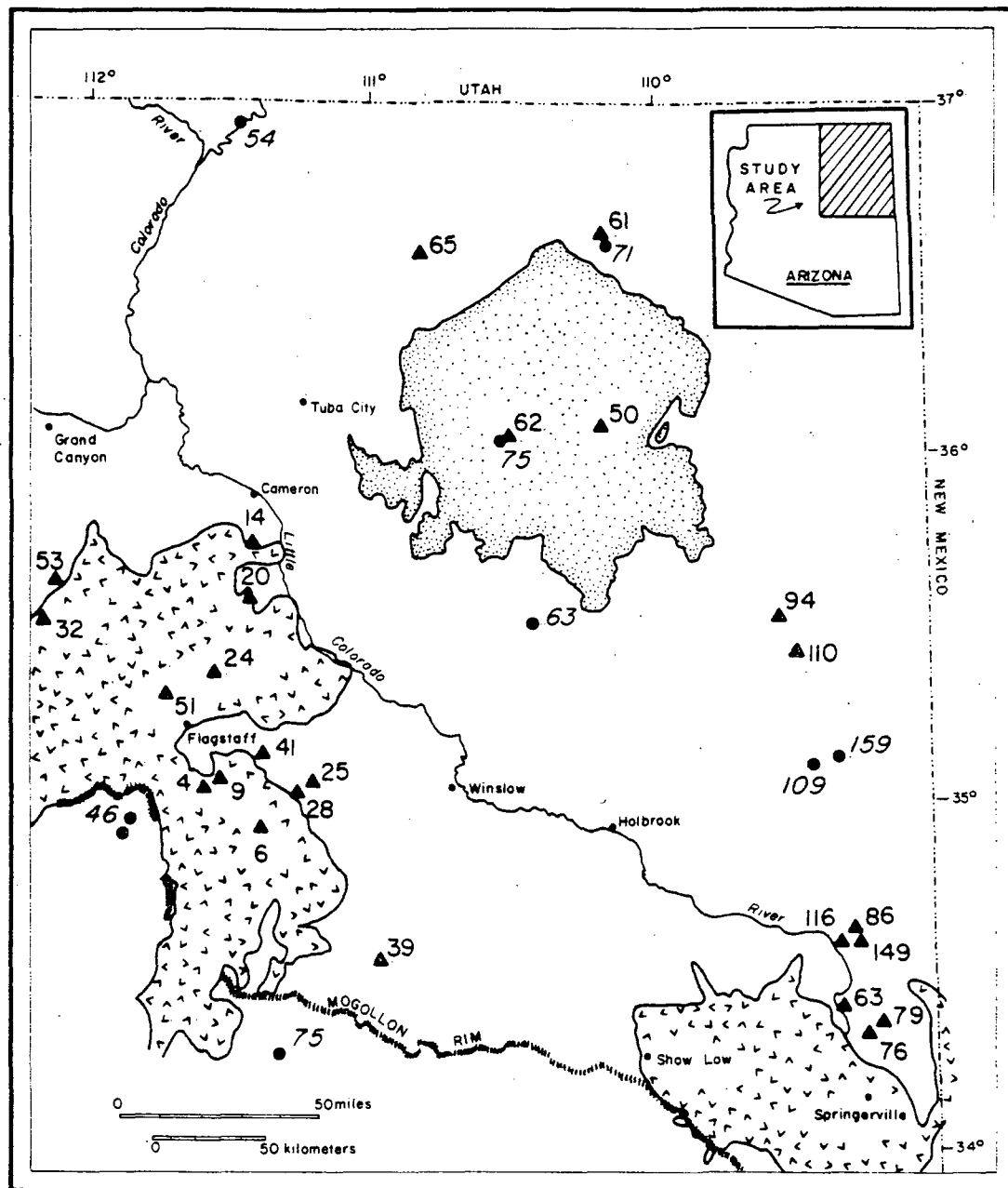


Figure 7. Map showing locations of wells (triangles) and heat-flow estimates for the present study. Also shown (as solid dots) are the published heat flows of Reiter and Shearer (1979) and Shearer and Reiter (1981).

has somewhat lower heat flows than sites to the north; however, they are high enough to be considered outside of the "cooler interior" of Bodell and Chapman (1982).

DISCUSSION

It should be emphasized that the estimates presented in the previous section are subject to large uncertainties and do not merit status as heat-flow measurements. No undue significance should be attached to any individual value; however, suitable groups of data probably contain information on the regional variation of heat flow. In Table 15, we calculate means for the three sub-provinces with some shuffling around of points dictated partly by the rather arbitrary initial groupings and partly by putting the present estimates in the context of previously published heat flows.

The San Francisco volcanic field is clearly a sub-province of low conductive flux. We believe that this is due primarily to the extensive recharge at higher elevations, pervasive and rapid lateral flow (with a downward vertical component of velocity) within a laterally continuous regional aquifer and the consequent discharge at low elevation in the Verde, Little Colorado, and Colorado valleys. A full understanding of the thermal regime of this tectonically active sub-province requires the acquisition of thermal data from deep wells (~ 1 km or deeper) which penetrate the basement rocks. Many such wells have been drilled in the past, but for various reasons are inaccessible below the regional aquifer. The total thermal budget (conductive and convective) is also an important field of study. Perhaps as much as 70 mWm^{-2} of regional heat flux is being carried laterally and discharged at fairly low enthalpy at lower elevations. Some of the discharge may be below the surface in streams which makes it difficult to evaluate quantitatively. Nevertheless, a systematic study of discharge rates and temperatures of known thermal springs and careful thermal and geochemical studies of thermal wells in the Verde Valley and elsewhere will be of great value in determining just where the heat that is being released beneath the San Francisco volcanic field is going. The same comments apply to the Mogollon Rim area which is represented by only one heat-flow determination (CVL, Figures 1 and 7) in this study.

If we exclude the high values from CORN and WIDE (Figure 7; Table 15), our values from Black Mesa are in reasonable agreement with those of Reiter and Shearer (1979) (although somewhat lower) and conform quite well to Bodell and Chapman's (1982) contour for the cool interior region of the plateau.

Finally, if we leave CVL by itself and add CORN and WIDE to our previously defined south-central province (Table 15), the data define a group of sites characterized by high heat flow. This data-set confirms and extends somewhat the previously documented high heat-flow terrane in the southeastern Colorado Plateau.

TABLE 15. Averages of heat-flow estimates for three provinces within the study area

Province	N*	q_{ave} mWm ⁻²	S.D.	S.E.
San Francisco Volcanic Field	11	27.1	16.4	4.9
Black Mesa [†]	a) 6	73.7	23.1	9.4
	b) 4	59.5	6.6	3.3
South-central Colorado Plateau ^{††}	a) 7	86.8	35.9	13.6
	b) 6	94.8	31.9	13.0
	c) 8	96.6	27.5	9.7

*N is number of values; q_{ave} , arithmetic mean heat flow; S.D., standard deviation; and S.E., standard error.

[†]a) all values; b) excluding CORN and WIDE.

^{††}a) all values; b) excluding CVL; c) b + CORN and WIDE.

REFERENCES

- Akers, J. P., 1964, Geology and ground water in the central part of Apache County, Arizona: U.S. Geological Survey Water Supply Paper 1771, 107 p.
- Appel, C. L., and Bills, D. J., 1980, Maps showing ground-water conditions in the Canyon Diablo area, Coconino and Navajo Counties, Arizona - 1979: U.S. Geological Survey Open-File Report 80-747, scale 1:125,000.
- Appel, C. L., and Bills, D. J., 1981, Maps showing ground-water conditions in the San Francisco Peaks area, Coconino County, Arizona - 1979: U.S. Geological Survey Open-File Report 81-914, scale 1:125,000.
- Bahr, C. W., 1962, The Holbrook anticline, Navajo country, Arizona: New Mexico Geological Society, Thirteenth Field Conference, p. 118-122.
- Bills, D. J., and Sass, J. H., 1982, Hydrologic and near-surface thermal regimes of the San Francisco Volcanic Field: U.S. Geological Survey Professional Paper, in press.
- Birch, Francis, 1950, Flow of heat in the Front Range, Colorado: Geological Society of America Bulletin, v. 61, p. 567-630.
- Blackwell, D. D., 1971, The thermal structure of the continental crust, in Heacock, J. G., ed., The structure and physical properties of the earth's crust: American Geophysical Union Geophysical Monograph 14, p. 169-184.
- Bodell, J. M., and Chapman, D. S., 1982, Heat flow in the north-central Colorado Plateau: Journal of Geophysical Research, v. 87, p. 2869-2884.
- Clark, S. P., Jr., and Niblett, E. R., 1956, Terrestrial heat flow in the Swiss Alps: Monthly Notices of the Royal Astronomical Society, Geophysical Supplement 7, p. 176-195.
- Cooley, M. E., 1976, Spring flow from Pre-Pennsylvanian rocks in the southwestern part of the Navajo Indian Reservation, Arizona: U.S. Geological Survey Professional Paper 521-F, 15 p.
- Cooley, M. E., Harshbarger, J. W., Akers, J. P., and Hardt, W. F., 1969, Regional hydrogeology of the Navajo and Hopi Indian Reservations, Arizona, New Mexico, and Utah; with a section on vegetation by O. N. Hicks: U.S. Geological Survey Professional Paper 521-A, 61 p.
- Damon, P. E., Shafiqullah, M., and Leventhal, J. S., 1974, K-Ar chronology for the San Francisco volcanic field and rate of erosion of the Little Colorado River, in Karlstrom, T. N. V., Swann, G. A., and Eastwood, R. L., eds., Geology of Northern Arizona: Geological Society of America Rocky Mountain Section Meeting, p. 221-235.
- DuBois, S. M., Sbar, M. L., and Nowak, T. A., Jr., 1981, Historical seismicity in Arizona: Arizona Bureau of Geology and Mineral Technology Open-File Report 82-2, Tucson, 199 p.

- Eychaner, J. H., 1981, Geohydrology and effects of water use in the Black Mesa area, Navajo and Hopi Indian Reservations, Arizona: U.S. Geological Survey Open-File Report 81-911, 46 p.
- Farrar, C. D., 1979a, Maps showing ground-water conditions in the Kaibito and Tuba City areas, Coconino and Navajo Counties, Arizona - 1978: U.S. Geological Survey Open-File Report 79-58, scale 1:125,000.
- Farrar, C. D., 1979b, Maps showing ground-water conditions in the Bodaway Mesa area, Coconino County, Arizona - 1977: U.S. Geological Survey Open-File Report 79-58, scale 1:125,000.
- Farrar, C. D., 1980, Maps showing ground-water conditions in the Hopi area, Coconino and Navajo Counties, Arizona - 1977: U.S. Geological Survey Open-File Report 80-3, scale 1:125,000.
- Geologic Atlas of the Rocky Mountain Region, 1972, Rocky Mountain Association of Geologists, Denver, 331 p.
- Harper, R. W., and Anderson, T. W., 1976, Maps showing ground-water conditions in the Concho, St. Johns, and White Mountains areas, Apache and Navajo Counties, Arizona - 1975: U.S. Geological Survey Open-File Report 76-104, scale 1:125,000.
- Harshbarger and Associates and John Carollo Engineers, 1974, Inner Basin aquifer report - City of Flagstaff, Arizona: Harshbarger and Associates and John Carollo Engineers, duplicate report, 67 p.
- Johnson, P. W., and Sanderson, R. B., 1968, Spring flow into the Colorado River, Lees Ferry to Lake Mead, Arizona: Arizona State Land Department, Water-Resources Report Number Thirty-Four, 26 p.
- Levings, G. W., and Farrar, C. D., 1977a, Maps showing ground-water conditions in the Monument Valley and northern part of Black Mesa area, Navajo, Apache, and Coconino Counties, Arizona - 1976: U.S. Geological Survey Open-File Report 77-44, scale 1:125,000.
- Levings, G. W., and Farrar, C. D., 1977b, Maps showing ground-water conditions in the southern part of the Black Mesa area, Navajo, Apache, and Coconino Counties, Arizona - 1976: U.S. Geological Survey Open-File Report 77-41, scale 1:125,000.
- Levings, G. W., and Farrar, C. D., 1977c, Maps showing ground-water conditions in the northern part of the Chinle area, Apache County, Arizona - 1976: U.S. Geological Survey Open-File Report 77-35, scale 1:150,000.
- Levings, G. W., and Farrar, C. D., 1977d, Maps showing ground-water conditions in the southern part of the Chinle area, Apache County, Arizona - 1976: U.S. Geological Survey Open-File Report 77-50, scale 1:125,000.

- Levings, G. W., and Mann, L. J., 1980, Maps showing ground-water conditions in the upper Verde River area, Yavapai and Coconino Counties, Arizona - 1978: U.S. Geological Survey Open-File Report 80-726, scale 1:125,000.
- Luedke, R. G., and Smith, R. L., 1978, Map showing distribution, composition, and age of Late Cenozoic volcanic centers in Arizona - New Mexico: U.S. Geological Survey Miscellaneous Investigations Series Map I-1091A, scale 1:1,000,000.
- Mann, L. J., 1976, Ground-water resources and water use in southern Navajo County, Arizona: Arizona Water Commission Bulletin 10, prepared by U.S. Geological Survey, 106 p.
- Mann, L. J., 1977, Maps showing ground-water conditions in the Puerco-Zuni area, Apache and Navajo Counties, Arizona - 1975: U.S. Geological Survey Open-File Report 77-5, scale 1:125,000.
- Merrill, R. K., 1974, The Late Cenozoic geology of the White Mountains, Apache County, Arizona: Unpublished Ph.D. dissertation, Arizona State University, Tempe, 202 p.
- Merrill, R. K., and Péwé, T. L., 1977, Late Cenozoic geology of the White Mountains, Arizona: Arizona Bureau of Geology and Mineral Technology Special Paper No. 1, 65 p.
- Moore, R. B., Wolfe, E. W., and Ulrich, G. E., 1974, Geology of the eastern and northern parts of the San Francisco volcanic field, Arizona, in Karlstrom, T. N. V., Swann, G. A., and Eastwood, R. L., eds., Geology of Northern Arizona: Geological Society of America Rocky Mountain Section Meeting, p. 465-494.
- Peirce, H. W., 1976, Elements of Paleozoic tectonics in Arizona: Arizona Geological Society Digest X, p. 37-57.
- Peirce, H. W., Keith, S. B., and Wilt, J. C., 1970, Coal, oil, natural gas, helium, and uranium in Arizona: Arizona Bureau of Mines Bulletin 182, Tucson, 289 p.
- Reiter, M., Edwards, C. L., Hartman, H., and Weidman, C., 1975, Terrestrial heat flow along the Rio Grande Rift, New Mexico and Southern Colorado: Geological Society of America Bulletin, v. 86, p. 811-818.
- Reiter, M., and Shearer, C., 1979, Terrestrial heat flow in eastern Arizona-- A first report: Journal of Geophysical Research, v. 84, p. 6115-6120.
- Roy, R. F., Blackwell, D. D., and Decker, E. R., 1972, Continental heat flow, in Robertson, E. C., ed., The nature of the solid earth: New York, McGraw-Hill, p. 506-544.
- Sass, J. H., Clark, S. P., Jr., and Jaeger, J. C., 1967, Heat flow in the Snowy Mountains of Australia: Journal of Geophysical Research, v. 72, p. 2635-2647.

- Sass, J. H., Lachenbruch, A. H., and Munroe, R. J., 1971a, Thermal conductivity of rocks from measurements on fragments and its application to heat-flow determinations: *Journal of Geophysical Research*, v.76, p. 3391-3401.
- Sass, J. H., Lachenbruch, A. H., Munroe, R. J., Greene, G. W., and Moses, T. H., Jr., 1971b, Heat flow in the western United States: *Journal of Geophysical Research*, v. 76, p. 6376-6413.
- Shearer, Charles, and Reiter, Marshall, 1981, Terrestrial heat flow in Arizona: *Journal of Geophysical Research*, v. 86, p. 6249-6260.
- Shoemaker, E. M., Squires, R. L., and Abrams, M. J., 1974, The Bright Angel and Mesa Butte fault systems of northern Arizona, in Karlstrom, T. N. V., Swann, G. A., and Eastwood, R. L., eds., *Geology of Northern Arizona: Geological Society of America Rocky Mountain Section Meeting*, p. 355-391.
- Smiley, T. L., 1958, The geology and dating of Sunset Crater, Flagstaff, Arizona, in Black Mesa basin, northeastern Arizona: *New Mexico Geological Society Guidebook, 9th Field Conference*, p. 186-190.
- Sobels, B. E., 1962, Mogollon Rim volcanism and geochronology: *New Mexico Geological Survey, 13th Field Conference Guidebook*, p. 100-106.
- Sutton, R. L., 1974, The geology of Hopi Buttes, Arizona, in Karlstrom, T. N. V., Swann, G. A., and Eastwood, R. L., eds., *Geology of Northern Arizona: Geological Society of America Rocky Mountain Section Meeting*, p. 647-671.
- Twenter, F. R., 1962, Rocks and water in Verde Valley, Arizona: *New Mexico Geological Survey, 13th Field Conference Guidebook*, p. 135-139.
- Twenter, F. R., and Metzger, D. G., 1963, Geology and ground water in the Verde Valley - the Mogollon Rim region, Arizona: *U.S. Geological Survey Bulletin 1177*, 132 p.
- Wilson, R. F., 1974, Mesozoic stratigraphy of northeastern Arizona, in Karlstrom, T. N. V., Swann, G. A., and Eastwood, R. L., eds., *Geology of Northern Arizona: Geological Society of America Rocky Mountain Section Meeting*, p. 192-207.
- Woodside, W., and Messmer, J. H., 1961, Thermal conductivity of porous media, I. Unconsolidated sands: *Journal of Applied Physics*, v. 32, p. 1688-1699.

APPENDIX A
Individual temperature profiles and tabulations
for the San Francisco Volcanic Field (see Figures 1 and 2)

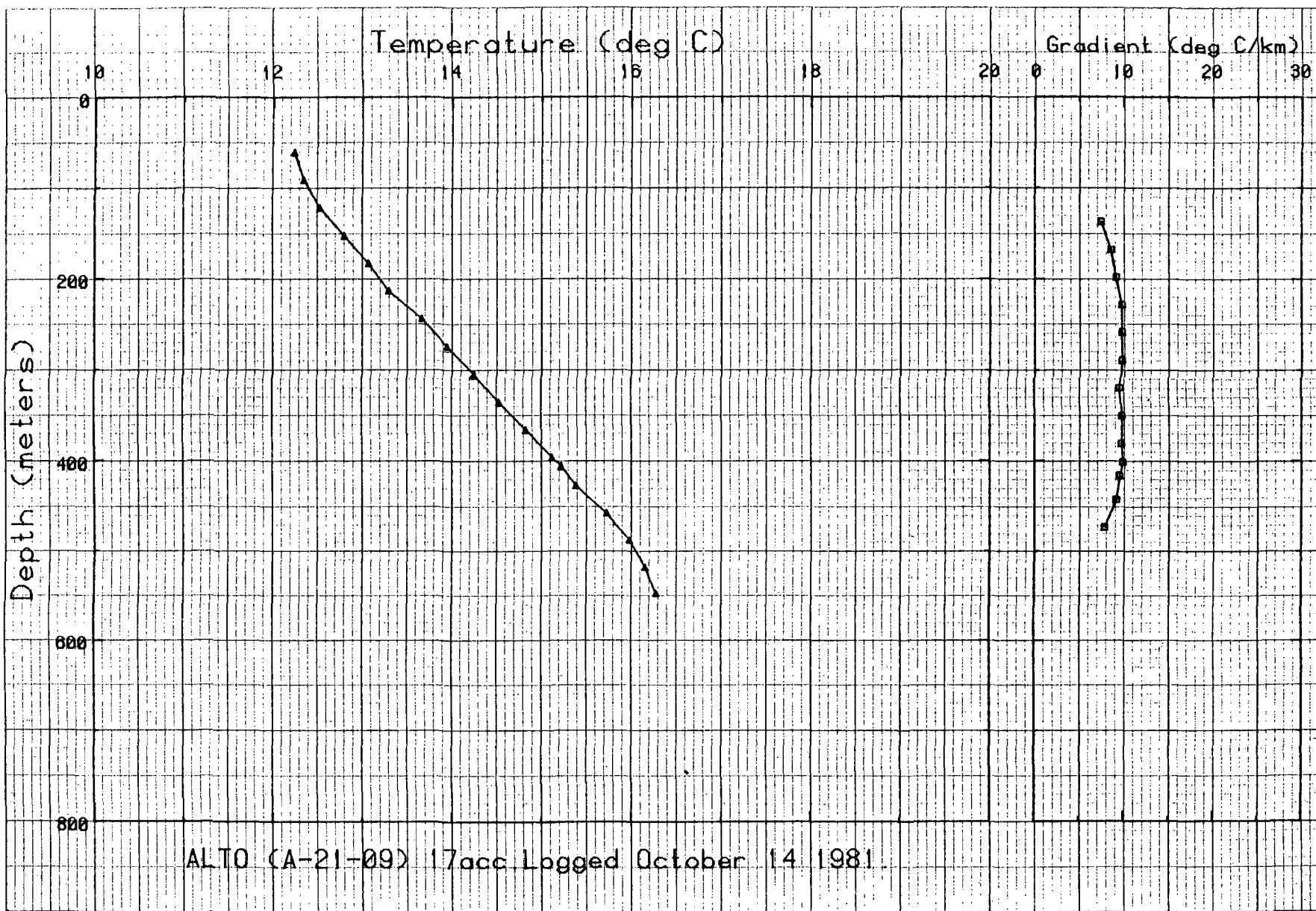


Figure A-1.

Depth,m	Temp,C	Depth,m	Temp,C
60.9	12.241	91.4	12.346
121.9	12.527	152.4	12.799
182.8	13.069	213.3	13.294
243.8	13.665	274.3	13.944
304.8	14.241	335.2	14.53
365.7	14.828	396.2	15.121
405.3	15.223	426.7	15.39
457.2	15.73	487.6	15.984
518.1	16.159	547.4	16.282

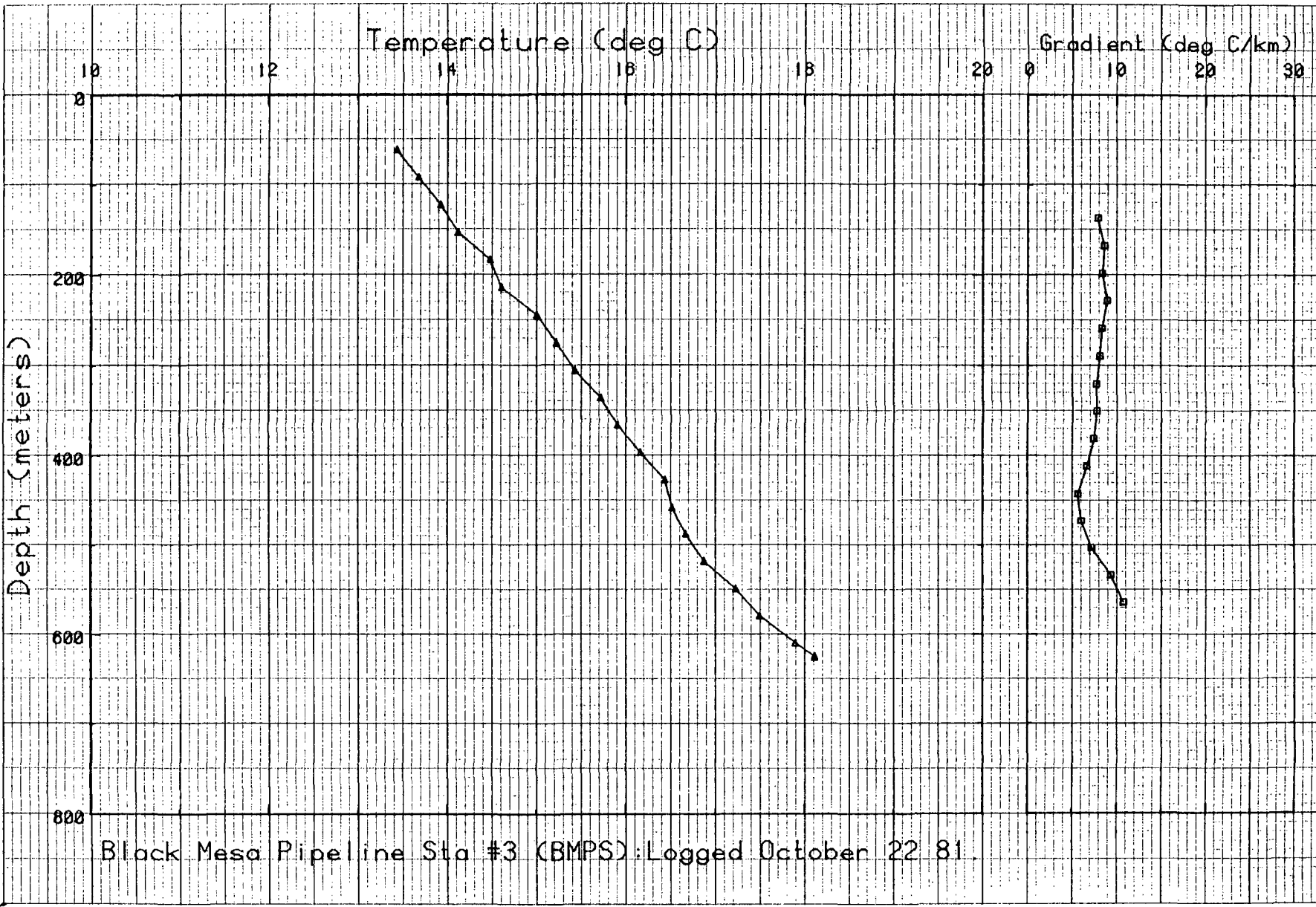


Figure A-2.

Depth,m	Temp,C	Depth,m	Temp,C
60.9	13.442	91.4	13.686
121.9	13.931	152.4	14.125
182.8	14.487	213.3	14.613
243.8	15.009	274.3	15.231
304.8	15.441	335.2	15.728
365.7	15.914	396.2	16.169
426.7	16.442	457.2	16.52
487.6	16.674	518.1	16.877
548.6	17.234	579.1	17.501
609.6	17.899	624.8	18.116

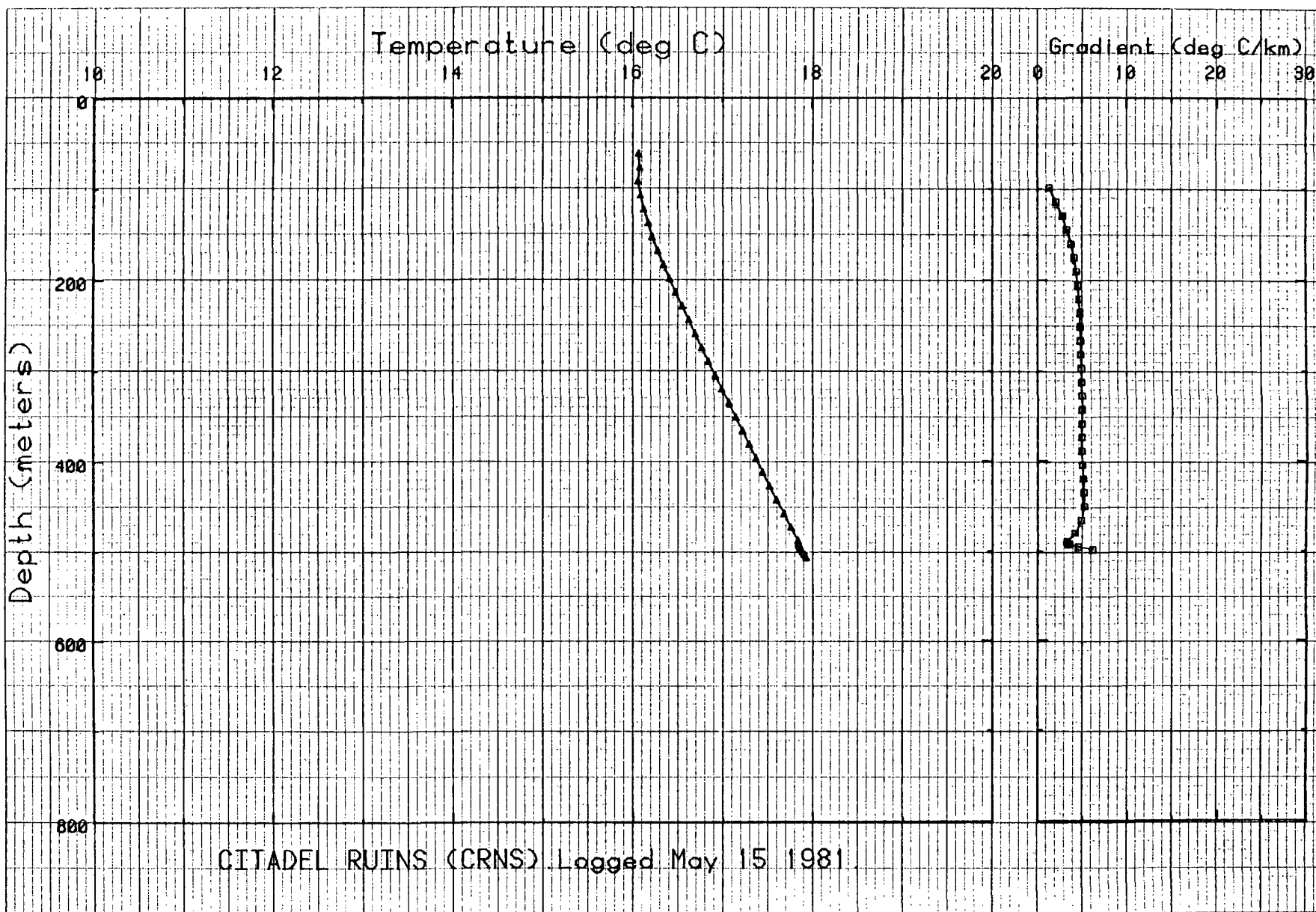


Figure A-3.

Depth,m	Temp,C	Depth,m	Temp,C
60.9	16.069	76.2	16.082
91.4	16.066	106.6	16.094
121.9	16.13	137.1	16.175
152.4	16.219	167.6	16.282
182.8	16.347	198.1	16.412
213.3	16.479	228.6	16.553
243.8	16.627	259	16.697
274.3	16.771	289.5	16.843
304.8	16.92	320	16.993
335.2	17.069	350.5	17.145
365.7	17.219	381	17.294
396.2	17.367	411.4	17.444
426.7	17.52	441.9	17.599
457.2	17.681	472.4	17.759
487.6	17.837	490.7	17.844
493.7	17.85	496.8	17.86
499.8	17.889	502.9	17.907
505.9	17.927		

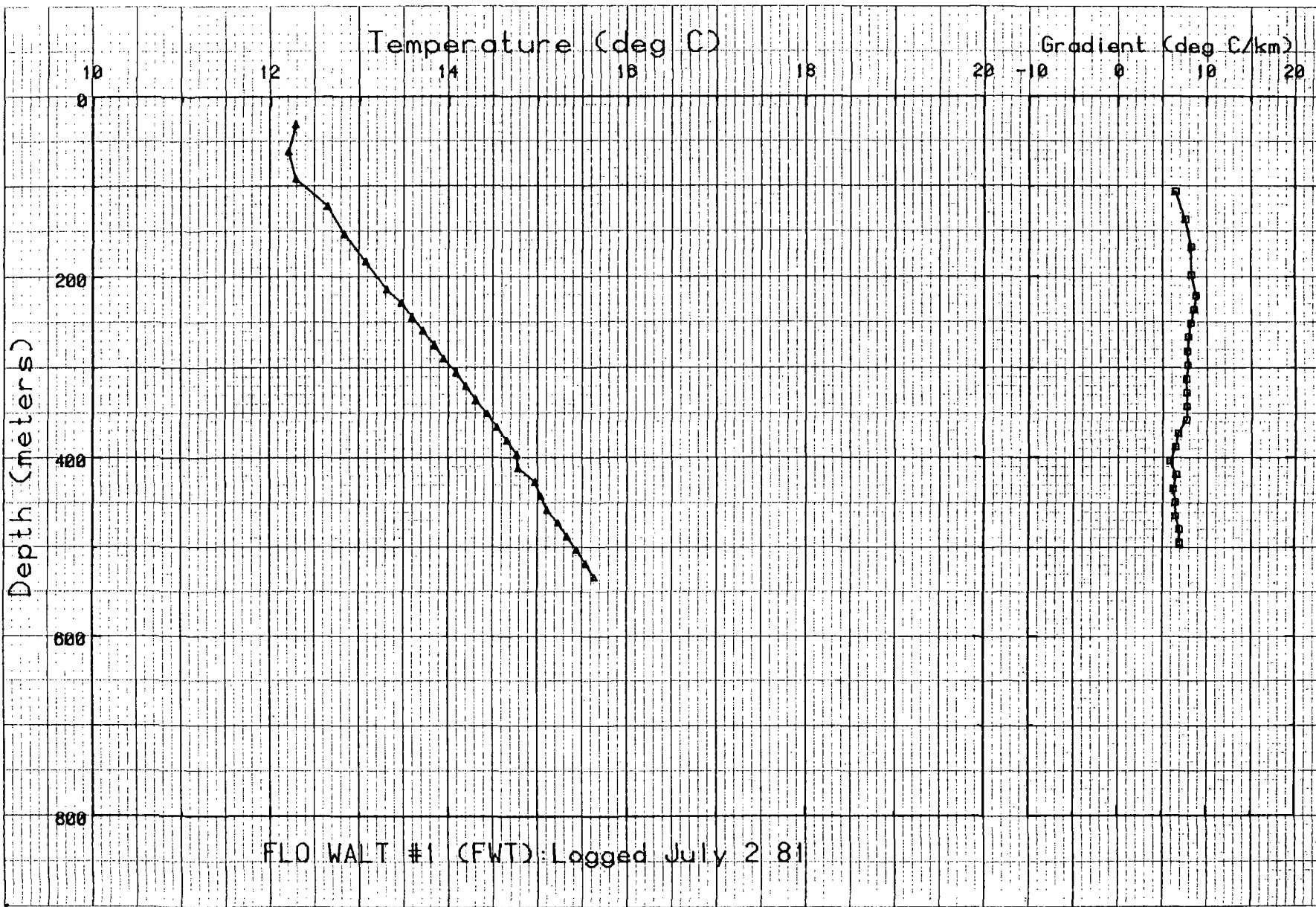


Figure A-4.

Depth,m	Temp,C	Depth,m	Temp,C
30.4	12.282	60.9	12.203
91.4	12.284	121.9	12.643
152.4	12.831	182.8	13.075
213.3	13.309	228.6	13.472
243.8	13.593	259	13.715
274.3	13.84	289.5	13.943
304.8	14.083	320	14.192
335.2	14.303	350.5	14.428
365.7	14.547	381	14.661
396.2	14.769	411.4	14.781
426.7	14.969	441.9	15.032
457.2	15.107	472.4	15.23
487.6	15.333	502.9	15.439
518.1	15.544	533.4	15.639

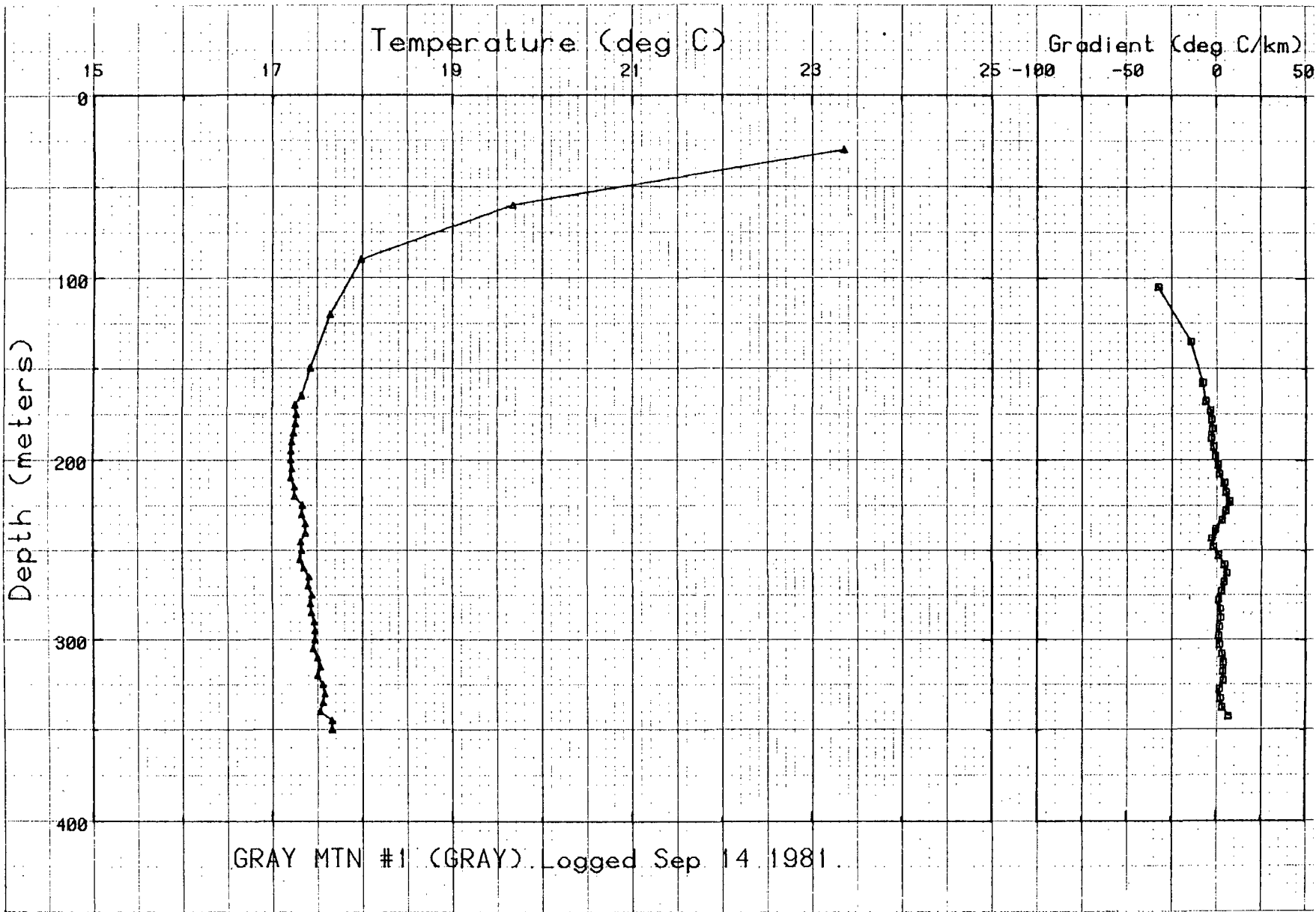


Figure A-5.

Depth,m	Temp,C	Depth,m	Temp,C
30	23.35	59.9	19.67
89.9	17.98	119.9	17.64
149.9	17.42	165	17.32
170	17.25	175	17.27
179.9	17.26	184.9	17.24
189.9	17.22	194.9	17.21
199.9	17.21	204.9	17.22
209.9	17.21	214.9	17.25
219.9	17.25	224.9	17.34
229.9	17.33	234.9	17.37
239.9	17.37	244.9	17.32
249.9	17.33	254.9	17.31
259.9	17.35	264.9	17.41
269.9	17.4	274.9	17.44
279.9	17.42	284.9	17.43
289.9	17.46	294.9	17.47
299.9	17.47	304.9	17.45
309.9	17.5	314.9	17.53
319.9	17.5	324.9	17.56
329.9	17.58	334.9	17.56
339.9	17.53	344.9	17.66
349.9	17.66	350	17.66

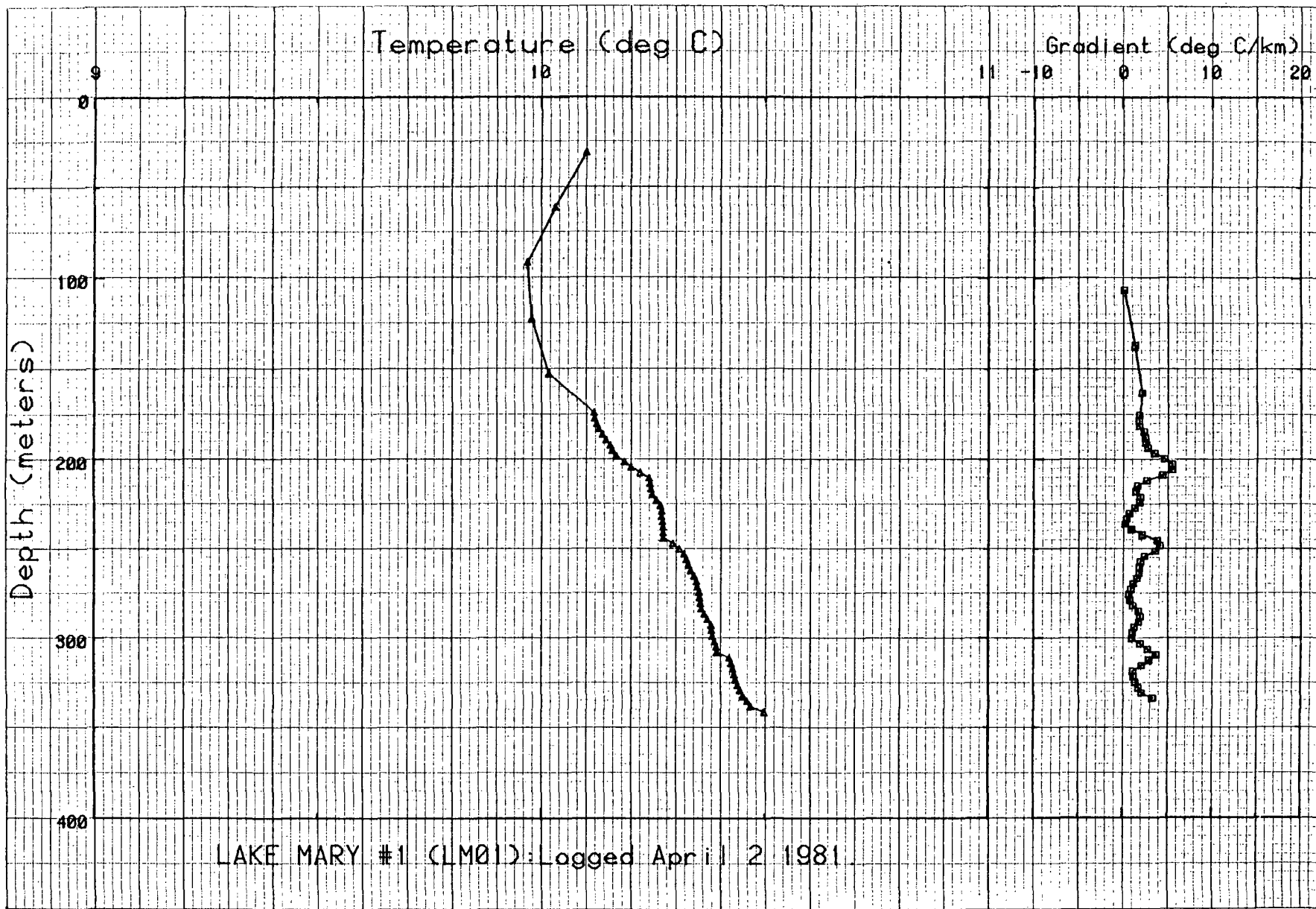


Figure A-6.

Depth,m	Temp,C	Depth,m	Temp,C
30.4	10.101	60.9	10.032
91.4	9.97	121.9	9.979
152.4	10.018	173.7	10.119
176.7	10.12	179.8	10.125
182.8	10.13	185.9	10.138
188.9	10.146	192	10.155
195	10.16	198.1	10.169
201.1	10.187	204.2	10.202
207.2	10.222	210.3	10.242
213.3	10.244	216.4	10.246
219.4	10.249	222.5	10.258
225.5	10.266	228.6	10.269
231.6	10.269	234.7	10.271
237.7	10.272	240.8	10.272
243.8	10.272	246.9	10.294
249.9	10.308	252.9	10.319
256	10.324	259	10.329
262.1	10.334	265.1	10.342
268.2	10.347	271.2	10.349
274.3	10.353	277.3	10.354
280.4	10.356	283.4	10.358
286.5	10.365	289.5	10.372
292.6	10.38	295.6	10.381
298.7	10.383	301.7	10.388
304.8	10.392	307.8	10.393
310.9	10.421	313.9	10.425
317	10.429	320	10.432
323.1	10.435	326.1	10.44
329.1	10.445	332.2	10.451
335.2	10.46	338.3	10.468
341.3	10.499		

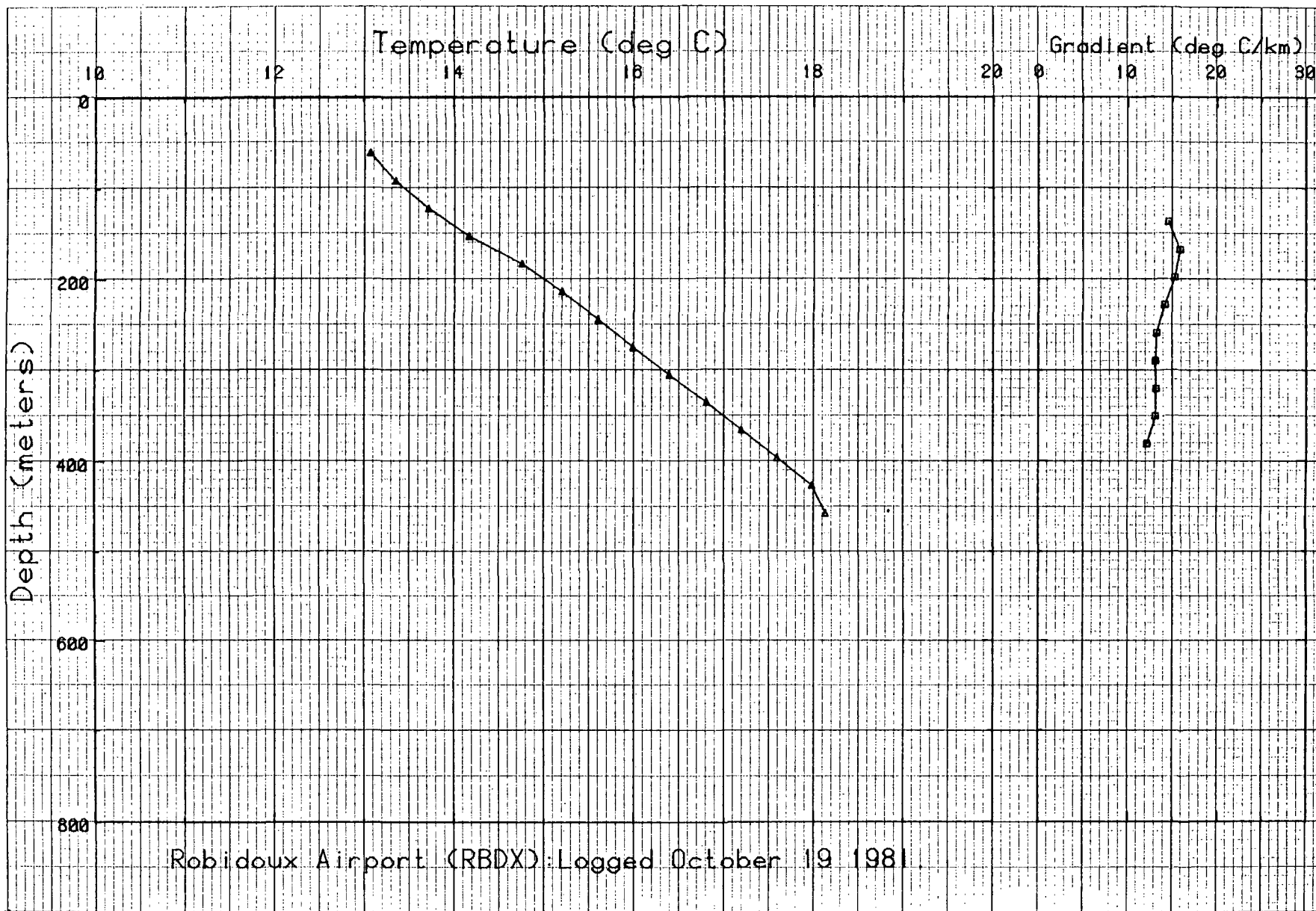


Figure A-7.

Depth,m

Temp,C

Depth,m

Temp,C

60.9
121.9
182.8
243.8
304.8
365.7
426.7

13.066
13.715
14.754
15.609
16.394
17.199
17.985

91.4
152.4
213.3
274.3
335.2
396.2
457.2

13.35
14.164
15.204
15.994
16.808
17.595
18.135

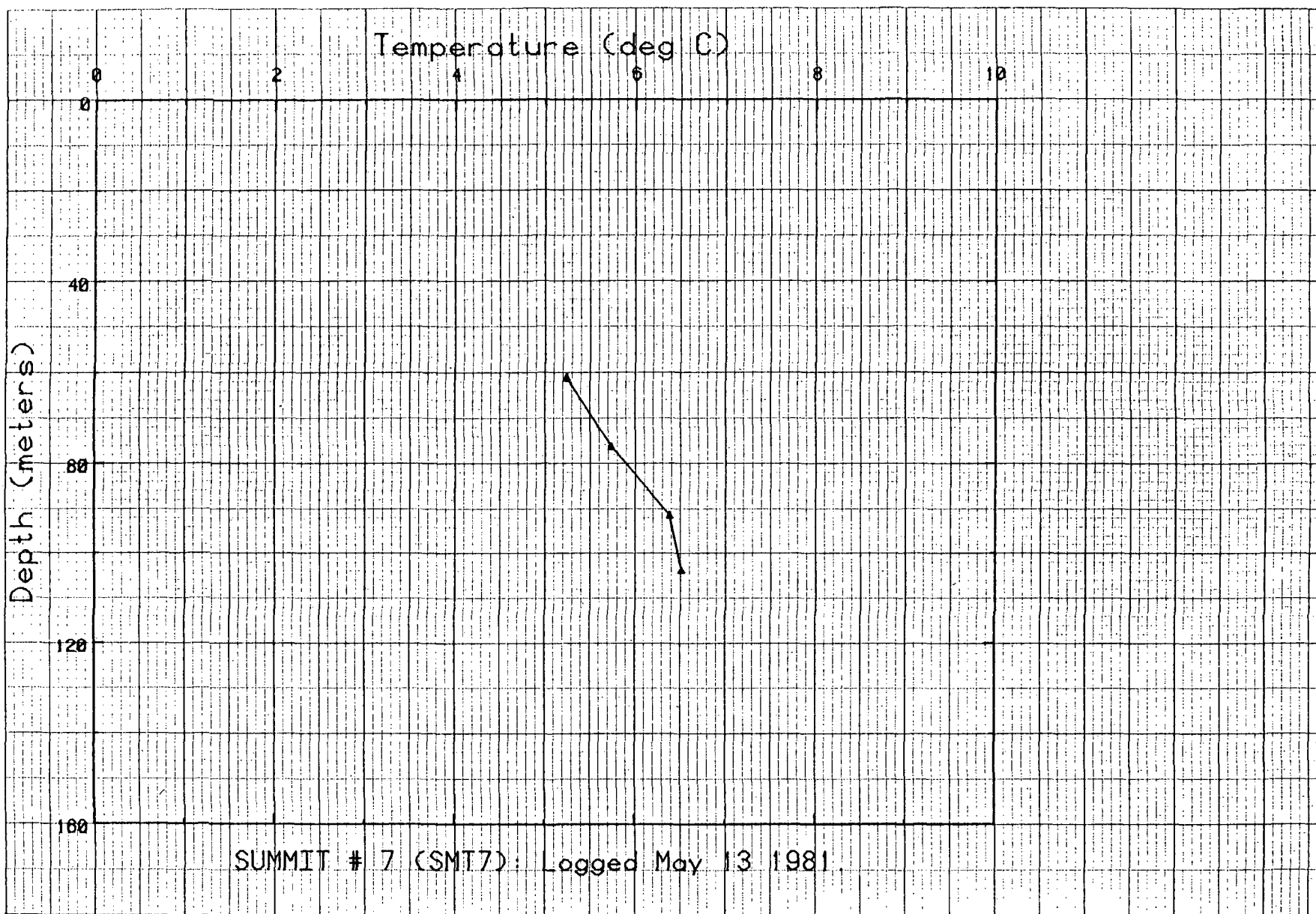


Figure A-8.

Depth,m

Temp,C

Depth,m

Temp,C

60.9
91.45.246
6.38976.2
103.85.741
6.517

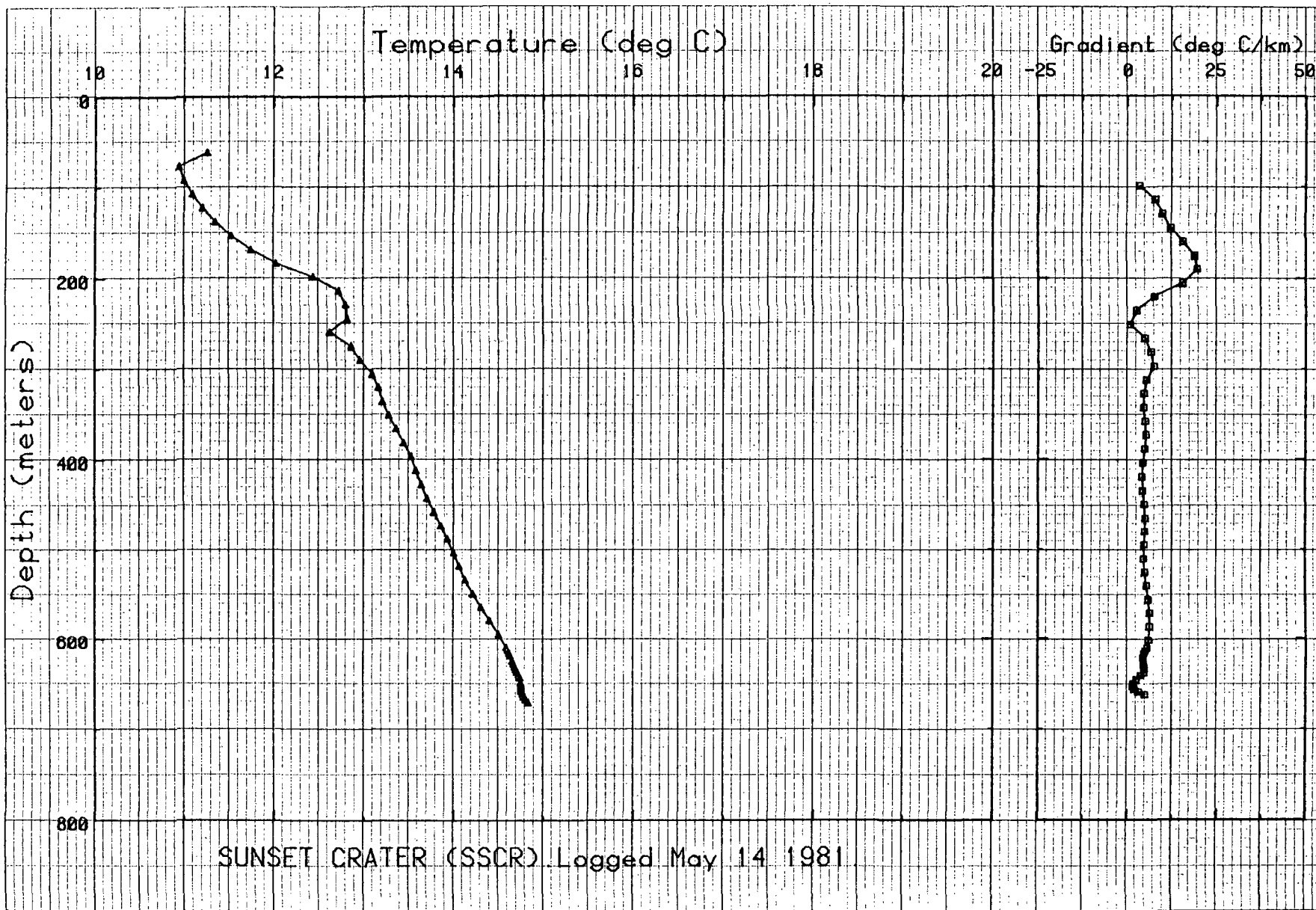


Figure A-9.

Depth,m	Temp,C	Depth,m	Temp,C
60.9	11.248	76.2	10.932
91.4	10.987	106.6	11.083
121.9	11.197	137.1	11.346
152.4	11.525	167.6	11.746
182.8	12.025	198.1	12.439
213.3	12.723	228.6	12.799
243.8	12.814	259	12.618
274.3	12.86	289.5	12.955
304.8	13.088	320	13.159
335.2	13.204	350.5	13.276
365.7	13.358	381	13.443
396.2	13.527	411.4	13.578
426.7	13.64	441.9	13.702
457.2	13.772	472.4	13.851
487.6	13.925	502.9	13.995
518.1	14.055	533.4	14.124
548.6	14.208	563.8	14.299
579.1	14.396	594.3	14.498
609.6	14.582	612.6	14.599
615.7	14.616	618.7	14.628
624.8	14.65	627.9	14.667
630.9	14.679	633.9	14.693
637	14.707	640	14.724
643.1	14.738	649.2	14.746
652.2	14.749	655.3	14.753
658.3	14.758	661.4	14.766
664.4	14.777	667.5	14.803
670.5	14.829		

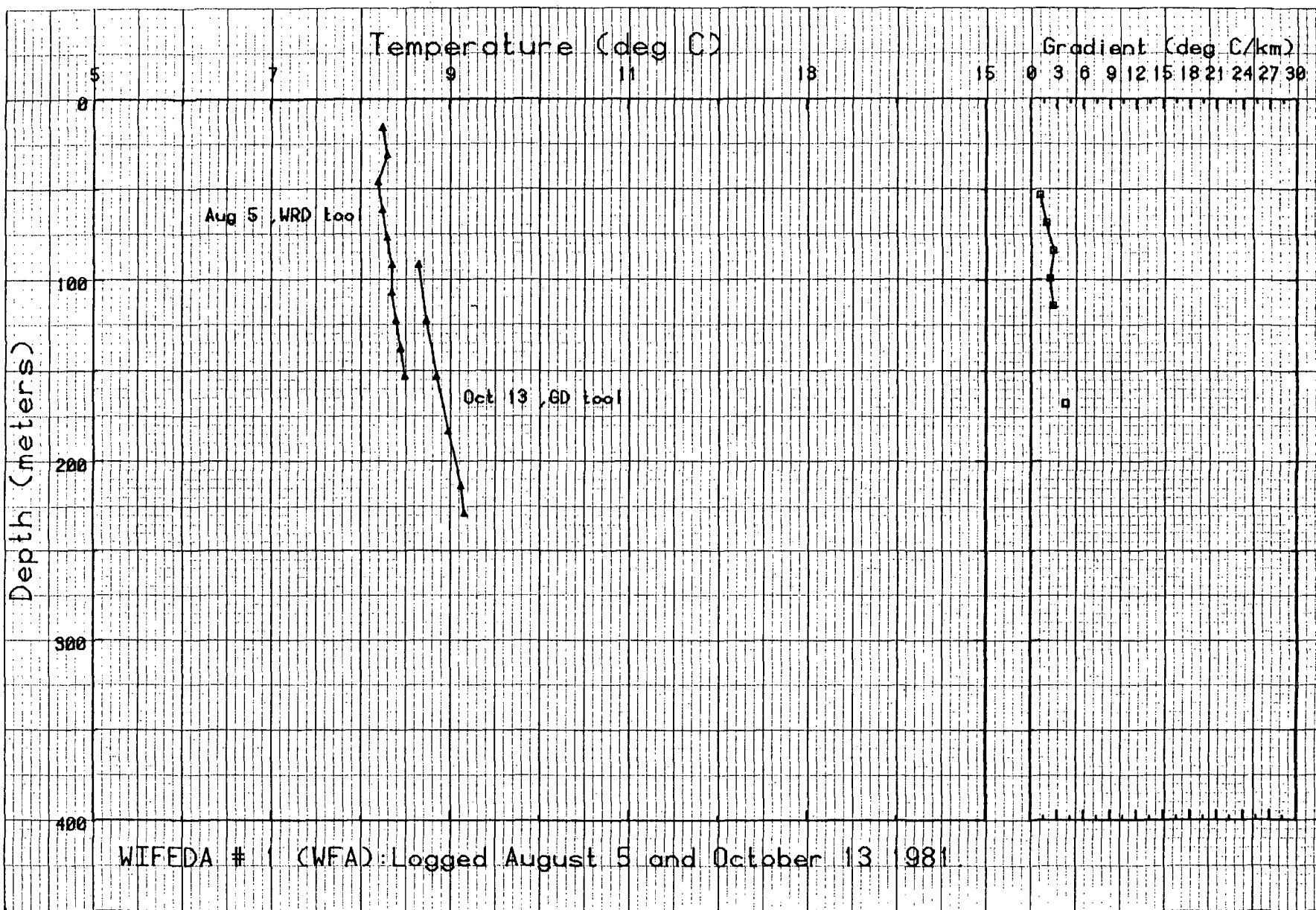


Figure A-10.

TLOGS/AZ/CP/WFA/AUG0581

Depth,m	Temp,C	Depth,m	Temp,C
15.2	8.25	30.4	8.3
45.7	8.2	60.9	8.25
76.2	8.3	91.4	8.35
106.6	8.35	121.9	8.4
137.1	8.45	152.4	8.5

Hole: A-17-09 11b0d

TLOGS/AZ/CP/WFA/OCT1381

Depth,m	Temp,C	Depth,m	Temp,C
91.4	8.649	121.9	8.738
152.4	8.854	182.8	8.983
213.3	9.128	228.6	9.167

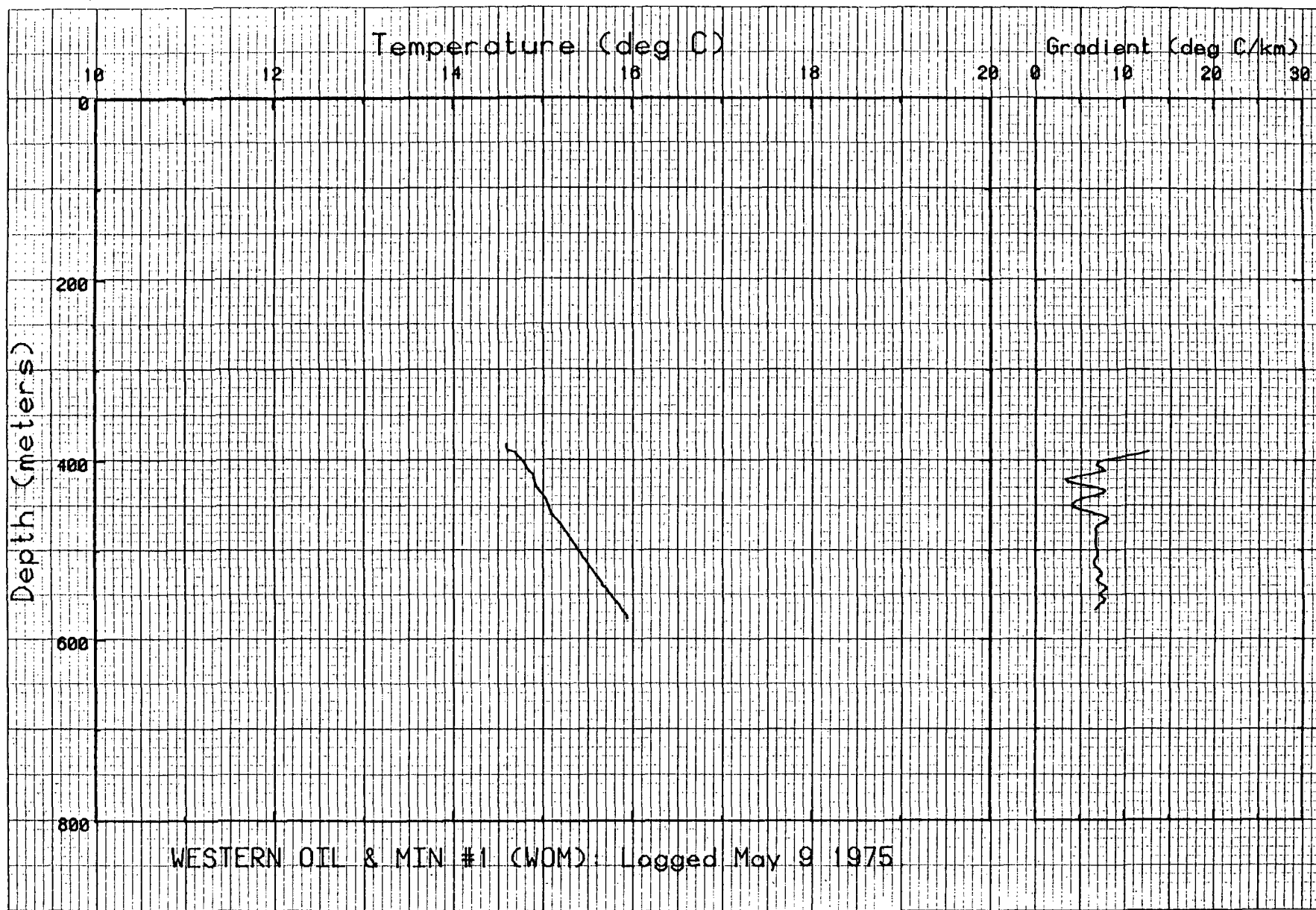


Figure A-11.

Depth,m	Temp,C	Depth,m	Temp,C
381	14.6	384	14.604
387.1	14.609	390.1	14.7
393.2	14.716	396.2	14.751
399.3	14.779	402.3	14.799
405.3	14.815	408.4	14.834
411.4	14.857	414.5	14.9
417.5	14.905	420.6	14.912
423.6	14.921	426.7	14.93
429.7	14.95	432.8	14.978
435.8	15.007	438.9	15.028
441.9	15.044	445	15.056
448	15.071	451.1	15.083
454.1	15.092	457.2	15.108
460.2	15.13	463.3	15.16
466.3	15.184	469.4	15.209
472.4	15.231	475.5	15.247
478.5	15.27	481.5	15.292
484.6	15.312	487.6	15.332
490.7	15.353	493.7	15.375
496.8	15.393	499.8	15.415
502.9	15.439	505.9	15.457
509	15.481	512	15.501
515.1	15.519	518.1	15.539
521.2	15.563	524.2	15.581
527.3	15.607	530.3	15.631
533.4	15.651	536.4	15.669
539.5	15.686	542.5	15.723
545.6	15.743	548.6	15.765
551.7	15.784	554.7	15.806
557.7	15.837	560.8	15.858
563.8	15.876	566.9	15.895
569.9	15.921	573	15.943
576	15.947		

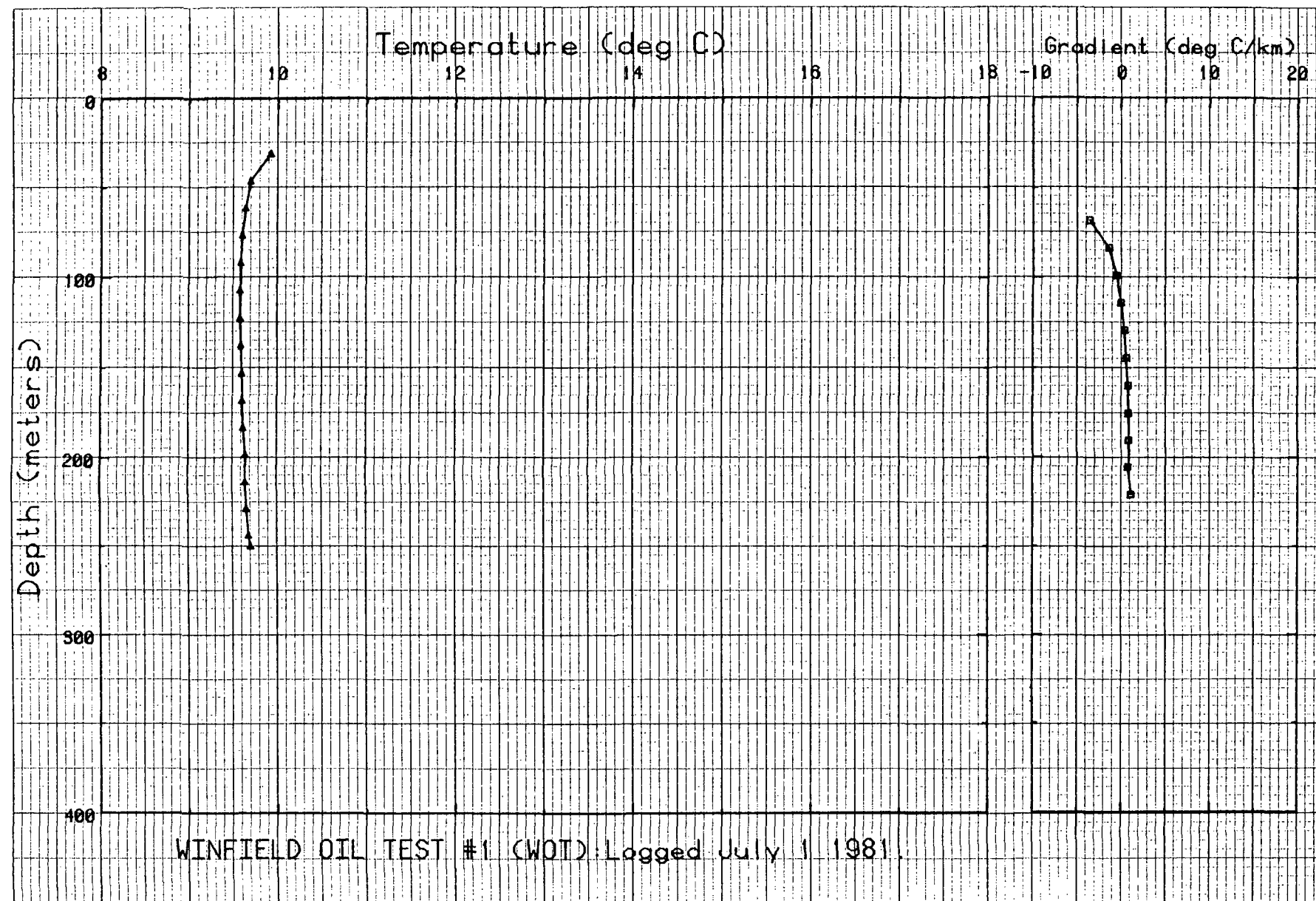


Figure A-12.

Depth,m	Temp,C	Depth,m	Temp,C
30.4	9.92	45.7	9.692
60.9	9.638	76.2	9.601
91.4	9.581	106.6	9.58
121.9	9.58	137.1	9.589
152.4	9.599	167.6	9.609
182.8	9.619	198.1	9.645
213.3	9.647	228.6	9.655
243.8	9.679	249.9	9.701

APPENDIX B
Individual temperature profiles and tabulations
for the Black Mesa region (see Figures 1 and 3)

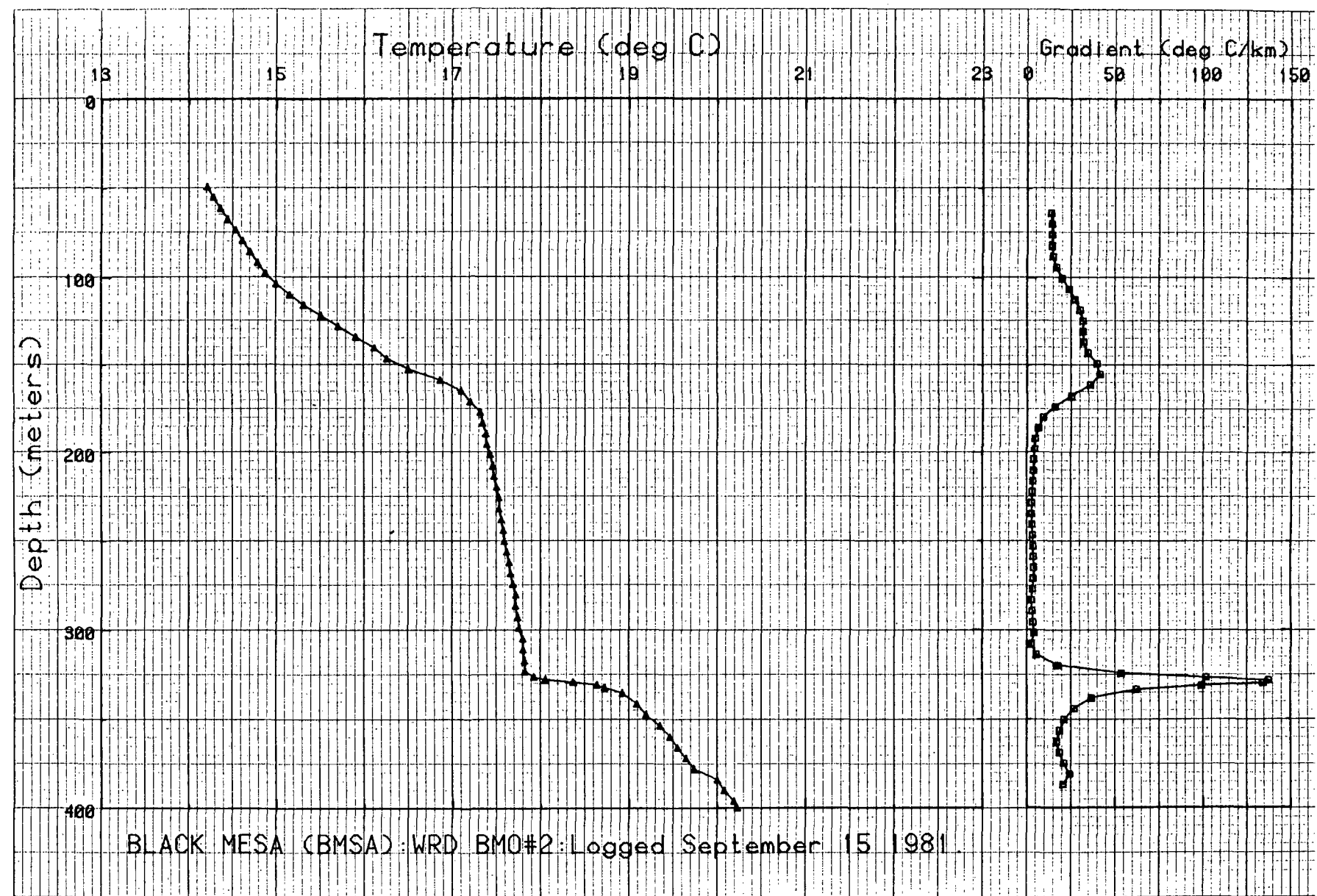


Figure B-1.

Depth,m	Temp,C	Depth,m	Temp,C
48.7	14.204	54.8	14.275
60.9	14.355	67	14.438
73.1	14.532	79.2	14.615
85.3	14.7	91.4	14.787
97.5	14.875	103.6	14.999
109.7	15.154	115.8	15.315
121.9	15.512	128	15.707
134.1	15.908	140.2	16.119
146.3	16.261	152.4	16.506
158.5	16.866	164.6	17.101
170.7	17.199	176.7	17.313
182.8	17.339	188.9	17.38
195	17.391	201.1	17.43
207.2	17.46	213.3	17.471
219.4	17.501	225.5	17.528
231.6	17.528	237.7	17.554
243.8	17.576	249.9	17.589
256	17.614	262.1	17.642
268.2	17.657	274.3	17.685
280.4	17.717	286.5	17.712
292.6	17.736	298.7	17.753
304.8	17.801	310.9	17.804
317	17.818	323.1	17.823
326.1	17.924	327.6	18.054
329.1	18.371	330.7	18.638
332.2	18.727	335.2	18.927
341.3	19.09	347.4	19.195
353.5	19.351	359.6	19.465
365.7	19.55	371.8	19.646
377.9	19.737	384	20.001
390.1	20.08	396.2	20.189
401.4	20.241		

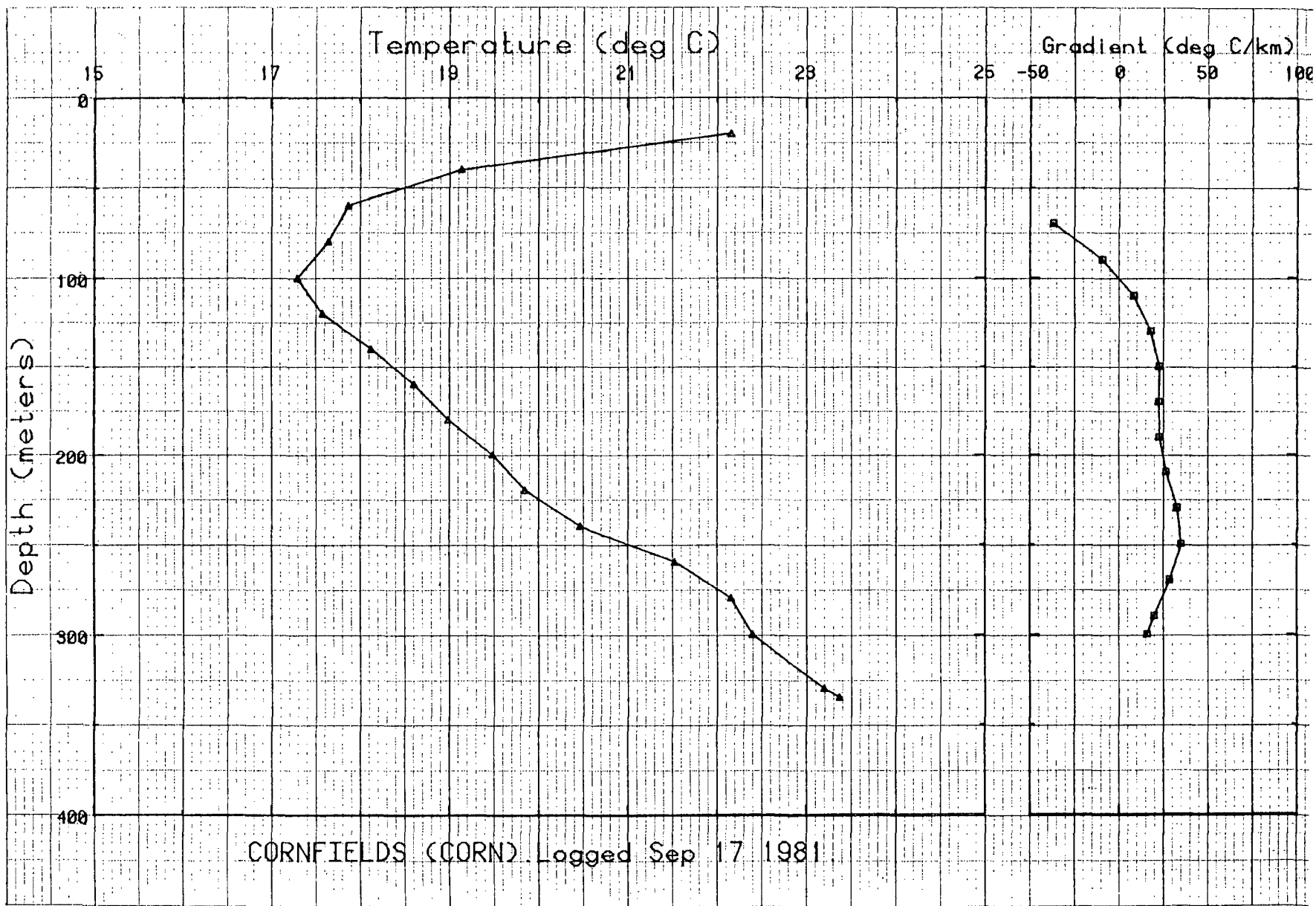


Figure B-2.

Depth,m	Temp,C	Depth,m	Temp,C
20	22.16	40	19.14
59.9	17.87	79.9	17.65
99.9	17.3	119.9	17.58
139.9	18.13	159.9	18.61
179.9	18.99	199.9	19.49
219.9	19.85	239.9	20.47
259.9	21.53	279.9	22.16
299.9	22.4	300	22.4
330	23.2	335	23.37

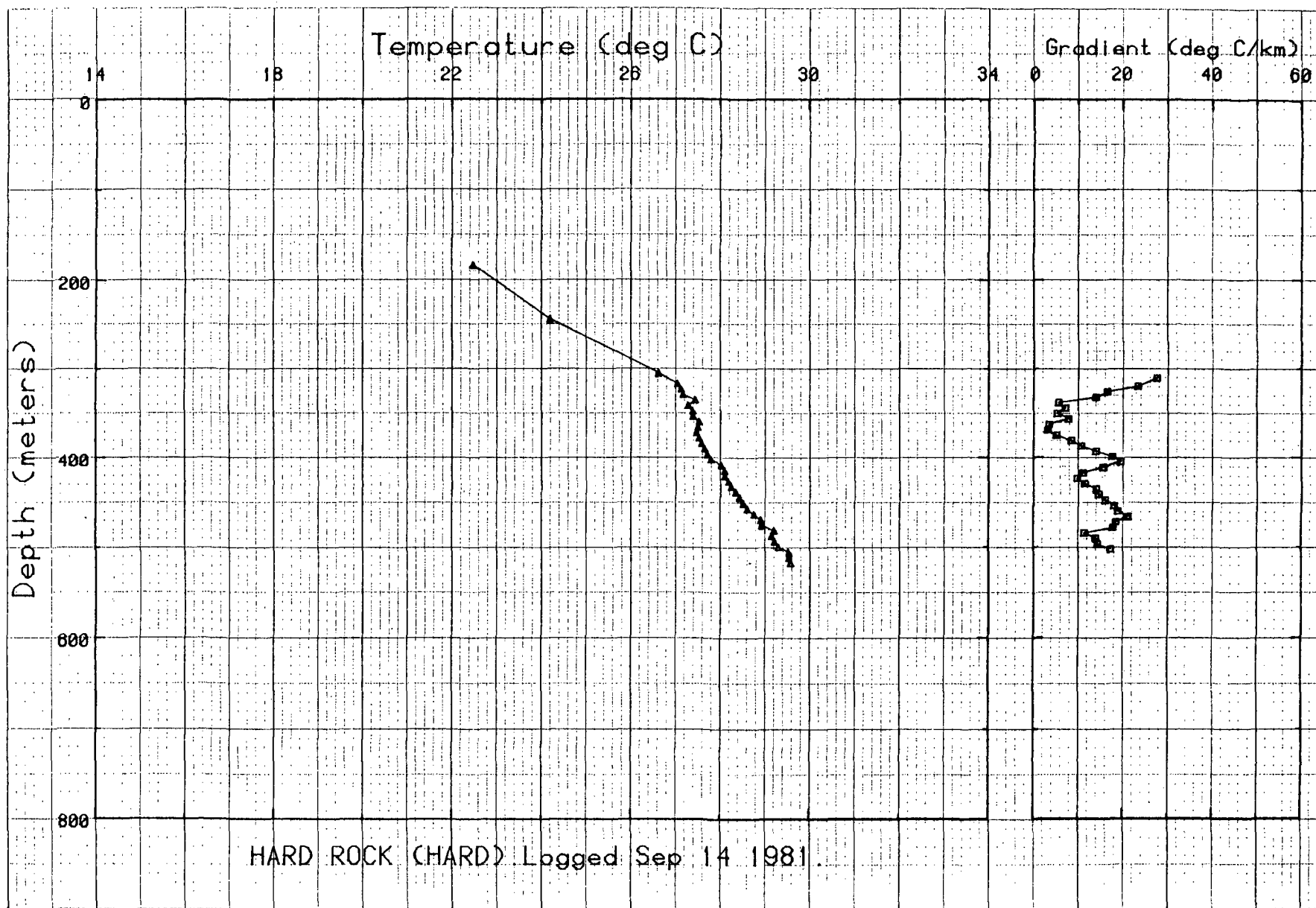


Figure B-3.

Depth,m

Temp,C

Depth,m

Temp,C

60.9	19.36	121.9	18.22
182.8	22.48	243.8	24.2
304.8	26.62	317	27.05
323.1	27.13	329.1	27.18
335.2	27.45	341.3	27.29
347.4	27.39	353.5	27.39
359.6	27.53	365.7	27.5
371.8	27.47	377.9	27.53
384	27.59	390.1	27.66
396.2	27.72	402.3	27.8
408.4	28.03	414.5	28.11
420.6	28.11	426.7	28.19
432.8	28.25	438.9	28.35
445	28.44	451.1	28.53
457.2	28.62	463.3	28.77
469.4	28.92	475.5	28.94
481.5	29.22	487.6	29.16
493.7	29.23	499.8	29.32
505.9	29.54	512	29.54
518.1	29.58		

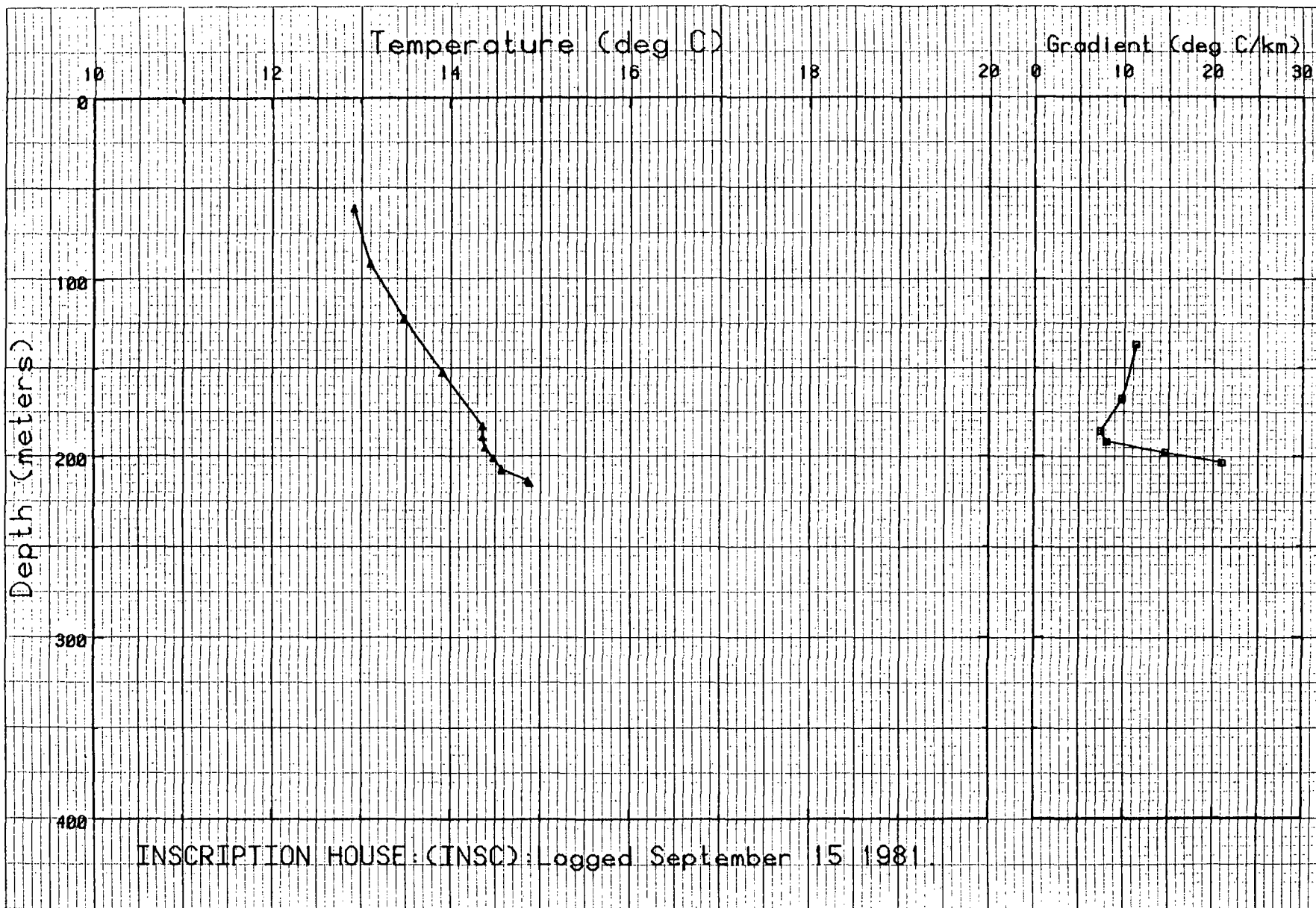


Figure B-4.

Depth,m

Temp,C

Depth,m

Temp,C

30.4

13.861

60.9

12.923

91.4

13.108

121.9

13.482

152.4

13.913

182.8

14.362

188.9

14.359

195

14.388

201.1

14.482

207.2

14.569

213.3

14.861

214.8

14.883

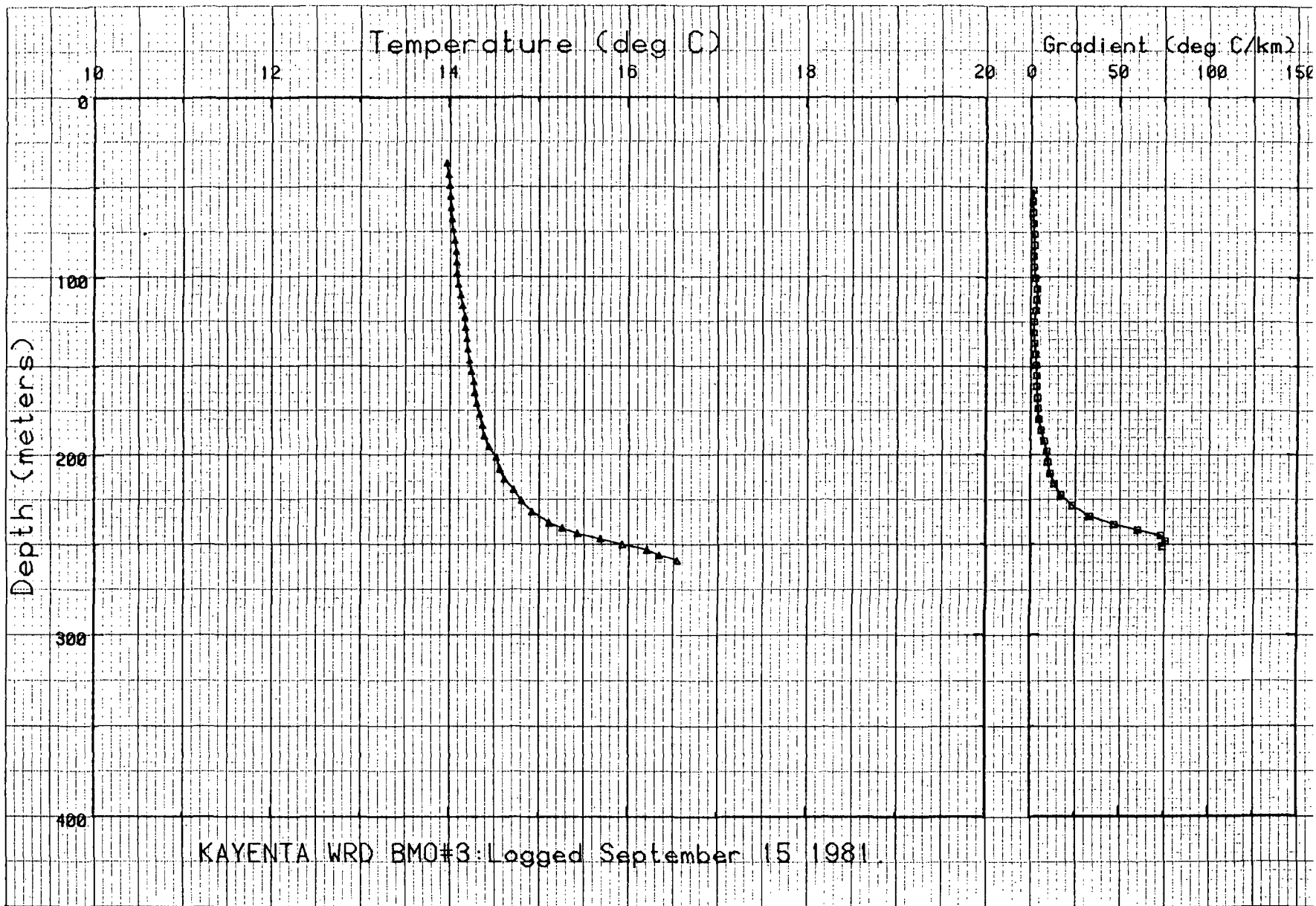


Figure B-5.

Depth,m	Temp,°C	Depth,m	Temp,°C
36.5	13.977	42.6	13.997
48.7	14.008	54.8	14.016
60.9	14.024	67	14.031
73.1	14.042	79.2	14.058
85.3	14.075	91.4	14.08
97.5	14.085	103.6	14.101
109.7	14.131	115.8	14.155
121.9	14.179	128	14.185
134.1	14.198	140.2	14.206
146.3	14.227	152.4	14.246
158.5	14.275	164.6	14.285
170.7	14.309	176.7	14.343
182.8	14.372	188.9	14.391
195	14.441	201.1	14.529
207.2	14.566	213.3	14.62
219.4	14.723	225.5	14.812
231.6	14.928	237.7	15.122
240.8	15.27	243.8	15.442
246.9	15.699	249.9	15.939
252.9	16.213	256	16.349
259	16.551		

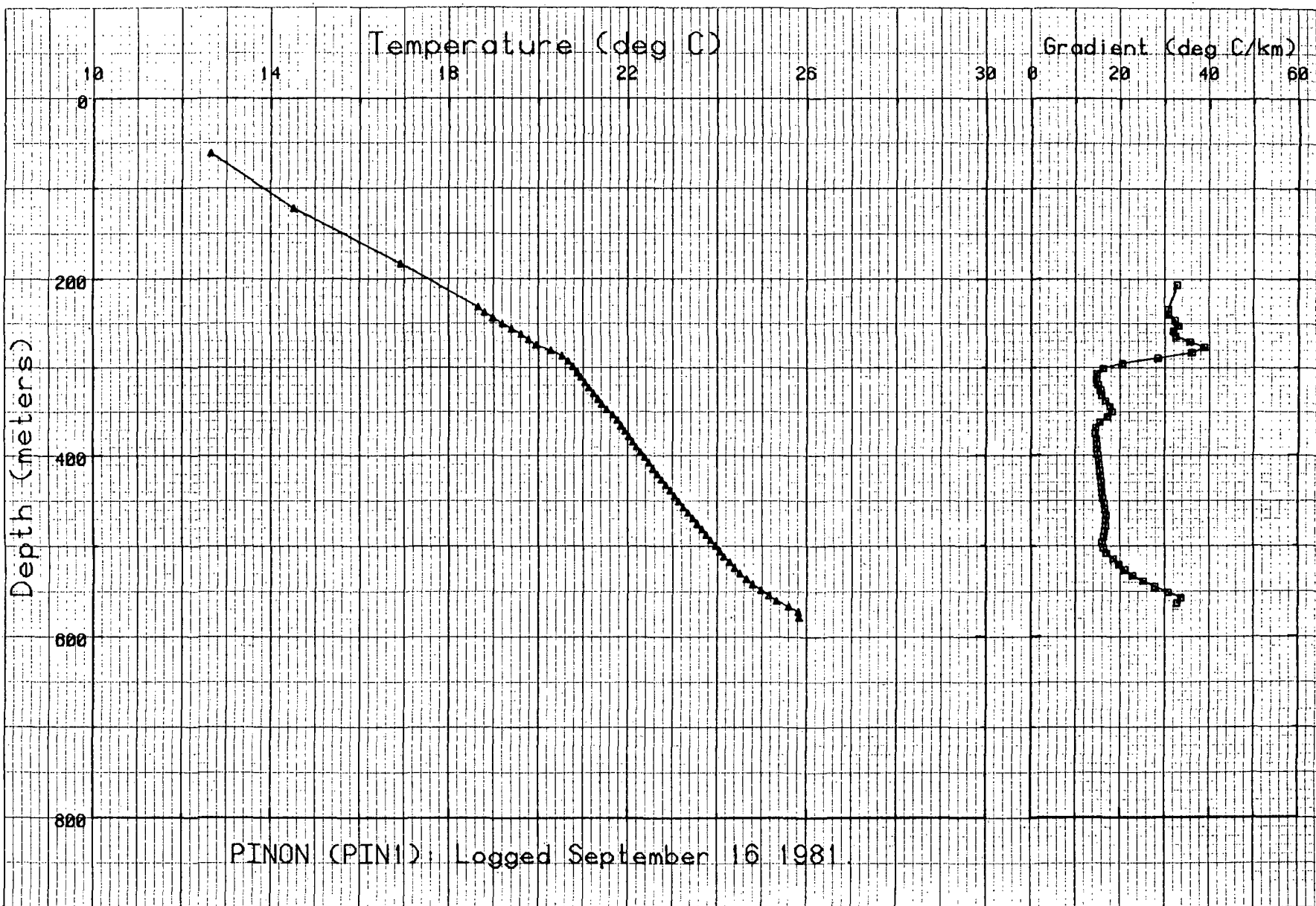


Figure B-6.

Depth,m	Temp,C	Depth,m	Temp,C
60.9	12.639	121.9	14.512
182.8	16.92	231.6	18.661
237.7	18.804	243.8	18.987
249.9	19.201	256	19.406
262.1	19.615	268.2	19.78
274.3	19.946	280.4	20.273
286.5	20.53	292.6	20.665
298.7	20.774	304.8	20.867
310.9	20.95	317	21.04
323.1	21.126	329.1	21.229
335.2	21.328	341.3	21.416
347.4	21.523	353.5	21.659
359.6	21.761	365.7	21.843
371.8	21.93	377.9	22.015
384	22.11	390.1	22.198
396.2	22.287	402.3	22.378
408.4	22.475	414.5	22.566
420.6	22.661	426.7	22.756
432.8	22.853	438.9	22.951
445	23.047	451.1	23.143
457.2	23.247	463.3	23.346
469.4	23.456	475.5	23.55
481.5	23.661	487.6	23.758
493.7	23.856	499.8	23.962
505.9	24.051	512	24.141
518.1	24.274	524.2	24.386
530.3	24.509	536.4	24.655
542.5	24.791	548.6	24.979
554.7	25.161	560.8	25.337
566.9	25.614	573	25.82
579.1	25.837		

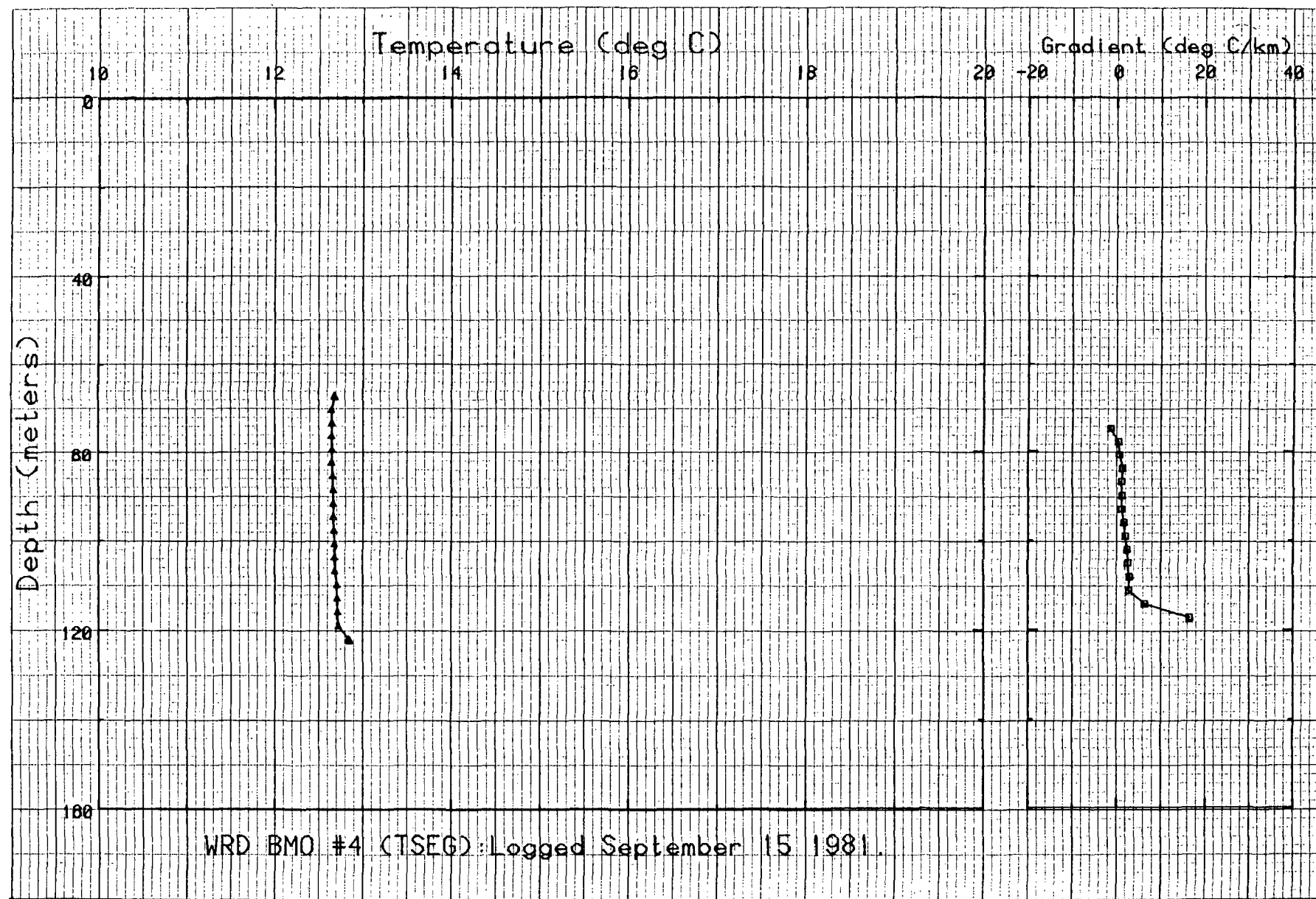


Figure B-7.

Depth,m	Temp,C	Depth,m	Temp,C
67	12.684	70.1	12.647
73.1	12.65	76.2	12.647
79.2	12.65	82.3	12.647
85.3	12.659	88.4	12.66
91.4	12.663	94.5	12.664
97.5	12.67	100.5	12.678
103.6	12.684	106.6	12.688
109.7	12.705	112.7	12.711
115.8	12.715	118.8	12.726
121.9	12.838	122.2	12.856

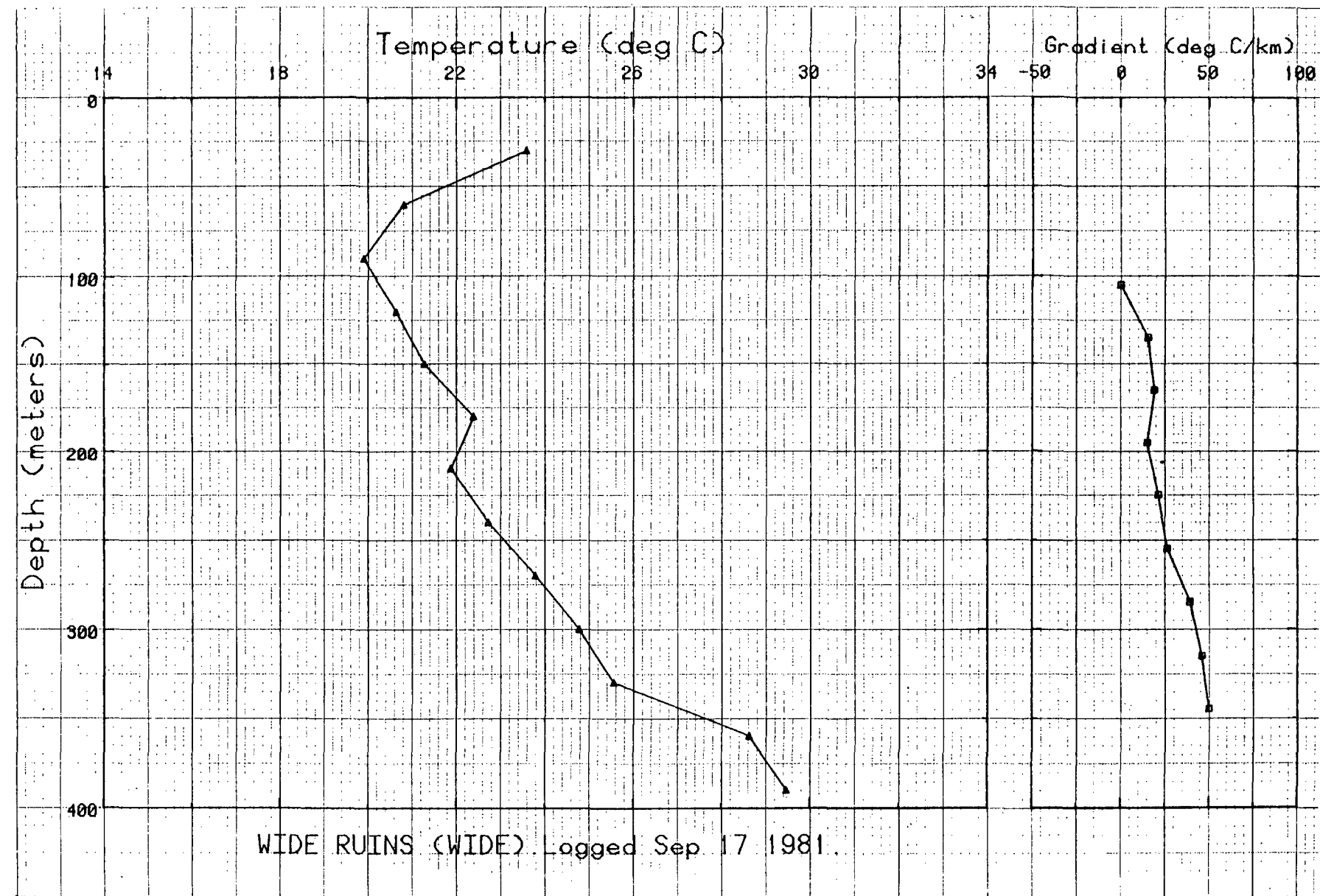


Figure B-8.

Depth,m

Temp,C

Depth,m

Temp,C

30

23.58

59.9

20.81

89.9

19.9

119.9

20.65

149.9

21.29

179.9

22.39

209.9

21.88

239.9

22.73

269.9

23.79

299.9

24.78

329.9

25.56

359.9

28.63

389.9

29.47

390

29.47

APPENDIX C

Individual temperature profiles and tabulations
for the south-central Colorado Plateau (see Figures 1 and 4)

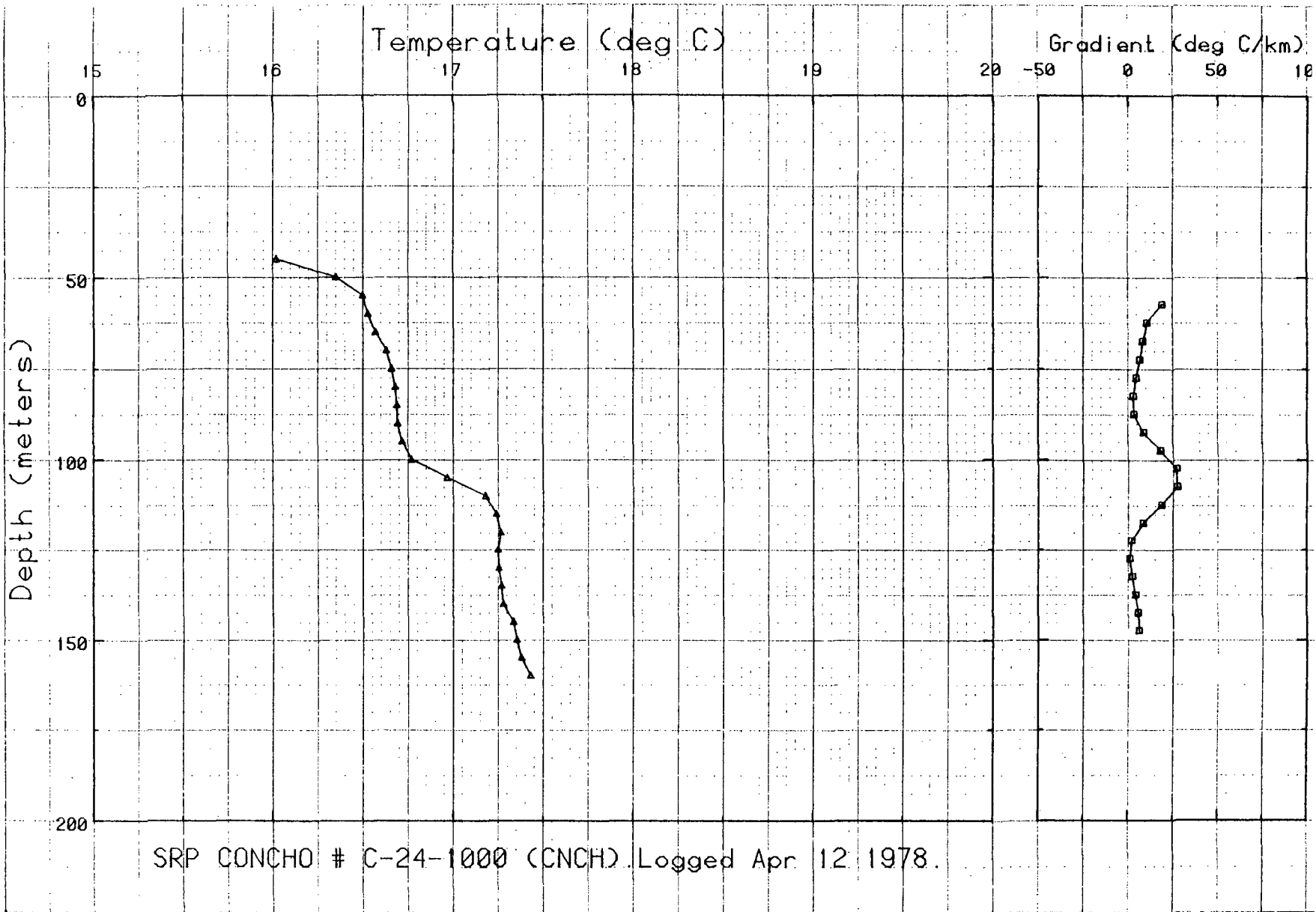


Figure C-1.

Depth,m	Temp,C	Depth,m	Temp,C
45	16.02	50	16.35
55	16.5	59.9	16.53
64.9	16.57	69.9	16.63
74.9	16.66	79.9	16.68
84.9	16.69	89.9	16.695
94.9	16.72	99.9	16.77
104.9	16.97	109.9	17.18
114.9	17.24	119.9	17.265
124.9	17.25	129.9	17.255
134.9	17.27	139.9	17.28
144.9	17.335	149.9	17.355
154.9	17.38	159.9	17.43

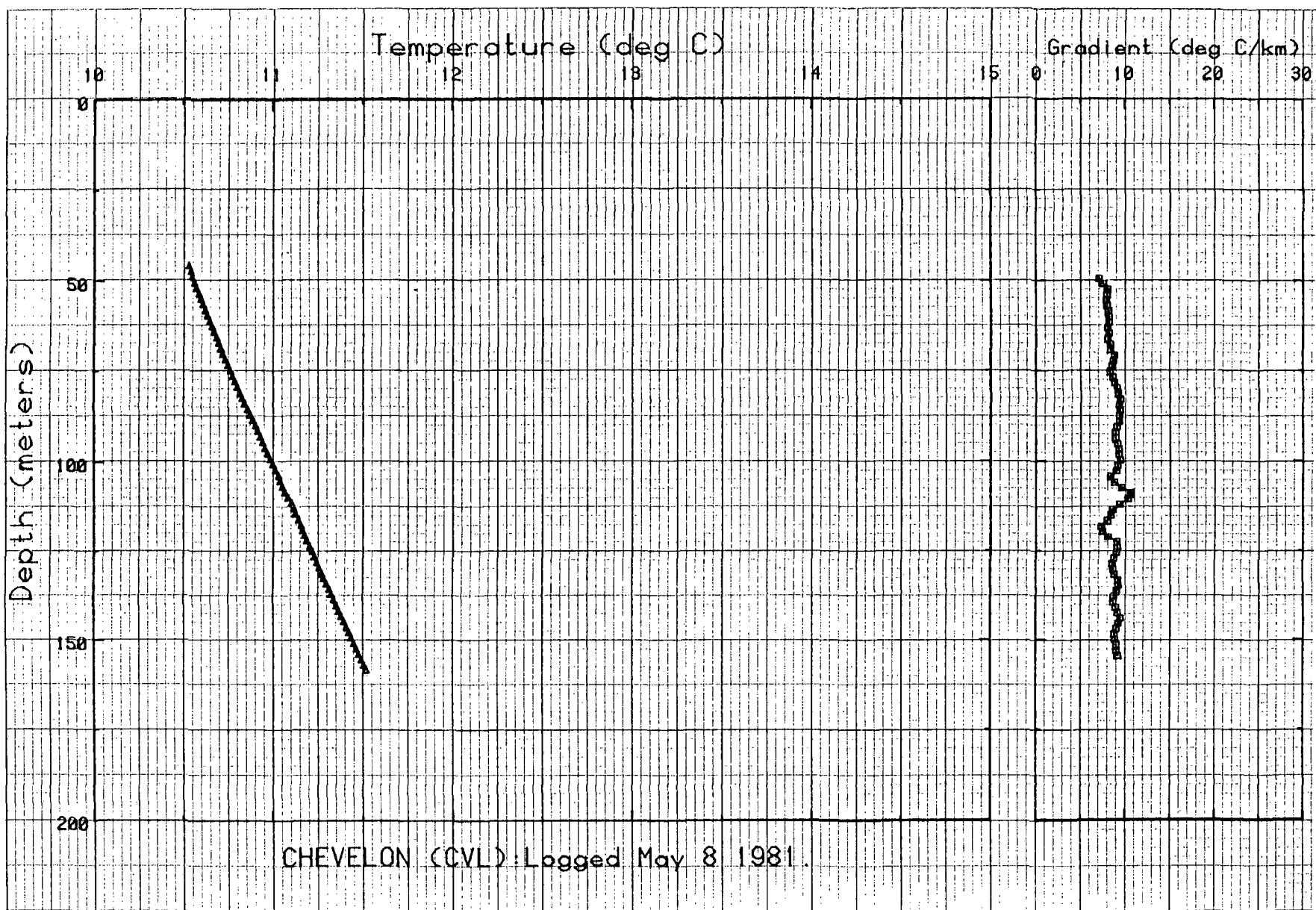


Figure C-2.

Depth,m	Temp,C	Depth,m	Temp,C
44.2	10.584	45.7	10.534
47.2	10.546	48.7	10.553
50.3	10.565	51.8	10.576
53.3	10.59	54.8	10.602
56.4	10.613	57.9	10.626
59.4	10.638	60.9	10.651
62.4	10.664	64	10.675
65.5	10.689	67	10.7
68.5	10.714	70.1	10.725
71.6	10.74	73.1	10.754
74.6	10.767	76.2	10.778
77.7	10.792	79.2	10.806
80.7	10.82	82.3	10.833
83.8	10.849	85.3	10.863
86.8	10.877	88.4	10.891
89.9	10.907	91.4	10.92
92.9	10.933	94.5	10.947
96	10.961	97.5	10.975
99	10.99	100.5	11.004
102.1	11.017	103.6	11.035
105.1	11.043	106.6	11.057
108.2	11.071	109.7	11.088
111.2	11.108	112.7	11.121
114.3	11.129	115.8	11.146
117.3	11.16	118.8	11.167
120.4	11.179	121.9	11.19
123.4	11.207	124.9	11.22
126.5	11.234	128	11.247
129.5	11.26	131	11.274
132.6	11.285	134.1	11.301
135.6	11.316	137.1	11.329
138.6	11.342	140.2	11.355
141.7	11.369	143.2	11.382
144.7	11.398	146.3	11.412
147.8	11.426	149.3	11.438
150.8	11.452	152.4	11.467
153.9	11.479	155.4	11.494
156.9	11.508	158.3	11.521

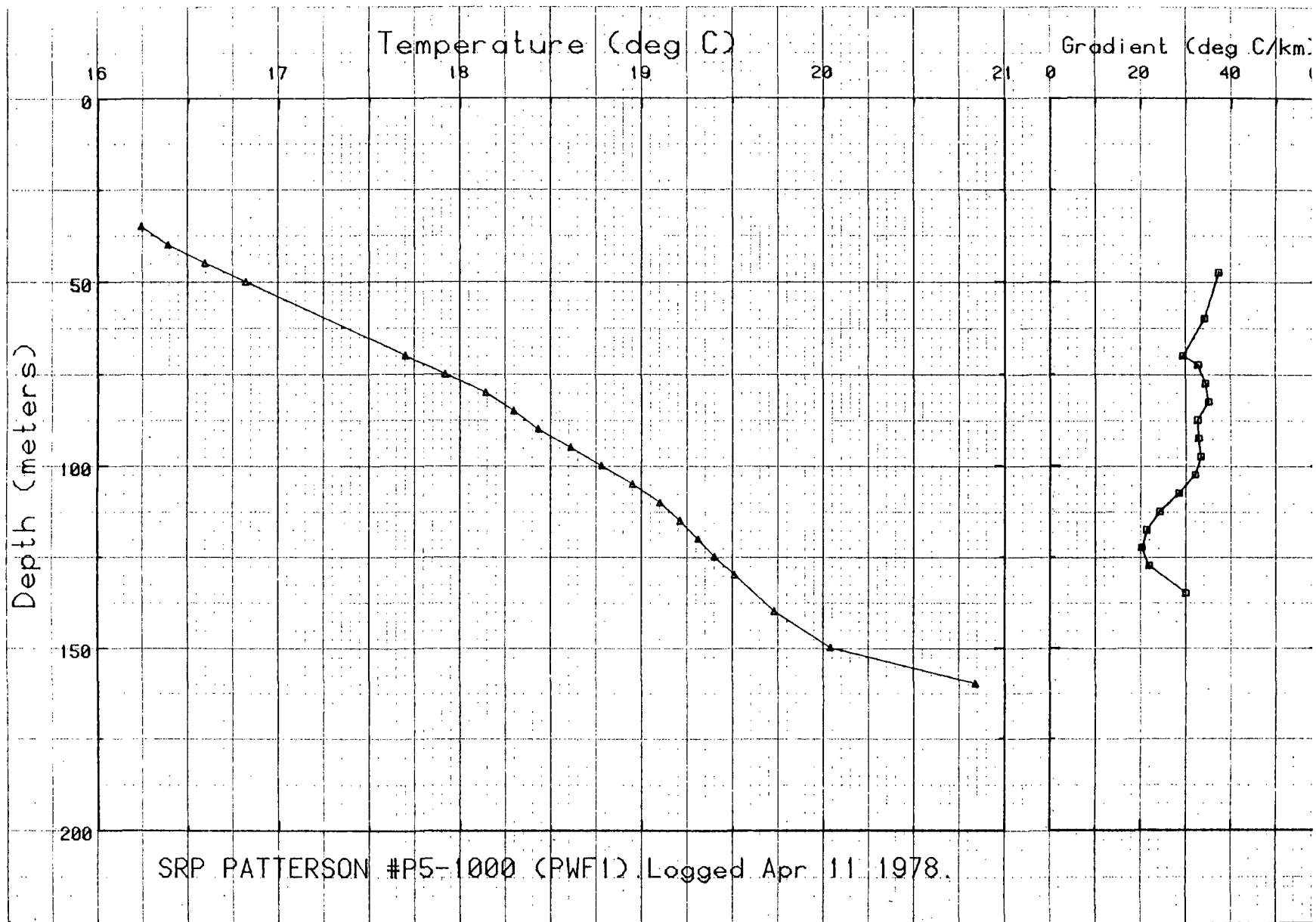


Figure C-3.

Depth,m	Temp,C	Depth,m	Temp,C
35	16.24	40	16.39
45	16.595	50	16.82
69.9	17.7	70	17.7
75	17.92	80	18.14
85	18.295	90	18.43
95	18.61	100	18.78
105	18.95	110	19.1
115	19.21	120	19.31
125	19.4	130	19.51
140	19.73	150	20.04
160	20.84		

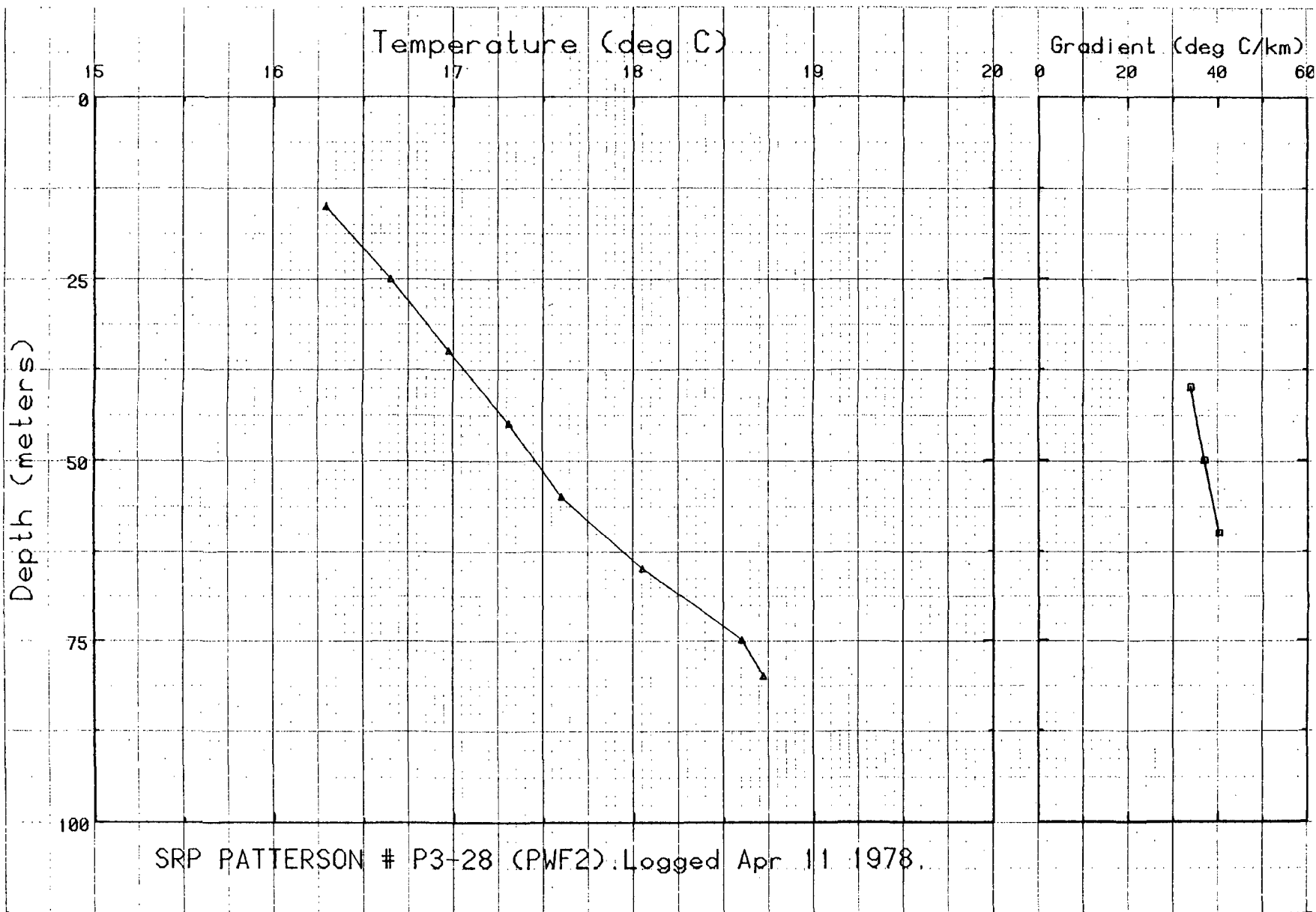


Figure C-4.

Depth,m

Temp,C

Depth,m

Temp,C

15
35
55
74.9

16.29
16.97
17.6
18.6

25
45
64.9
80

16.65
17.31
18.05
18.72

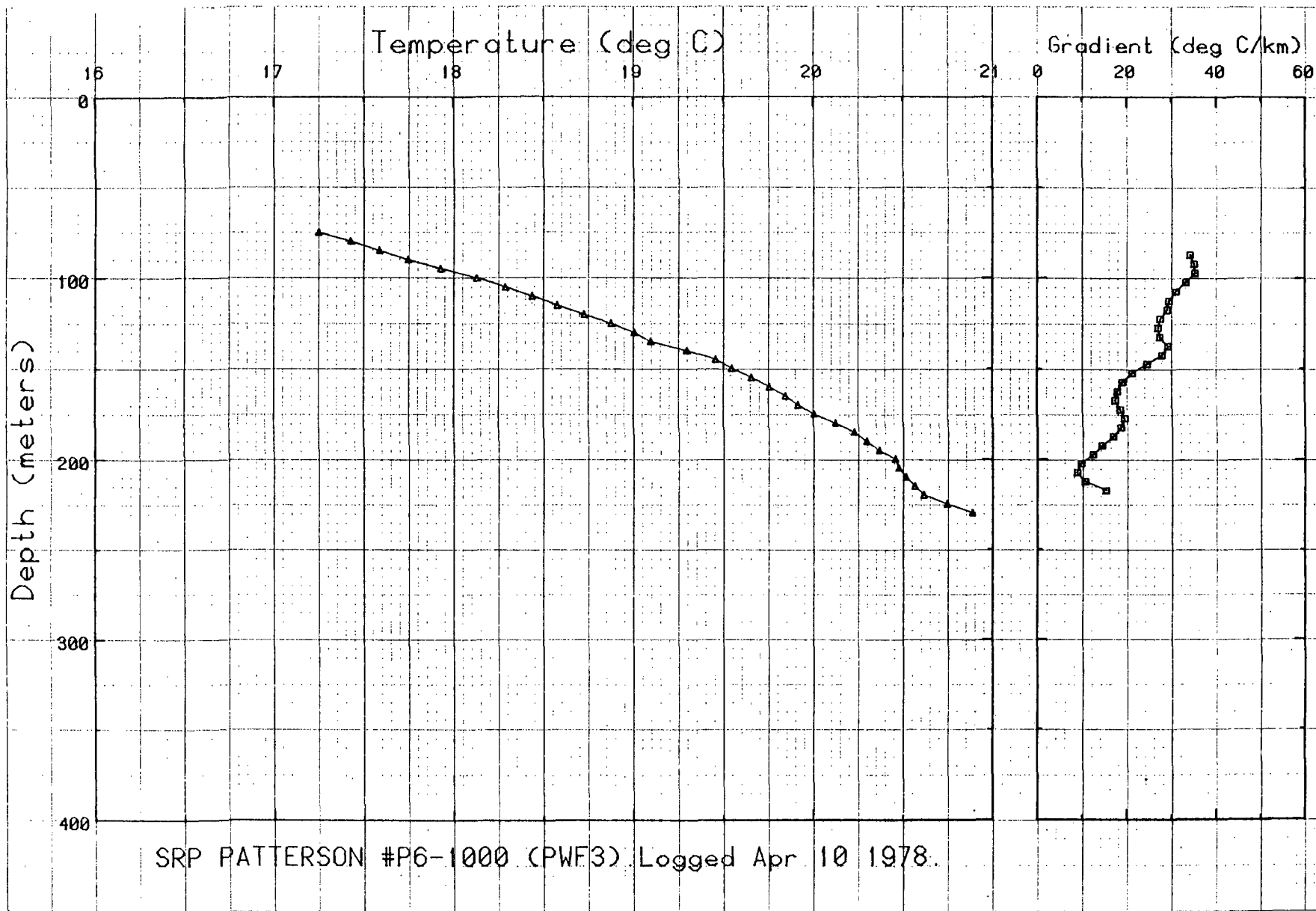


Figure C-5.

Depth,m	Temp,C	Depth,m	Temp,C
75	17.25	80	17.43
85	17.59	90	17.75
95	17.93	100	18.13
105	18.29	110	18.44
115	18.58	120	18.73
125	18.88	130	19.01
135	19.1	140	19.3
145	19.46	150	19.55
155	19.66	160	19.76
165	19.85	170	19.92
175	20.01	179.9	20.13
184.9	20.23	189.9	20.3
194.9	20.37	199.9	20.46
204.9	20.48	209.9	20.52
214.9	20.57	219.9	20.62
224.9	20.75	229.9	20.89

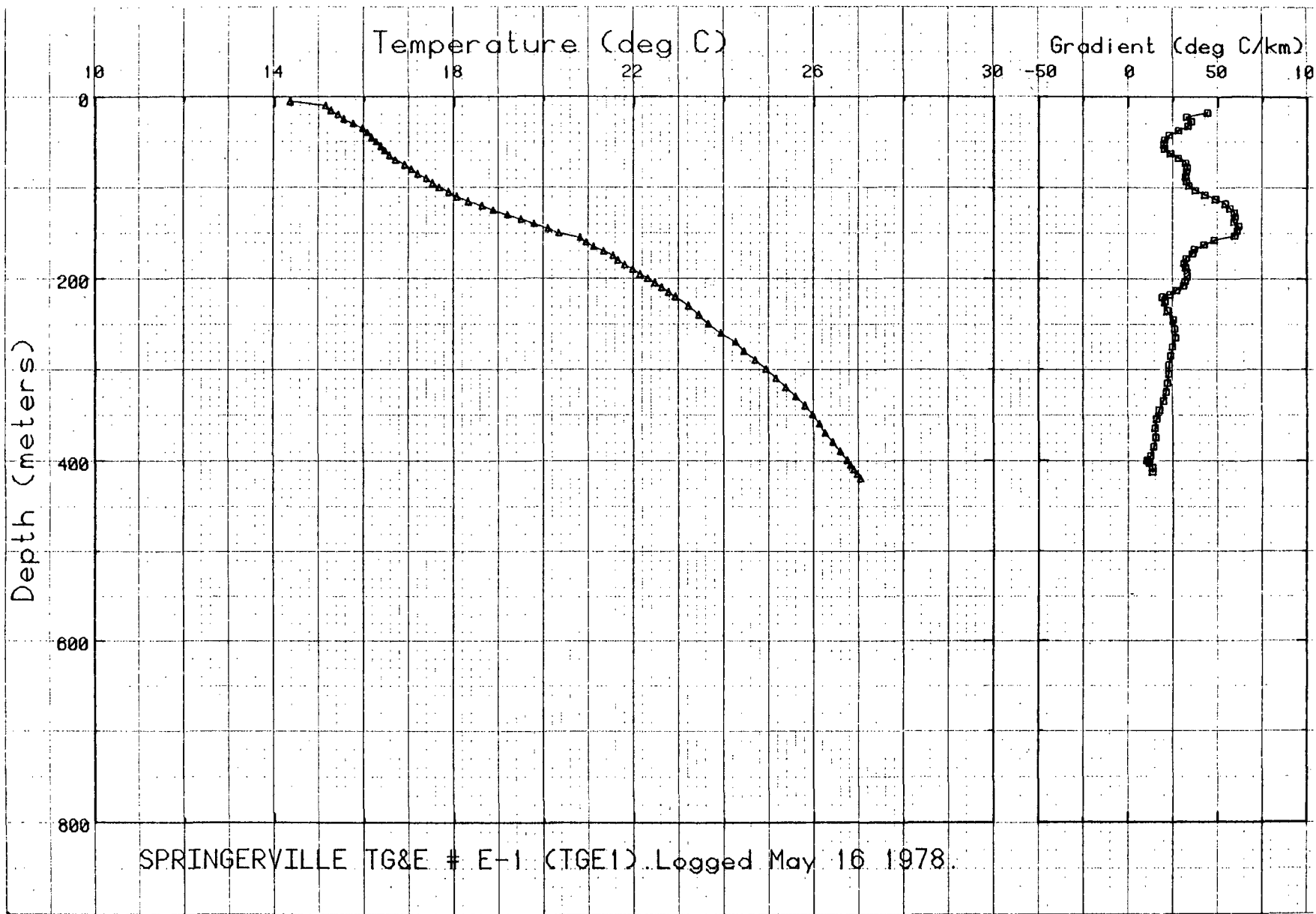


Figure C-6.

Depth,m	Temp,C	Depth,m	Temp,C
5	14.34	10	15.13
15	15.25	20	15.41
25	15.54	30	15.75
35	15.96	40	16.07
45	16.16	50	16.27
55	16.37	59.9	16.455
64.9	16.56	69.9	16.69
74.9	16.9	79.9	17.05
84.9	17.19	89.9	17.38
94.9	17.52	99.9	17.67
104.9	17.88	109.9	18.06
114.9	18.31	119.9	18.62
124.9	18.87	129.9	19.19
134.9	19.49	139.9	19.78
144.9	20.09	149.9	20.33
154.9	20.81	159.9	20.945
164.9	21.11	169.9	21.33
174.9	21.54	179.9	21.65
184.9	21.8	189.9	21.98
194.9	22.14	199.9	22.31
204.9	22.47	209.9	22.615
214.9	22.77	219.9	22.92
220	22.92	230	23.21
240	23.44	250	23.655
260	23.935	270	24.265
280	24.45	290	24.7
299.9	24.94	309.9	25.16
319.9	25.38	329.9	25.6
339.9	25.81	349.9	25.98
359.9	26.13	369.9	26.25
379.9	26.42	389.9	26.585
399.9	26.74	400	26.74
405	26.815	410	26.89
415	26.97	419.9	27.04
420	27.04		

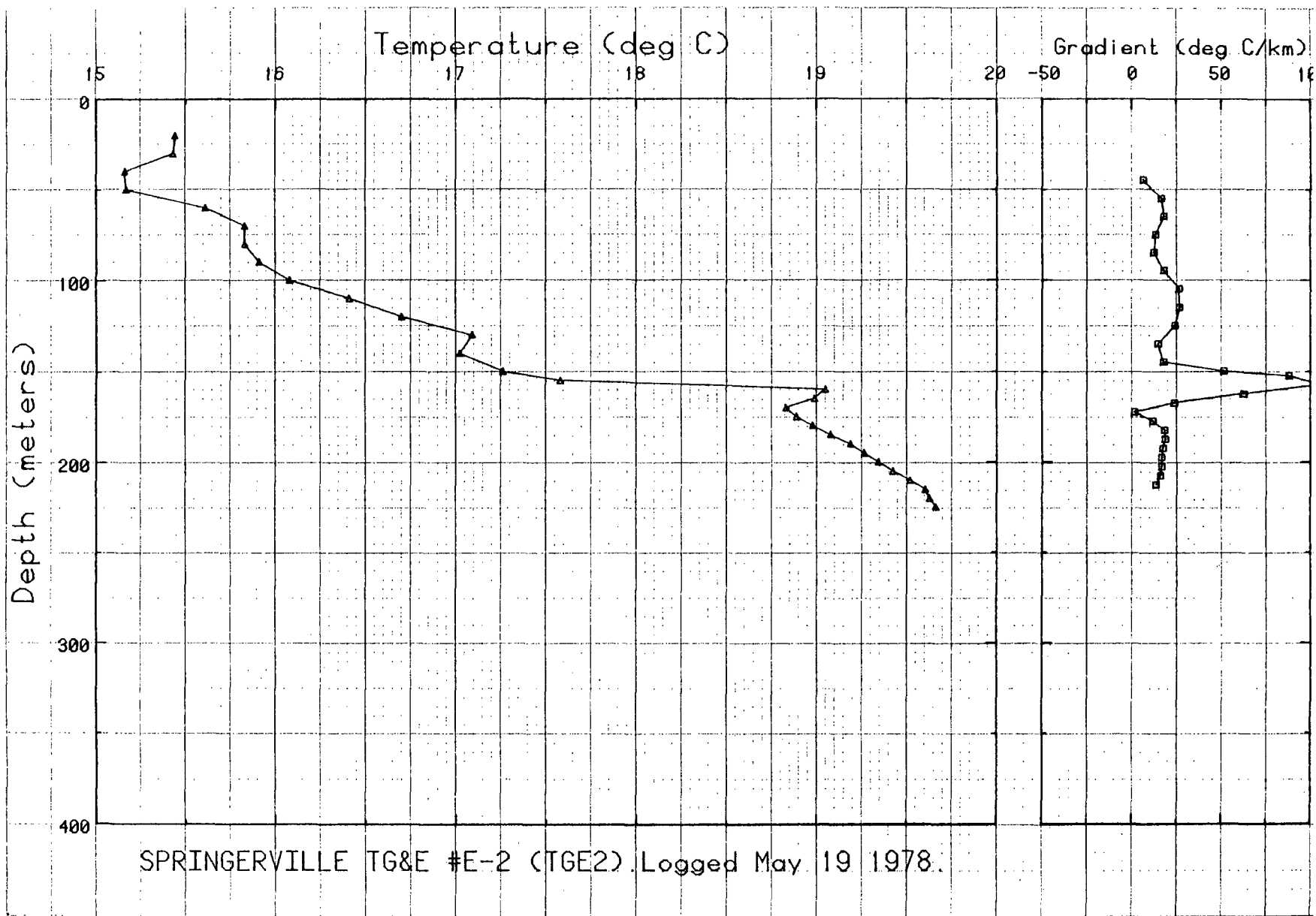


Figure C-7.

Depth,m	Temp,C	Depth,m	Temp,C
10	18.06	20	15.44
30	15.43	40	15.16
50	15.17	59.9	15.61
69.9	15.83	79.9	15.83
89.9	15.91	99.9	16.08
109.9	16.41	119.9	16.7
129.9	17.09	139.9	17.02
149.9	17.26	150	17.26
155	17.58	160	19.05
165	18.99	170	18.83
175	18.89	179.9	18.98
184.9	19.08	189.9	19.19
194.9	19.265	199.9	19.345
204.9	19.425	209.9	19.52
214.9	19.605	219.9	19.63
224.9	19.665		

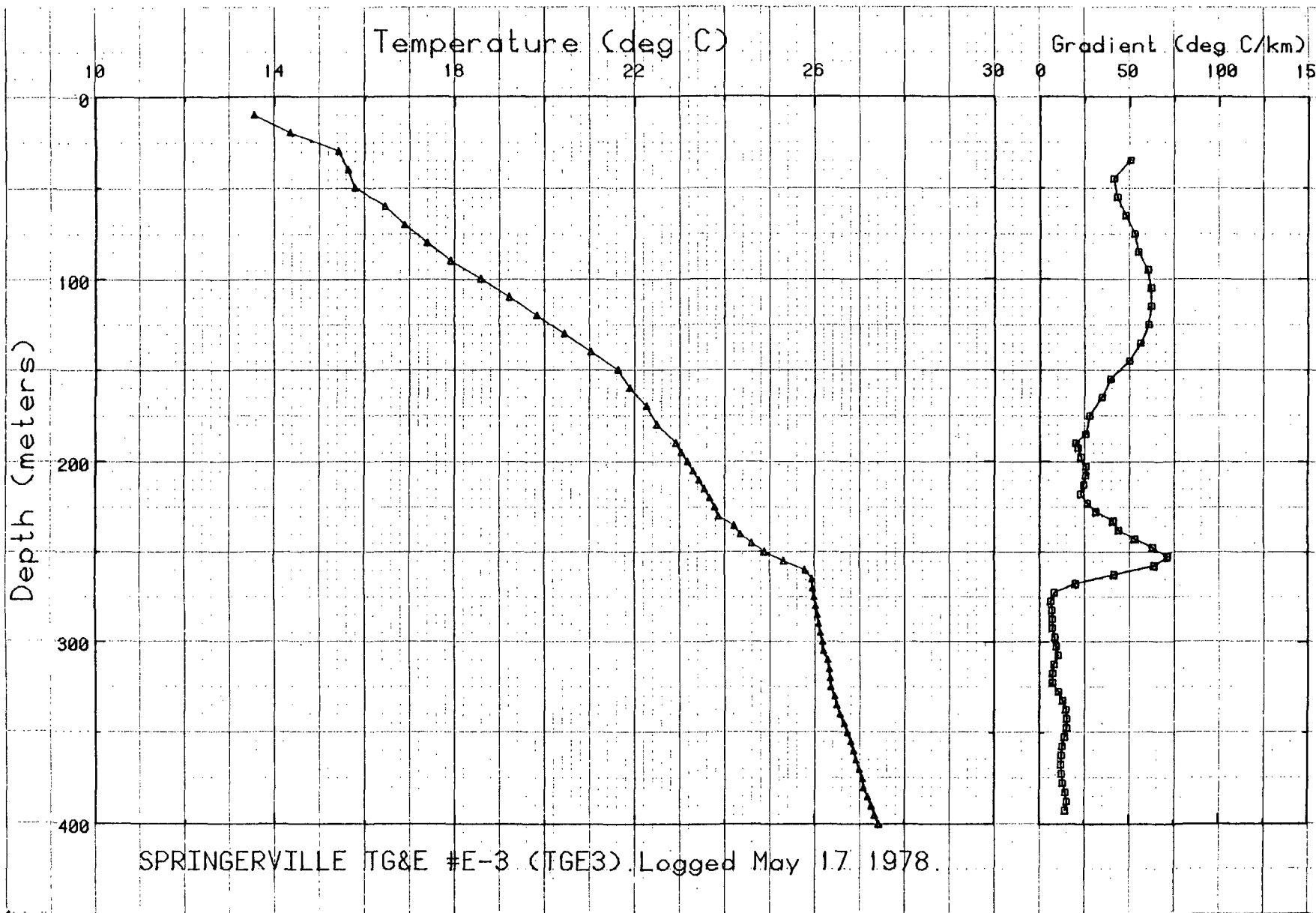


Figure C-8.

Depth,m	Temp,C
10	13.55
30	15.41
50	15.78
69.9	16.88
89.9	17.91
109.9	19.21
129.9	20.44
149.9	21.63
169.9	22.27
189.9	22.91
194.9	23.03
204.9	23.29
214.9	23.55
224.9	23.78
234.9	24.21
244.9	24.6
254.9	25.32
264.9	25.94
274.9	25.98
284.9	26.055
294.9	26.12
304.9	26.19
314.9	26.32
324.9	26.355
334.9	26.49
344.9	26.66
354.9	26.81
364.9	26.915
374.9	27.06
384.9	27.19
394.9	27.34
400	27.43

Depth,m	Temp,C
20	14.35
40	15.63
59.9	16.45
79.9	17.39
99.9	18.58
119.9	19.83
139.9	21.03
159.9	21.89
179.9	22.49
189.9	22.91
199.9	23.17
209.9	23.43
219.9	23.67
229.9	23.86
239.9	24.35
249.9	24.89
259.9	25.79
269.9	25.95
279.9	26.015
289.9	26.085
299.9	26.17
309.9	26.29
319.9	26.34
329.9	26.44
339.9	26.57
349.9	26.73
359.9	26.87
369.9	26.99
379.9	27.09
389.9	27.27
399.9	27.43

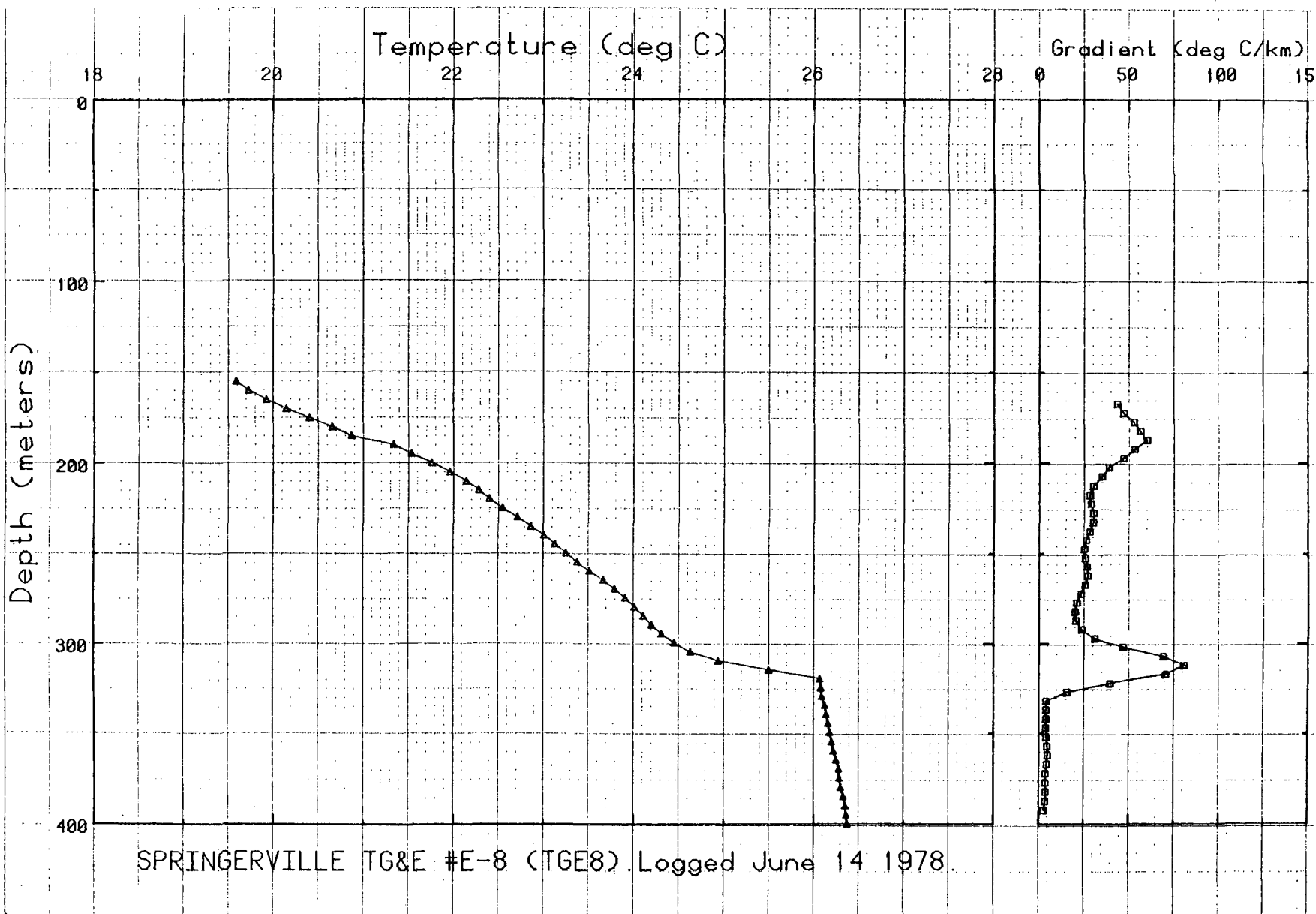


Figure C-9.

Depth,m

Temp,C

Depth,m

Temp,C

155	19.59	160	19.73
165	19.93	170	20.15
175	20.41	179.9	20.655
184.9	20.87	189.9	21.34
194.9	21.535	199.9	21.76
204.9	21.96	209.9	22.145
214.9	22.28	219.9	22.4
224.9	22.545	229.9	22.71
234.9	22.865	239.9	23.01
244.9	23.135	249.9	23.255
254.9	23.38	259.9	23.515
264.9	23.67	269.9	23.795
274.9	23.91	279.9	24.01
284.9	24.11	289.9	24.2
294.9	24.31	299.9	24.45
304.9	24.63	309.9	24.94
314.9	25.5	319.9	26.07
324.9	26.08	329.9	26.09
334.9	26.125	339.9	26.14
344.9	26.16	349.9	26.18
354.9	26.2	359.9	26.22
364.9	26.25	369.9	26.28
374.9	26.285	379.9	26.3
384.9	26.33	389.9	26.35
394.9	26.36	399.9	26.37
400	26.37		